




University of  
Stavanger

Faculty of Science and Technology

## MASTER'S THESIS

Study program/ Specialization:  Petroleum Engineering – Master of Science Degree Programme / Reservoir Engineering	Spring semester, 2011  Open
Writer: Marthe Gilje Fossmark	 (Marthe Gilje Fossmark)
Faculty supervisor: Svein Magne Skjæveland  External supervisor: Øivind Fevang (Statoil ASA)	
Titel of thesis:  Multiphase-Flow Correlations' Ability to Model Vertical Lift Performance	
Credits (ECTS): 30	
Key words: Multiphase Flow Pressure-Gradient Equation Accuracy of correlations Modification of correlations	Pages: 103  + enclosure: 26  Stavanger, 9th of June/2011 Date/year



## Abstract

The Statfjord Field has entered a drainage strategy where the reservoir will be depleted such that gas liberates from the remaining oil in the reservoirs. Adequate modelling of vertical lift performance is needed to predict a realistic liquid offtake and thereby pressure-depletion rate. Wells in the Statfjord Formation have been producing from a gas cap in which some areas of the formation has disappeared. Production tests from wells located in such areas have been used as basis when analysing multiphase-flow correlations' ability to model vertical lift performance.

Calculations are done in Prosper, a well performance, design and optimization program developed by Petroleum Experts. Conceptual test data describing liquid and gas-condensate wells were sett up to study prediction of pressure drop, and differences between correlations. Measured downhole pressures from 203 production tests, from six wells located in the Statfjord Formation, were used to compare accuracy of correlations. Petroleum Experts, Petroleum Experts 2 and Petroleum Experts 3 were found to be the most accurate correlations, and were recommended to use when creating lift curves for the Statfjord full field model.

A trend of too low pressures predicted at low gas-liquid ratio (GLR), and too high pressures predicted at higher GLR was observed. An attempt of making the correlation even more accurate for a wider gas-liquid range was done by tuning in Prosper. None of the attempted modifications gave increased accuracy for the whole GLR range studied. It was proposed that modification to equations for liquid holdup, or in flow regime boundaries may improve accuracy over a wider GLR range.

A study of using tuned correlations and possible errors introduced when predicting future performance was performed. Only small errors were observed for a narrow GLR range (as for the Brent Group, 50 – 300 Sm<sup>3</sup>/Sm<sup>3</sup>), and one correlation can be used for the entire time range. With higher gas-liquid ratios, errors introduced by using correlations tuned to test data may be significant, and it was recommended to change correlation as function of GLR development. A recommendation of correlations to use and how they may be modified when predicting future performance of the Statfjord Field is included.

## Acknowledgements

There are several people I would like to express my gratitude towards in making of this thesis. First I gratefully acknowledge Statoil ASA and the University of Stavanger for allowing me to write this thesis. I would like to thank Kari Nordaas Kulkarni for posing the thesis and Svein Magne Skjæveland for his guidance and support as my faculty supervisor.

I am heartily thankful to my supervisor, Øivind Fevang. He has encouraged, guided and supported me from the beginning to the final level, and through this enabled me to develop an understanding of the subject.

I would like to show my gratitude to Håvard Thomassen Lauritsen for guidance, discussions and support. He has made the development of this thesis enjoyable and educational by being accessible and friendly.

My good friends and fellow students, Dagny Håmsø and Kristian Grepstad, have been supportive and encouraging. We have helped and pushed each other through the process, especially when difficulties were encountered, and for this I owe them gratitude.

I am grateful for love, support and understanding from my dear husband Marius Fossmark and my loving parents Ann Elin Gilje and Dag Bergslien.

Lastly I would like to thank all of those who supported me in any respect during the completion of my thesis.

Marthe Gilje Fossmark

## Nomenclature

$A$	=	pipe cross-sectional area
$C$	=	liquid holdup parameter
$C$	=	correction factor
$CN_L$	=	corrected liquid viscosity number
$d$	=	pipe inside diameter
$E_k$	=	dimensionless kinetic-energy pressure gradient
$f$	=	correction factor
$f$	=	friction factor
$f$	=	no-slip volume fraction
$g$	=	gravity
$H_G$	=	gas holdup
$H_L$	=	liquid holdup
$L$	=	length
$L_B$	=	bubble-slug boundary
$L_M$	=	transition-Mist boundary
$L_S$	=	slug-transition boundary
$n$	=	correction factor
$N_D$	=	dimensionless diameter number
$N_{Fr}$	=	Froude number
$N_{GV}$	=	dimensionless gas velocity number
$N_L$	=	dimensionless liquid viscosity number
$N_{LV}$	=	dimensionless liquid velocity number
$N_{Re}$	=	Reynolds number
$N_v$	=	dimensionless velocity number
$p$	=	pressure
$q$	=	volumetric flow rate
$R$	=	superficial liquid/gas ratio
$S$	=	slip ratio
$t$	=	time
$v$	=	velocity
$v_b$	=	bubble rise velocity

$Z$  = length  
 $\Gamma$  = liquid distribution coefficient  
 $\Delta$  = difference  
 $\varepsilon$  = pseudo wall roughness factor  
 $\varepsilon/d$  = relative roughness  
 $\varepsilon'$  = roughness variable  
 $\theta$  = inclination angle from vertical  
 $\lambda$  = no-slip fraction  
 $\mu$  = viscosity  
 $\rho$  = density  
 $\sigma$  = surface tension  
 $\tau$  = shear stress  
 $\psi$  = correction factor

### **Subscripts**

a = acceleration  
F = Fanning  
f = friction  
G = gas  
h = hydrostatic  
L = liquid  
M = Moody  
m = mixture of liquid and gas  
n = no-slip  
o = oil  
S = superficial  
s = slip  
t = total  
TP = two-phase  
w = water

## Abbreviations

BB =	Beggs and Brill
DRm =	Duns and Ros Modified
DRo =	Duns and Ros Original
FB =	Fancher and Brown
Fm =	Formation
GLR =	Gas-liquid ratio
Gm =	Gray Modified
GOR =	Gas-oil ratio
Gp =	Group
H3P =	Hydro-3 Phase
HB =	Hagedorn and Brown
MB =	Mukherjee and Brill
O =	Orkiszewski
O2P =	OLGAS 2-phase
O3P =	OLGAS 3-phase
O3PE =	OLGAS 3-phase Extended
OD =	Outer diameter
P1 =	Parameter 1, tuning parameter for hydrostatic gradient
P2 =	Parameter 2, tuning parameter fro the frictional gradient
PE =	Petroleum Experts
PE2 =	Petroleum Experts 2
PE3 =	Petroleum Experts 3
PE4 =	Petroleum Experts 4
PE5 =	Petroleum Experts 5
PI =	Productivity index
THP =	Tubing-head pressure
THT =	Tubing-head temperature
VLP =	Vertical lift performance
WCT =	Water cut

# Table of Contents

<b>1</b>	<b>Introduction and Objectives .....</b>	<b>1</b>
<b>2</b>	<b>Theory .....</b>	<b>3</b>
2.1	Single-Phase Flow .....	3
2.1.1	<i>Pressure-Gradient Equation</i> .....	3
2.2	Multiphase Flow .....	8
2.2.1	<i>Holdup</i> .....	8
2.2.2	<i>Velocities</i> .....	10
2.2.3	<i>Mixture-Fluid Properties</i> .....	11
2.2.4	<i>Pressure-Gradient Equation</i> .....	12
2.2.5	<i>Flow Regimes</i> .....	13
2.3	Calculation of Pressure-drop in Long Pipelines .....	16
2.4	Pressure-Drop Correlations.....	18
2.4.1	<i>Fancher and Brown Correlation (Fancher and Brown 1963)</i> .....	19
2.4.2	<i>Gray Correlation (Gray 1974)</i> .....	21
2.4.3	<i>Hagedorn and Brown Correlation (Hagedorn and Brown 1965)</i> .....	23
2.4.4	<i>Duns and Ros Correlation (Duns and Ros 1963)</i> .....	26
2.4.5	<i>Orkiszewski Correlation (Orkiszewski 1967)</i> .....	29
2.4.6	<i>Beggs and Brill Correlation (Beggs and Brill 1973)</i> .....	34
2.4.7	<i>Petroleum Experts' Correlations (Petroleum Experts 2010)</i> .....	38
<b>3</b>	<b>Study of Pressure-Drop Prediction in Liquid and Gas-Condensate Wells ..</b>	<b>40</b>
3.1	Liquid Wells.....	41
3.2	Gas-Condensate Wells .....	47
3.2.1	<i>Effects of Increasing Gas-Rate on Pressure-Drop Prediction</i> .....	47
3.2.2	<i>Effects of Varying Oil-Water Ratio on Pressure-Drop Prediction</i> .....	53
3.3	Conclusions.....	57
<b>4</b>	<b>Comparison of Measured and Predicted Bottomhole Pressures.....</b>	<b>58</b>
4.1	Accuracy of Correlations .....	59
4.2	Effect of Input Data on Accuracy of Correlations .....	63
4.3	Conclusions.....	65
<b>5</b>	<b>Modification of Correlations to Match Measured Bottomhole Pressures....</b>	<b>66</b>
5.1	VLP Matching Method with Prosper (Petroleum Experts 2010).....	66
5.2	Effect of Tuning Correlations to Test Data.....	67
5.3	Studying Manual Tuning in Prosper .....	73
5.4	Conclusions.....	76
<b>6</b>	<b>Effect of Using Tuned Correlations in Simulations.....</b>	<b>77</b>
6.1	Simulation with ProdPot.....	78
6.2	Simulations with Tuned Correlations .....	79
6.2.1	<i>Low GLR Development</i> .....	79
6.2.2	<i>High GLR Development</i> .....	84
6.3	Sensitivity Analysis .....	87
6.4	Conclusions.....	91
<b>7</b>	<b>Main Conclusions and Recommendations.....</b>	<b>92</b>
7.1	Recommendations.....	93
<b>8</b>	<b>Sources of Error .....</b>	<b>94</b>
<b>9</b>	<b>References.....</b>	<b>95</b>
<b>Appendix A</b>	<b>Description of Wells.....</b>	<b>98</b>
<b>Appendix B</b>	<b>Figures.....</b>	<b>105</b>



# 1 Introduction and Objectives

Calculation of pressure drop in oil and gas wells will be important for cost effective design and of well completions and production optimization (Persad 2005). Flow up the tubing will usually be multiphase. Gas and liquid tend to separate and will normally not travel with the same velocities. Both temperature and pressure conditions will change in upwards multiphase flow. Calculation of pressure drop will thereby not be straight forward (Time 2009). Nevertheless, accurate prediction of pressure drop in oil and gas wells is needed to forecast well deliverability and to optimize depletion (Reinicke et al. 1987).

Many multiphase flow correlations are proposed. Still, none of them are proven to give good results for all conditions that may occur when producing hydrocarbons (Pucknell et al. 1993). Analyze of available correlations are often the best way to determine which one to use (Brill and Mukherjee 1999). Some will be good for liquid wells, whereas others for gas. Most of the correlations available are to some degree empirical and will thereby be limited to conditions of which the correlations are based on (Pucknell et al. 1993).

The Statfjord Field has entered a drainage strategy where the reservoir will be depleted such that gas liberates from the remaining oil in the reservoirs. There are two reservoirs, the Statfjord Formation and the Brent Group, exposed to this strategy. Most of the future gas reserves are predicted to come from the Brent Group. Pressure-depletion rate is one of the important factors influencing the gas reserves. Adequate modeling of vertical lift performance (VLP) is needed to predict a realistic liquid offtake and thereby pressure-depletion rate.

Main objective of this thesis is to give a recommendation of which correlation(s) to be used when generating VLP curves for the Statfjord full field model. Furthermore, modifications of correlations and how this may affect simulation result are studied to give a recommendation of how correlations should be used when generating lift curves. The correlation(s) recommended should give good result over the range of

production conditions expected regarding drainage strategy, and modifications should not introduce errors that may increase with time.

Production tests from selective wells located in the Statfjord Formation have been used as basis when investigating the different correlations. Calculations are performed using Prosper, a well performance, design and optimization program developed by Petroleum Experts (2010). Wells in the Statfjord Formation have been producing from a gas cap which in some areas of the formation has disappeared. These wells have therefore been producing with various gas-liquid ratios (GLR), one of the main parameters influencing lift. Wells in the Brent Group have currently low GLR, but with depressurization GLR will increase. The correlation's accuracy when predicting bottomhole pressures with varying GLR is studied. Furthermore, modifications of correlations and the effect on simulation results are studied.

## 2 Theory

### 2.1 Single-Phase Flow

Single-phase flow is unexpected in a producing well. Even if only one phase is produced from the reservoir, pressure depletion across the pipeline may generate multiphase flow (Time 2009). Before heading into multiphase flow, a general understanding of single-phase flow is useful. Calculations for single-phase flow act as basis for multiphase flow (Brill and Mukherjee 1999). In this section, the steady-state pressure-gradient equation for single phase flow will be described. The different terms will be discussed, and a brief description of laminar and turbulent flow is given.

#### 2.1.1 Pressure-Gradient Equation

The steady-state pressure-gradient equation is found by combining equations for conservation of mass,

$$\frac{dp}{dt} + \frac{\partial(\rho v)}{\partial L} = 0, \dots\dots\dots(2.1)$$

and linear momentum,

$$\frac{\partial}{\partial t}(\rho v) + \frac{\partial}{\partial L}(\rho v^2) = -\frac{\partial p}{\partial L} - \tau \frac{\pi d}{A} - \rho g \cos \theta, \dots\dots\dots(2.2)$$

where  $p$  is pressure,  $t$  is time,  $\rho$  density,  $v$  velocity,  $L$  length,  $\tau$  shear stress,  $d$  pipe diameter,  $A$  pipe cross-sectional area,  $g$  gravity and  $\theta$  inclination angle from vertical. By assuming steady-state flow the pressure-gradient equation may be expressed as,

$$\frac{dp}{dL} = -\tau \frac{\pi d}{A} - \rho g \cos \theta - \rho v \frac{dv}{dL} . \dots\dots\dots(2.3)$$

As seen from Eq. 2.3, the total pressure gradient in a pipeline may be expressed as the sum of three components,

$$\left(\frac{dp}{dL}\right)_t = \left(\frac{dp}{dL}\right)_f + \left(\frac{dp}{dL}\right)_h + \left(\frac{dp}{dL}\right)_a, \dots\dots\dots(2.4)$$

where  $(dp/dL)_t$  is total pressure gradient,  $(dp/dL)_f$  frictional pressure gradient,  $(dp/dL)_h$  hydrostatic pressure gradient and  $(dp/dL)_a$  acceleration pressure gradient (Brill and Mukherjee 1999).

When calculating frictional pressure drop in single-phase flow, it is important to discriminate between laminar and turbulent flow. The type of flow is determined from Reynolds number

$$N_{Re} = \frac{\rho v d}{\mu}, \dots\dots\dots(2.5)$$

where  $N_{Re}$  is Reynolds number and  $\mu$  is viscosity.

One may discriminate between flow regimes the following way:

- $N_{Re} \leq 2000$ : Laminar flow
- $2000 < N_{Re} \leq 4000$ : Transition between laminar and turbulent flow
- $N_{Re} > 4000$ : Turbulent flow

In single-phase laminar flow, at constant flow velocity and pipe diameter, the frictional pressure drop is given by:

$$\left(\frac{dp}{dL}\right)_f = \frac{4}{d} \frac{16}{N_{Re}} \frac{1}{2} \rho v^2, \dots\dots\dots(2.6)$$

if the Fanning friction factor is used. The Moody type friction factor may also be used for laminar flow. Then the number 4 in equation 2.6 is included in the friction factor term,

$$\left(\frac{dp}{dL}\right)_f = \frac{1}{d} \frac{64}{N_{Re}} \frac{1}{2} \rho v^2 \dots\dots\dots(2.7)$$

The result will be exactly the same whether Fanning friction factor

$$f_F \equiv \frac{16}{N_{Re}}, \dots\dots\dots(2.8)$$

or Moody friction factor

$$f_M \equiv \frac{64}{N_{Re}}, \dots\dots\dots(2.9)$$

is used.

For laminar flow, the friction factor may be determined exactly from the theory, due to the well defined parabolic velocity profile. In turbulent flow, the velocity profile becomes more uniform, although fluctuating. Larger velocity fall-off towards the pipe wall results in a larger shear rate. Thereby various equations exist for calculating turbulent friction factors (Time 2009). For smooth pipes, and high Reynolds number one may use the following equation to determine the friction factor:

$$f = CN_{Re}^n, \dots\dots\dots(2.10)$$

where  $C$  and  $n$  are correction factors. The correction factors are found experimentally. When  $C = 0.316$  and  $n = -0.25$ , Time (2009) refers to equation 2.10 as the Blasius form.

The pipe wall is normally not smooth, and one must account for the wall roughness. In turbulent flow the friction factor has been found to depend on relative roughness and the Reynolds number. Brill and Mukherjee (1999) write that Nikuradse rough pipe friction factor correlation,

$$\frac{1}{\sqrt{f}} = 1.74 - 2 \log\left(\frac{2\varepsilon}{d}\right), \dots\dots\dots(2.11)$$

is based on the relative roughness ( $\varepsilon/d$ ).

If the friction factor varies both with Reynolds number and relative roughness, the region is defined as transition or partially rough wall. Colebrook friction factor,

$$\frac{1}{\sqrt{f}} = 1.74 - 2 \log\left(\frac{2\varepsilon}{d} + \frac{18.7}{N_{Re} \sqrt{f}}\right), \dots\dots\dots(2.12)$$

is made to describe the variation of friction factor in the transition region (Brill and Mukherjee 1999). For fully developed turbulent flow (rough pipe flow) with large Reynolds number, Eq. 2.12 degenerates to Eq. 2.11.

A Moody diagram is often used to find friction factors. For a given Reynolds number and relative roughness one may read a friction factor. The Moody diagram in figure 2.1, shows the variations of friction factors based on Eq. 2.12 and the friction factor in laminar flow (Brill and Mukherjee 1999; Time 2009).

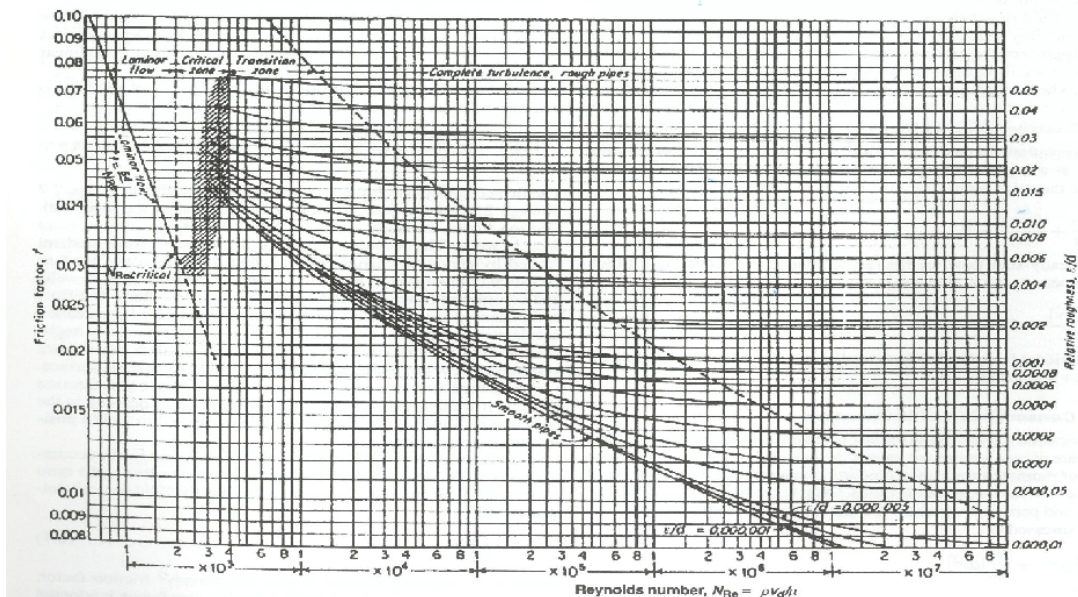


**Figure 2.1: Moody Diagram (Brill and Mukherjee 1999)**

The gravity term is given by the fluid density and the pipe inclination relative to the vertical direction ( $\theta$ ):

$$\left(\frac{dp}{dL}\right)_h = \rho g \cos \theta . \dots\dots\dots(2.13)$$

Contribution from the acceleration term is normally insignificant. Acceleration may give a relatively small contribution if the velocity of the producing fluid changes rapidly (e.g. in a gas well operating at low wellhead pressure) (Time 2009). Rapid change in velocity may cause a pressure change, and contribute to the total pressure gradient. The acceleration pressure gradient (one dimensional) is given as (Brill and Mukherjee 1999):

$$\left(\frac{dp}{dL}\right)_a = -\rho v \frac{dv}{dL} . \dots\dots\dots(2.14)$$

## 2.2 Multiphase Flow

Multiphase-flow behavior is much more complex than single-phase flow. If gas and liquid flows simultaneously, they tend to separate because of differences in fluid properties. The fluids will give different shear stress due to differences in density and viscosity. Gas and liquid will normally not travel with the same velocity. In vertical flow the gas phase tends to have a higher velocity compared to the liquid phase. This occurs because gas is more compressible, less dense and less viscous than liquid (Brill and Mukherjee 1999). There will be several forces acting on the fluids, buoyancy, turbulence, inertia and surface tension. The relative magnitude of these forces may change along the pipe, resulting in different flow regimes (Brennen 2005).

To deal with the complex nature of multiphase flow, many flow parameters and various “mixing rules” are defined. These make it possible to use the same basic pressure gradient equation as for single phase flow, modified for multiphase flow. The basic definitions of flow parameters, flow patterns and general equations for mixing are presented in this section.

### 2.2.1 Holdup

The proportion of the pipe cross-section or volume that is occupied by the liquid phase is defined as the liquid holdup ( $H_L$ ) (Brill and Mukherjee 1999).

Experimentally it is found by averaging liquid or gas volume versus total amount of fluid, see equations 2.16 - 2.18, ( $a = \text{gas or liquid}$ ). If gas is used, the liquid holdup is found as,

$$H_L = (1 - H_G), \dots\dots\dots(2.15)$$

because the sum of fraction gas and liquid should be one.

Generally it is discriminated between line-average

$$H_a = \frac{L_a}{L}, \dots\dots\dots(2.16)$$

area-average



$$H_a = \frac{A_a}{A}, \dots\dots\dots(2.17)$$

and volume-average

$$H_a = \frac{V_a}{V}, \dots\dots\dots(2.18)$$

given the averaging-measurement method used. If the mixture was completely homogeneous, the three methods should give the same fluid fractions (Time 2009).

It may be difficult to measure the fluid fractions, e.g., in a subsea pipeline. Estimation of the liquid holdup then becomes crucial. If the volumetric flow rates ( $q_L, q_G$ ) are known, the no-slip fractions (flux fraction) may be calculated. No-slip liquid fraction ( $\lambda_L$ ) is given by,

$$\lambda_L = \frac{q_L}{q_L + q_G}, \dots\dots\dots(2.19)$$

and no-slip gas fraction ( $\lambda_G$ ) as,

$$\lambda_G = \frac{q_G}{q_G + q_L}. \dots\dots\dots(2.20)$$

If the phase velocities are different, slip is present. Gas has higher mobility compared to liquid, giving gas a higher velocity. The ratio between the real phase velocities defines the slip ratio,

$$S = \frac{v_G}{v_L}. \dots\dots\dots(2.21)$$

Slippage of gas past liquid results in larger liquid holdup, compared to the situation of no-slip. If slip is present, the fluid fractions cannot be calculated using Eq. 2.19 and 2.20. If the slip ratio is known, the true fluid fractions may be determined using

$$H_L = \frac{A_L}{A} = \frac{A_L}{A_L + A_G} = \frac{q_L}{q_L + \frac{1}{S}q_G}, \dots\dots\dots(2.22)$$

for liquid and

$$H_G = \frac{A_G}{A} = \frac{A_G}{A_G + A_L} = \frac{q_G}{q_G + Sq_L}, \dots\dots\dots(2.23)$$

for gas. From Eq. 2.22 and 2.23,  $H_L = \lambda_L$  and  $H_G = \lambda_G$  if  $S = 1$  (Time 2009). How liquid holdup is estimated in multiphase-flow correlations varies amongst the authors. This will be described in greater detail in section 2.4.

### 2.2.2 Velocities

Superficial velocity is defined as the velocity of a phase if it was occupying the entire pipe area. Superficial velocity ( $v_s$ ) for liquid is given by:

$$v_{SL} = \frac{q_L}{A}, \dots\dots\dots(2.24)$$

and for gas

$$v_{SG} = \frac{q_G}{A} \dots\dots\dots(2.25)$$

The real average velocity in a pipe, defined as the total mixture velocity ( $v_m$ ), may be found as the sum of superficial velocities,

$$v_m = \frac{q_L + q_G}{A} = v_{SL} + v_{SG} \dots\dots\dots(2.26)$$

Real phase velocities may be defined locally or as time- and space-averaged velocities. If holdup is known, one may determine the real flowing cross sections for liquid and gas, and thus the real phase velocities by:

$$v_L = \frac{q_L}{A_L}, \dots\dots\dots(2.27)$$

and

$$v_G = \frac{q_G}{A_G} . \dots\dots\dots(2.28)$$

The difference between the real gas velocity and the real liquid velocity is defined as the slip velocity ( $v_s$ ) (Time 2009),

$$v_s = v_G - v_L . \dots\dots\dots(2.29)$$

### 2.2.3 Mixture-Fluid Properties

Multiphase-flow correlations in general consider only two phases, liquid and gas. Water and oil may be combined and treated as one equivalent fluid and referred to as the liquid phase (Petroleum Experts 2010). In this thesis mixing rules for oil and water will not be included, but there exist various ways to combine water and oil to one fluid.

Many equations to calculate fluid properties for a mixture of gas and liquid have been proposed. If the equations consider slip or no-slip fractions is the main difference between them. Mixture density with slip ( $\rho_m$ ) can be found by,

$$\rho_m = \rho_L H_L + \rho_G (1 - H_L) . \dots\dots\dots(2.30)$$

Mixture density with no-slip ( $\rho_{mn}$ ) is found by replacing  $H_L$  with  $\lambda_L$  (Brill and Mukherjee 1999):

$$\rho_{mn} = \rho_L \lambda_L + \rho_G (1 - \lambda_L) . \dots\dots\dots(2.31)$$

Several models to determine mixture viscosity exist. These arise because mixture viscosity is strongly dependant on dynamical processes, including bubble size, flow regime etc (Time 2009). The most common equations are listed below:

- $\mu_m = \mu_L H_L + \mu_G (1 - H_L) \dots\dots\dots(2.32)$

- $\mu_m = \mu_L^{H_L} \mu_G^{(1-H_L)} \dots\dots\dots(2.33)$

- $\mu_{mn} = \mu_L \lambda_L + \mu_G (1 - \lambda_L) \dots\dots\dots(2.34)$

#### 2.2.4 Pressure-Gradient Equation

Pressure-drop calculation for two-phase flow is quite similar that of single-phase flow. The main difference is the use of mixed fluid properties for two-phase flow. The total pressure-gradient equation takes the same form as for single-phase flow, Eq. 2.4. Each term is modified for two phases, and is described in the following section.

Frictional pressure drop may be expressed as (Brill and Mukherjee 1999):

$$\left(\frac{dp}{dL}\right)_f = \frac{4}{D} f \frac{1}{2} \rho_m v_m^2 \dots\dots\dots(2.35)$$

Various two-phase friction factors, and properties used when calculating the Reynolds number varies amongst authors. This will be described for different correlations in section 2.4.

Pressure drop caused by the hydrostatic term is normally the larges contribution to the total pressure drop, for wells producing liquid. For conditions of high gas velocities, the frictional pressure drop may exceed the contribution from the hydrostatic term.

Pressure drop caused by the hydrostatic term is found by:

$$\left(\frac{dp}{dL}\right)_h = \rho_m g \cos \theta \dots\dots\dots(2.36)$$

The mixture density is usually calculated using Eq. 2.30 (Brill and Mukherjee 1999). How the liquid holdup is correlated thus becomes crucial for the hydrostatic pressure drop.

As mentioned for single-phase flow, the acceleration pressure drop is normally negligible. It is considered mainly for cases of high fluctuating flow velocities. For two-phase flow the pressure-drop component caused by acceleration can be found from (Brill and Mukherjee 1999):

$$\left(\frac{dp}{dL}\right)_a = -\rho_m v_m \frac{dv_m}{dL} \dots\dots\dots(2.37)$$

### 2.2.5 Flow Regimes

Single-phase flow is divided into laminar and turbulent flow regimes. In multiphase flow the discrimination becomes more complex. Gas and liquid distribution may vary when flowing in a long pipe, resulting in different flow regimes (Time 2009). A brief description of the flow regimes that may occur in vertical flow will be given in this section.

In general one may discriminate between four flow regimes for vertical upward multiphase flow: bubble flow, slug flow, churn flow and annular flow, see figure 2.2. The flow regimes change in this order by increasing gas rate for a given liquid rate (Zavareh et al. 1988). The most important flow patterns for multiphase flow in wells are slug and churn flow patterns. They are often referred to as intermittent flow regimes (Brill 1987). Mist flow and annular-mist flow are other names for the annular flow regime (Brill and Mukherjee 1999).

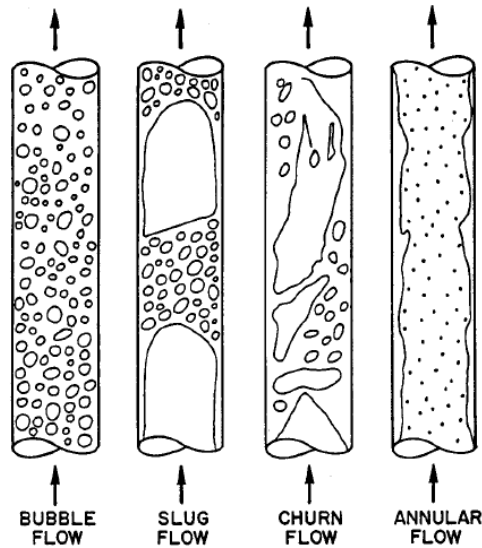


**Figure 2.2:** *Flow patterns for upward vertical flow (Brill 1987)*

In bubble flow, liquid is the continuous phase and the free-gas phase is presented as small bubbles. The gas-bubbles are randomly distributed in the liquid flow, and the diameter may vary. Due to different sizes of the gas-bubbles, they travel with different velocities. The liquid phase however moves with a more uniform velocity. The gas phase, except for its density, has little effect on the pressure drop (Orkiszewski 1967).

Slug flow is characterized by alternating slugs of liquid with large bubbles of gas. Large gas-bubbles are made as the smaller gas-bubbles coalesce, when gas velocity increases. The larger bubbles are called Taylor bubbles. Smaller bubbles of gas are contained in the liquid slugs. Liquid is still the continuous phase, because of a liquid film covering the Taylor bubbles (Zavareh et al. 1988).

As the gas velocity is increased further, the large gas-bubbles become unstable and may collapse. When this happens, churn flow occur. Churn flow is a highly turbulent and chaotic regime. Neither gas nor liquid phase appears to be continuous. Oscillatory, up and down motion of liquid, is characteristic for churn flow (Zavareh et al. 1988).

In annular flow, gas is the continuous phase. Gas flows with a high rate in the centre of the pipe. Liquid is found as a liquid film coating the pipe wall and as entrained droplets in the gas phase. The gas phase becomes the controlling phase (Orkiszewski 1967).

Determination of flow regime will be important for parameters such as holdup and thereby pressure-drop predictions. Result of study on flow regimes are often displayed in the form of a flow regime map (Brennen 2005). Flow maps are generated to relate flow patterns to flow rates and fluid properties. Boundaries in a flow regime map represents where a regime becomes unstable. A growth of the instability will lead to transition to another regime. These transitions can be rather unpredictable because they may depend on otherwise minor features of the flow, as the wall roughness or entrance conditions. Hence, the flow-pattern boundaries are not distinctive lines, but more poorly defined transition zones. Many different flow regime maps have been published, based on different correlations for flow-regime prediction. Most of them are dimensionless and applies only for the specific pipe size and fluids used when they were created (Brennen 2005; Zavareh et al. 1988).

### 2.3 Calculation of Pressure-drop in Long Pipelines

The pressure will drop when fluids flow from inlet to outlet in a long pipeline. The gas density, and thereby the gas velocity will change according to the pressure changes. As the pressure drop, more and more gas may evaporate from the oil phase into the gas phase. This will in turn increase the gas flow velocity, which again will lead to higher pressure drop and even higher evaporation. By this, the pressure at inlet and outlet determines the total flow velocity. At least one more factors complicate the calculations, namely temperature. A temperature profile along the pipeline and the heat conduction from the surroundings are needed to determine the pressure traverse (Time 2009).

The total pressure drop over a pipeline may be calculated by integrating the pressure gradient over the total length,

$$\Delta p = \int_0^L \left( \frac{dp}{dL} \right) dL \dots\dots\dots(2.38)$$

The challenge lies in the fact that the pressure gradient is dependent on pressure, temperature and inclination angle, and will vary throughout the pipe length. Properties like flow pattern, densities, rates etc. will be affected. A general approach is to divide the pipeline into segments, and calculate pressure stepwise along the pipe. The segments should be small enough so that the pressure gradient can be considered constant within the segment.

If the flow rates of oil and gas and the inlet pressure are known, it is possible to calculate the pressure at the outlet. Calculations may also be carried out the other way around. Pressure is calculated stepwise, and the flow rates are updated for each segment along the pipe. The pressure gradient is calculated for each segment and multiplied by the length of the segment,

$$\Delta p \approx \sum_{i=1}^n \left( \frac{dp}{dL} \right)_i \Delta L_i \dots\dots\dots(2.39)$$



The outlet pressure for segment  $i$  will be the inlet pressure for segment  $i+1$ . Pressure obtained at the end of the last segment will be the outlet pressure. The total pressure drop will be the sum of pressure drops calculated for each segment (Time 2009; Brill and Mukherjee 1999).

## 2.4 Pressure-Drop Correlations

A large range of different pressure-drop correlations are published. In addition many methods and correlations developed are kept confidential. As stated in by Time (2009); “There is no guarantee that the correlations kept confidential are better than other correlations. On the contrary, keeping methods secret is a way to avoid scientific testing, and the methods may have low validity.”

One may divide the pressure gradient calculations into two categories:

- 1) *Empirical correlations*, based on experimental data and dimensional analysis.
- 2) *Mechanistic models*, based on simplified mechanistic (physical) considerations like conservation of mass and energy.

It can be quite difficult to discriminate between empirical and mechanistic correlations. Often a combination is used to develop multiphase correlations (Yahaya and Gahtani 2010).

The empirical correlations are generated by establishing mathematical relations based on experimental data. Dimensional analysis is often used to select correlating variables. It is important to notice that application of empirical correlations is limited to the range of data used when it was developed (Ellul et al. 2004; Yahaya and Gahtani 2010). Further it is possible to divide the empirical correlations in groups regarding if slip and flow patterns are considered, see table 2.1.

The mechanistic models are based on a phenomenological approach and they take into account basic principles, like conservation of mass and energy (Yahaya and Gahtani 2010). In mechanistic models, flow regime determination is important. “Normally” a mechanistic transport equation is written for each of the phases in the multiphase flow. Separate models for predicting pressure drop, liquid holdup and temperature profile have been developed by flow regime determination and separating the phases (Ellul et al. 2004).

<b>Correlation</b>	<b>Category</b>	<b>Slip considered?</b>	<b>Flow regime considered?</b>
Fancher & Brown	Empirical	No	No
Gray	Empirical	Yes	No
Hagedorn & Brown	Empirical	Yes	No
Duns & Ros	Empirical	Yes	Yes
Orkiszewski	Empirical	Yes	Yes
Beggs & Brill	Empirical	Yes	Yes
Mukherjee & Brill	Empirical	Yes	Yes
Petroleum Experts (1,2,3)	Empirical	Yes	Yes
Petroleum Experts (4,5)	Mechanistic	Yes	Yes
Hydro 3-Phase	Mechanistic	Yes	Yes
OLGAS	Mechanistic	Yes	Yes

Most correlations defined as empirical in table 2.1 will be described regarding theory. In the experimental work, a few mechanistic models are used. These are the once listed in table 2.1, and will not be described here.

Similar equations for pressure drop are proposed for the empirical correlations. The main difference between the correlations is how liquid holdup, mixture density and friction factors are estimated. Descriptions of the various estimations for the respective correlations are found in the following sections.

#### *2.4.1 Fancher and Brown Correlation (Fancher and Brown 1963)*

Fancher and Brown proposed a correlation based on Poettmann and Carpenter's (1952) work. As table 2.1 describes, this is a no-slip correlation and the same correlation is used regardless of flow regime. An 8000 ft long experimental field well with 2 3/8 inch OD tubing was used for testing. Flow rates ranged from 75 – 936 B/D at various GLR from 105 to 9433 scf/bbl. Results from these tests were compared with Poettmann and Carpenter's (1952) correlation. Deviations occurred for low flow rates and for high GLR (outside the range of what Poettmann and Carpenter's correlation was designed for). The deviation was believed to originate from the

friction factor correlation. By adopting the pressure gradient equation from Poettmann and Carpenter (1952), a new correlation for friction factor was proposed. The pressure gradient equation may be expressed as,

$$\frac{dp}{dZ} = \frac{f\rho_{mn}v_m^2}{2d} + \rho_{mn}g, \dots\dots\dots(2.40)$$

for vertical flow of a homogeneous no-slip mixture (Brill and Mukherjee 1999).

Fancher and Brown found that GLR is a significant parameter in the friction factor correlation. Thereby three separate friction factor correlations were developed, divided by GLR ranges of 0-1.5 Mscf/7bbl, 1.5-3.0 Mscf/bbl and greater than 3.0 Mscf/bbl, see figures 2.3 to 2.5.

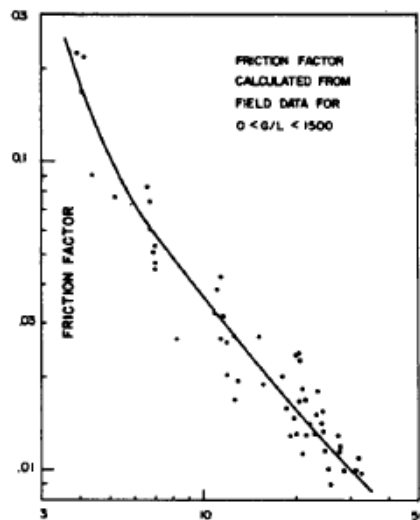


**Figure 2.3:** Friction factor correlation (Fancher and Brown 1963)

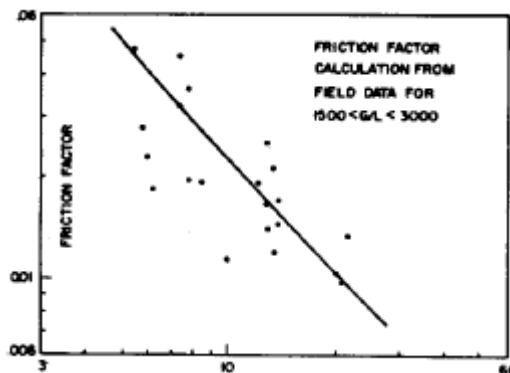


**Figure 2.4:** Friction factor correlation (Fancher and Brown 1963)

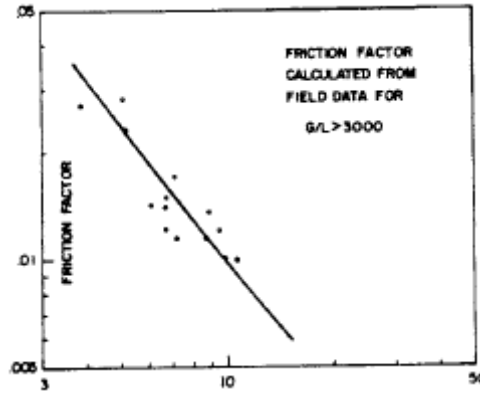


**Figure 2.5:** Friction factor correlation (Fancher and Brown 1963)

#### 2.4.2 Gray Correlation (Gray 1974)

Gray developed an empirical correlation for a vertical well producing gas and gas-condensate or water. Slip is considered, but it does not distinguish between different flow patterns, see table 2.1. The correlation is based on a total of 108 well test data, and Gray cautioned use of the correlation beyond the following limits:

- velocities higher than 50 ft/sec
- nominal diameters larger than 3.5 in
- condensate or liquid loadings above 50 bbl/MMscf
- water or liquid loadings above 5 bbl/MMscf

Pressure gradient for two-phase flow is given by:

$$\frac{dp}{dZ} = \frac{f\rho_{mn}v_m^2}{2d} + \rho_m g - \rho_{mn}^2 v_m^2 \frac{d}{dZ} \left( \frac{1}{\rho_{mn}} \right) \dots\dots\dots(2.41)$$

With basis in dimensional analysis, Gray’s correlation uses three dimensionless parameters to predict liquid holdup, namely velocity number

$$N_v = \frac{\rho_{mn}^2 v_m^4}{g\sigma_L(\rho_L - \rho_G)} \dots\dots\dots(2.42)$$

where  $\sigma_L$  is surface tension. Dimensionless diameter number

$$N_D = \frac{g(\rho_L - \rho_G)d^2}{\sigma_L}, \dots\dots\dots(2.43)$$

and superficial liquid-gas ratio

$$R = \frac{v_{SL}}{v_{SG}} \dots\dots\dots(2.44)$$

Gray proposed the following equation for predicting liquid holdup,

$$H_L = 1 - \frac{1 - \text{Exp}\left\{-2.314\left[N_v\left(1 + \frac{205.0}{N_D}\right)\right]^B\right\}}{R + 1}, \dots\dots\dots(2.45)$$

where

$$B = 0.0814\left[1 - 0.0554\ln\left(1 + \frac{730R}{R + 1}\right)\right] \dots\dots\dots(2.46)$$

The three dimensionless parameters defined above are intersected into equation 2.45 to estimate liquid holdup. When liquid holdup is determined, mixture density may be calculated using equation 2.30.

If both condensate and water are present, Gray suggested that surface tension should be calculated as

$$\sigma_L = \frac{f_o\sigma_o + 0.617f_w\sigma_w}{f_o + 0.617f_w}, \dots\dots\dots(2.47)$$

where  $f_{o,w}$  is no-slip volume fraction for condensate and water.

The friction loss model is a modified Darcy-Weisbach expression, and the flow is assumed to be turbulent. By this the energy loss is considered wholly dependent on a

pseudo wall roughness factor ( $\epsilon$ ). A Colebrook-White function together with pseudo wall roughness factor is used to obtain a two-phase friction factor. The pseudo wall roughness factor is correlated using a roughness variable defined by a modified Weber number. If  $R \geq 0.007$ , pseudo wall roughness is given by

$$\epsilon = \epsilon' = 28.5 \frac{\sigma_L}{\rho_{mn} v_m^2}, \dots\dots\dots(2.48)$$

where  $\epsilon'$  is a roughness variable. If  $R < 0.007$ , one should use

$$\epsilon = \epsilon_G + R \frac{(\epsilon' - \epsilon_G)}{0.007}, \dots\dots\dots(2.49)$$

when calculating pseudo wall roughness. The two-phase friction factor may then be read of a Moody diagram, see figure 2.1. By definition  $\epsilon$  must be larger or equal to  $2.77 \times 10^{-5}$ .

In Prosper a modified version of the Gray correlation is used. It was modified by Shell, but no paper documenting the modifications was found.

#### 2.4.3 Hagedorn and Brown Correlation (Hagedorn and Brown 1965)

The Hagedorn and Brown correlation is in the same category as the Gray correlation, see table 2.1. To develop the correlation an experimental vertical well of 1500 ft was used. The pressure gradient occurring during continuous two phase flow was studied in tubing with 1 in., 1 ¼ in. and 1 ½ in. nominal diameter. Air was used as the gas-phase. The liquid phase was varied. Water and crude oils with viscosities approximately 10, 30 and 110 cp were used. Liquid flow rates and GLR were also varied between the tests.

During development of the correlation, Hagedorn and Brown did not measure the liquid holdup. They developed a pressure-gradient equation, and by assuming a friction factor correlation they could calculate pseudo liquid holdup values to match

measured pressure gradients. The correlation for liquid holdup is therefore not based on true measurements of liquid holdup.

The pressure-gradient equation developed has the form:

$$\frac{dp}{dZ} = \frac{f\rho_m^2 v_m^2}{2\rho_m d} + \rho_m g + \frac{\rho_m \Delta(v_m^2)}{2dZ} \dots\dots\dots(2.50)$$

The holdup correlation is shown in figure 2.6. In order to determine holdup, a secondary correction factor ( $\psi$ ), and a corrected liquid-viscosity number ( $CN_L$ ) must be determined. These factors are found from figures 2.7 and 2.8 by using dimensionless groups proposed by Duns and Ros (1963). The dimensionless groups are liquid velocity number

$$N_{LV} = v_{SL} \sqrt[4]{\frac{\rho_L}{g\sigma}} \dots\dots\dots(2.51)$$

gas velocity number

$$N_{GV} = v_{SG} \sqrt[4]{\frac{\rho_L}{g\sigma}} \dots\dots\dots(2.52)$$

pipe diameter number

$$N_D = d \sqrt{\frac{\rho_L g}{\sigma}} \dots\dots\dots(2.53)$$

and liquid viscosity number

$$N_L = \mu_L \sqrt[4]{\frac{g}{\rho_L \sigma^3}} \dots\dots\dots(2.54)$$

When holdup is determined, the mixture density may be calculated using Eq. 2.30.



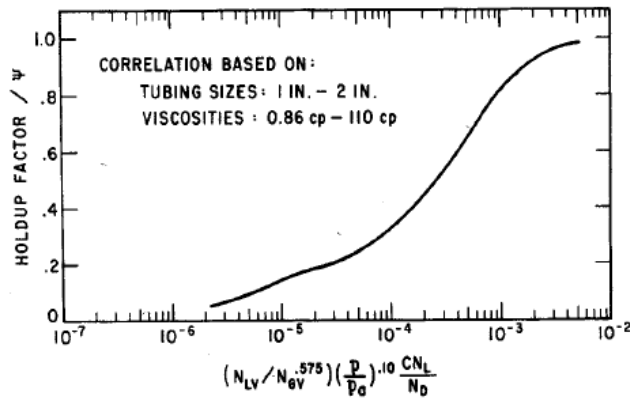


**Figure 2.6:** Holdup-factor correlation (Hagedorn and Brown 1965)

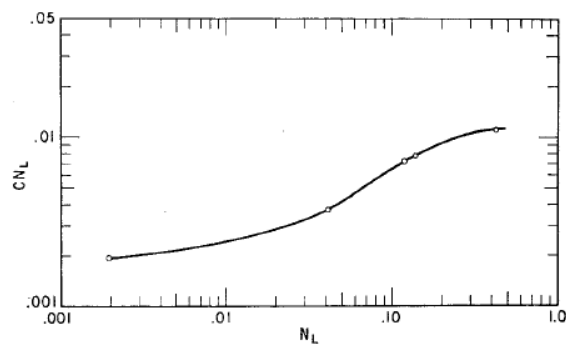


**Figure 2.7:** Correlation for liquid viscosity number (Hagedorn and Brown 1965)

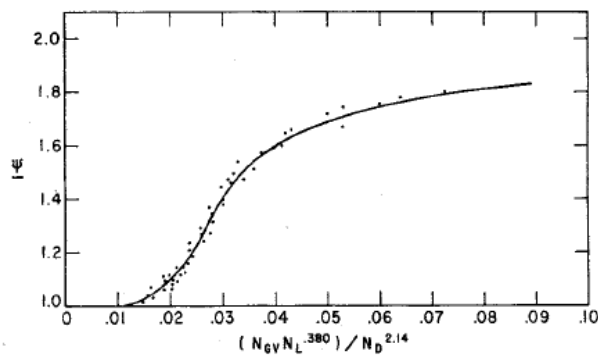


**Figure 2.8:** Correlation for secondary correction factor (Hagedorn and Brown 1965)

Darcy-Weisbach equation for single phase flow, relative roughness of the pipe and the two-phase Reynolds number are used to determine the two-phase friction factor from a Moody diagram, see figure 2.1. When calculating the Reynolds number, an assumption stating that the mixture of gas and liquid can be treated as a homogenous mixture over a finite interval is used. The Reynolds number for the two phase mixture may then be written as

$$(N_{Re})_{TP} = \frac{v_m \rho_{mm} d}{\mu_m}, \dots\dots\dots(2.55)$$

where  $\mu_m$  is defined by equation 2.33.

Modification has been proposed to the Hagedorn and Brown correlation. The refinements suggested by Brill and Hagedorn have been implemented in Prosper (Petroleum Experts 2010):

- Griffith correlation for bubble flow
- Limit on liquid holdup to always be greater than the no-slip holdup

Some additional refinements have been added to the basic Hagedorn and Brown correlation in Prosper (Petroleum Experts 2010):

- Beggs and Brill deviation correction for liquid holdup
- Explicit calculation of acceleration term

#### 2.4.4 Duns and Ros Correlation (Duns and Ros 1963)

The Duns and Ros method is an empirical correlation based on approximately 4000 two-phase flow experiments. Liquid holdup and pressure gradients were measured. The experiments were conducted as vertical flow, with pipe diameters ranging from 1.26 to 5.60 inches. Flow patterns were observed in a transparent section of the test tubing. In the Duns and Ros correlation it is discriminated between three main flow regimes. Liquid holdup and friction factor correlations were developed for each flow regime.

Duns and Ros correlation discriminates between three different flow regimes. These are shown in figure 2.9, described as regions. In region I, liquid is the continuous phase. Where gas and liquid phase's alternate is referred to as region II and in region III gas is the continuous phase. A transition regime is treated as a fourth regime in calculations. For flow in the transition regions linear interpolation may be used to approximate the pressure gradient.

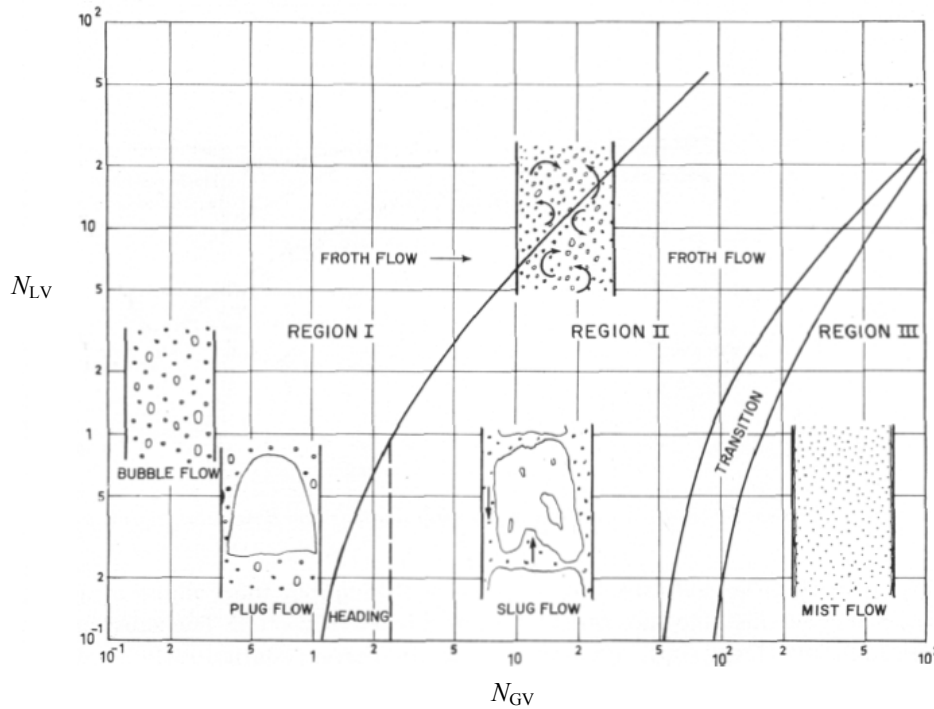


**Figure 2.9:** Flow regime map (Duns and Ros 1963)

Both friction factor and liquid holdup were found to depend on gas and liquid velocities, the pipe diameter and the liquid viscosity. These factors together with surface tension and liquid density are converted into four dimensionless groups as described in Eqs. 2.51 to 2.54.

Duns and Ros used a dimensionless slip velocity number,

$$S = v_s \sqrt[4]{\frac{\rho_l}{g\sigma}}, \dots\dots\dots(2.56)$$

to correlate liquid holdup,

$$H_L = \frac{v_s - v_m + \sqrt{(v_m - v_s)^2 + 4v_s v_{SL}}}{2v_s} \dots\dots\dots(2.57)$$

Determination of slip varies between the three regions, one correlation for each region. The correlations are based on liquid and gas velocity numbers and a given number of constants related to viscosity and diameter. For a more detailed description and equations it is referred to the original paper. When slip is determined from a respective correlation, Eq. 2.56 is solved for slip velocity. Furthermore liquid holdup is calculated using Eq. 2.57 and mixture density may be calculated using Eq. 2.30. The hydrostatic pressure gradient may be calculated as described in Eq. 2.36.

In region I and II, the pressure-gradient due to friction is found from

$$\left(\frac{dp}{dZ}\right)_f = \frac{f \rho_L v_{SL} v_m}{2d} \dots\dots\dots(2.58)$$

The friction factor correlation developed by Duns and Ros is based on experimental data. The following equation was proposed,

$$f = f_1 \frac{f_2}{f_3}, \dots\dots\dots(2.59)$$

where  $f_1$  is a function of the Reynolds number for liquid, and may be found from figure 2.10. Besides the transition region between laminar and turbulent flow, figure 2.10 is identical to the Moody diagram for single phase flow. The factors  $f_2$  and  $f_3$  are correction factors for in-situ GLR, and both liquid viscosity and in-situ GLR respectively.

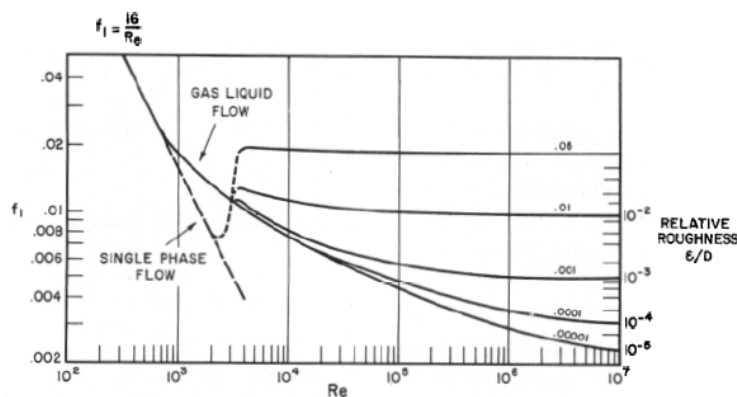


**Figure 2.10:** Non-dimensional  $f_1$  versus Reynolds number (Duns and Ros 1963)

In region III friction is assumed to originate from the drag of gas on the pipe wall. Due to this assumption the friction gradient is based on the gas phase,

$$\left(\frac{dp}{dZ}\right)_f = \frac{f\rho_G v_{SG}^2}{2d} \dots\dots\dots(2.60)$$

No slip gives  $f = f_1$ , and the Reynolds number should be calculated for the gas flow. The friction factor may then be read of figure 2.10.

Duns and Ros found that wall roughness actually is the roughness of the liquid film. Ripples in the liquid film are formed due to drag of gas, thus roughness will not be constant. They suggested a way to account for this effect. It is referred to original paper for details.

In Prosper the following refinements have been made to the basic Duns and Ros method (Petroleum Experts 2010):

- Beggs and Brill deviation correction for holdup
- Gould et al. (1974) flow map
- Explicit calculation of the acceleration term

*2.4.5 Orkiszewski Correlation (Orkiszewski 1967)*

Orkiszewski compared many of the published correlations against test data. He concluded that none of them sufficiently described two phase flow for all the flow regimes. Thereby a combination of the correlations that best described the test data was suggested to be used. Orkiszewski uses Griffith and Wallis method for slug flow, Duns and Ros for transition and mist flow, and he suggested a new method for slug flow.

Determination of flow regime is described in table 2.2. Griffith and Wallis have defined the boundary between bubble and slug, while Duns and Ros have defined the boundaries for the remaining three regimes. The variables are described in equations 2.61 to 2.63.

<b>Table 2.2: Flow-regime boundaries for Orkiszewski correlation</b>	
<b>Flow Regime</b>	<b>Limit</b>
Bubble	$v_{SG}/v_m < L_B$
Slug	$v_{SG}/v_m > L_B, N_{GV} < L_S$
Transition	$L_M > N_{GV} > L_S$
Mist	$N_{GV} > L_M$

Bubble-slug boundary ( $L_B$ ) is defined by

$$L_B = 1.071 - 0.2218 \frac{v_m^2}{d}, \dots\dots\dots(2.61)$$

with the constrain  $L_B \geq 0.13$ .

Slug-transition boundary, ( $L_S$ ) are given as

$$L_S = 50 + 36 N_{VG} \frac{q_L}{q_G}, \dots\dots\dots(2.62)$$

And transition-mist boundary ( $L_M$ ) is

$$L_M = 75 + 84 \left( \frac{v_G q_L}{q_G} \right)^{0.75} \dots\dots\dots(2.63)$$

In bubble flow liquid holdup given is given by:

$$H_L = 1 - \frac{1}{2} \left[ 1 + \frac{v_m}{v_s} - \sqrt{\left( 1 + \frac{v_m}{v_s} \right)^2 - \frac{4v_{SG}}{v_s}} \right] \dots\dots\dots(2.64)$$

According to Orkiszewski, Griffith suggested an average value of the slip velocity to be used as a constant equal to 0.8 ft/sec. The average flow density is found from Eq.

2.30, together with the liquid holdup the hydrostatic pressure-gradient may be calculated as described in equation 2.36.

The friction pressure-gradient is given by

$$\left(\frac{dp}{dZ}\right)_f = \frac{f\rho_L(v_{SL}/H_L)^2}{2d} \dots\dots\dots(2.65)$$

Friction factors are obtained from a Moody diagram using liquid Reynolds number,

$$N_{Re} = \frac{\rho_L(v_{SL}/H_L)d}{\mu_L} \dots\dots\dots(2.66)$$

and relative roughness.

The slip density for slug flow proposed by Orkiszewski is:

$$\rho_m = \frac{\rho_L(v_{SL} + v_b) + \rho_G v_{SG}}{v_m + v_b} + \Gamma\rho_L \dots\dots\dots(2.67)$$

where  $v_b$  is bubble rise velocity and  $\Gamma$  is a liquid distribution coefficient.  $\Gamma$  is correlated from oilfield data by Hagedorn and Brown (1965) as described in table 2.3. Bubble rise velocity is defined as

$$v_b = C_1 C_2 \sqrt{gd} \dots\dots\dots(2.68)$$

Here  $C_1$  and  $C_2$  are expressed as a function of bubble Reynolds number

$$N_{ReB} = \frac{\rho_L v_b d}{\mu_L} \dots\dots\dots(2.69)$$

and liquid Reynolds number,

$$N_{Re} = \frac{\rho_L v_m d}{\mu_L} \dots\dots\dots(2.70)$$

After calculating liquid and bubble Reynolds numbers,  $C_1$  and  $C_2$  may be read off figures 2.11 and 2.12 respectively.

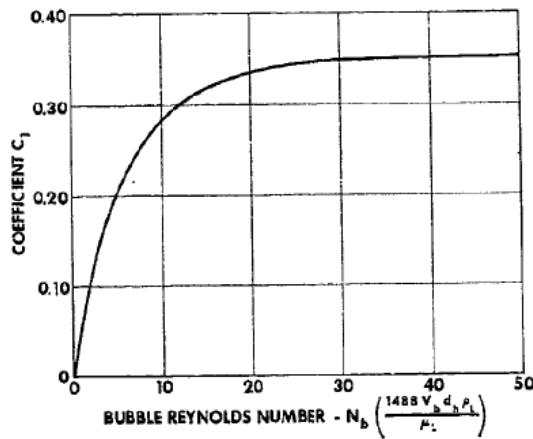


**Figure 2.11:** Griffith and Wallis'  $C_1$  versus Reynolds number (Orkiszewski 1967)

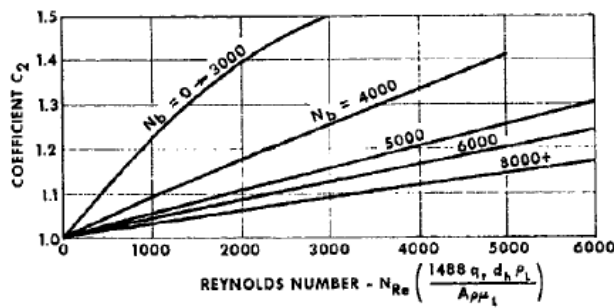


**Figure 2.12:** Griffith and Wallis  $C_2$  versus bubble Reynolds number and Reynolds number (Orkiszewski 1967)

The friction pressure-gradient may be found from

$$\left(\frac{dp}{dZ}\right)_f = \frac{f \rho_L v_m^2}{2d} \left[ \left( \frac{v_{SL} + v_b}{v_m + v_b} \right) + \Gamma \right] \dots\dots\dots(2.71)$$



Friction factor is obtained using a Moody diagram and liquid Reynolds number. The liquid distribution coefficient may be found as described in table 2.3 together with respective equations.

<b>Table 2.3: Liquid distribution coefficient equations</b>		
<b>Continuous liquid phase</b>	$v_m$	<b>Use equation number</b>
Water	<10	2.72
Water	>10	2.73
Oil	<10	2.74
Oil	>10	2.75

$$\Gamma = \left[ \frac{0.013 \log \mu_L}{d^{1.38}} \right] - 0.681 + 0.232 \log v_m - 0.428 \log d \dots\dots\dots(2.72)$$

$$\Gamma = \left[ \frac{0.045 \log \mu_L}{d^{0.799}} \right] - 0.709 - 0.162 \log v_m - 0.888 \log d \dots\dots\dots(2.73)$$

$$\Gamma = \left[ \frac{0.0127 \log(\mu_L + 1)}{d^{1.415}} \right] - 0.284 + 0.167 \log v_m + 0.113 \log d \dots\dots\dots(2.74)$$

$$\Gamma = \left[ \frac{0.0274 \log(\mu_L + 1)}{d^{1.371}} \right] + 0.161 + 0.569 \log d - \log v_m \left\{ \frac{0.01 \log(\mu_L + 1)}{d^{1.571}} + 0.379 + 0.63 \log d \right\} \dots\dots\dots(2.75)$$

The liquid distribution coefficient is constrained by the limit

$$\Gamma \geq -0.065 v_m, \dots\dots\dots(2.76)$$

if  $v_m < 10$  ft/sec, and

$$\Gamma \geq -\frac{v_b}{v_m + v_b} \left( 1 - \frac{\rho_m}{\rho_L} \right), \dots\dots\dots(2.77)$$

when  $v_m > 10$  ft/sec. The constraints are made to eliminate pressure-discontinuities between the flow regimes. Still significant discontinuities may occur (Petroleum Experts 2010).

For transition and mist flow, the correlations developed by Duns and Ros are to be used, see section 2.4.4.

#### 2.4.6 Beggs and Brill Correlation (Beggs and Brill 1973)

Beggs and Brill developed correlations for liquid holdup and friction factor. The correlations are based on experimental data from 90 ft long acrylic pipes. Fluids used were air and water and 584 tests were conducted. Gas rate, liquid rate and average system pressure was varied. Pipes of 1 and 1.5 inch diameter were used. First the pipe was horizontal, and the flow rates were varied in such a way that all horizontal flow patterns were observed, see figure 2.13. Afterwards the pipe inclination was changed, and liquid holdup ( $H_{L(\theta)}$ ) and pressure drop was measured. By this the effect of inclination on holdup and pressure drop could be studied. Beggs and Brill proposed the following pressure-gradient equation,

$$\frac{dp}{dL} = \frac{\frac{f\rho_n v_m^2}{2d} + \rho_m g \sin \theta}{1 - E_k}, \dots\dots\dots(2.78)$$

where  $E_k$ , dimensionless kinetic-energy pressure gradient, is defined by

$$E_k = \frac{v_m v_{SG} \rho_n}{p}, \dots\dots\dots(2.79)$$

and mixture density should be calculated as

$$\rho_m = \rho_L H_{L(\theta)} + \rho_G [1 - H_{L(\theta)}]. \dots\dots\dots(2.80)$$

Liquid holdup and friction factor should be found as described in the following.

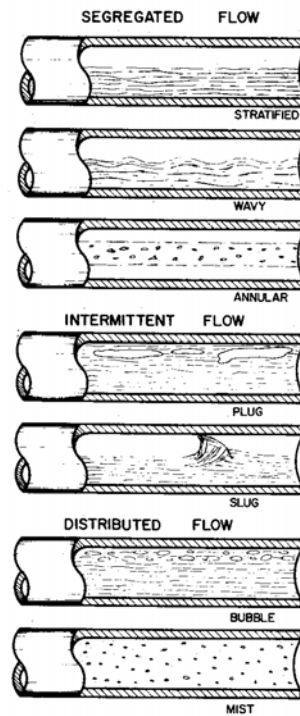


**Figure 2.13:** Horizontal flow patterns (Beggs and Brill 1973)

Beggs and Brill plotted liquid holdup versus angle of pipe from horizontal, see figure 2.14. They found that holdup has a definite dependency on angle. From the figure one can see that the curves have maximum and minimum at +/- 50° from the horizontal. The slippage and liquid holdup increase as the angle of the pipe increase, from horizontal towards vertical (flow upwards). Gravity forces act on the liquid, causing a decrease in the liquid velocity and thereby slippage and holdup is increased. By further increasing of the angle, liquid covers the entire cross section of the pipe. The slippage between the phases is reduced and liquid holdup reduces. Beggs and Brill observed that degree of holdup with angle varied with flow rates. To include effects of pipe inclination, it was decided to normalize liquid holdup. The following equation was proposed,

$$\psi = \frac{H_L(\theta)}{H_L(0)} , \dots\dots\dots(2.81)$$

where  $\psi$  is inclination correction factor,  $H_L(\theta)$  is holdup at angle  $\theta$  from horizontal, and  $H_L(0)$  is horizontal holdup.

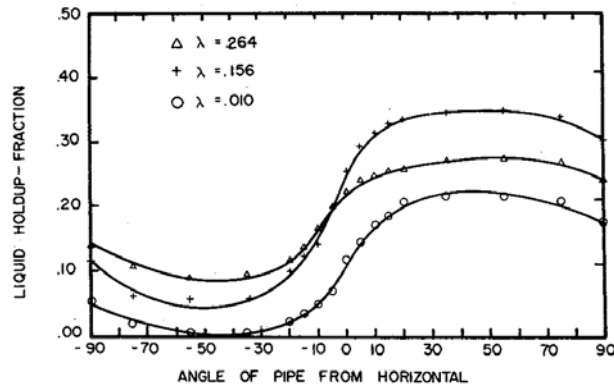


**Figure 2.14:** *Liquid holdup versus angle (Beggs and Brill 1973)*

The liquid holdup for horizontal flow should be calculated first, and corrected for inclination afterwards. The equations used for calculating liquid holdup is the same for all flow patterns, but there are different empirical coefficients for each flow pattern. The equation for calculating liquid holdup for horizontal flow is:

$$H_L(0) = \frac{a\lambda_L b}{N_{Fr}^c}, \dots\dots\dots(2.82)$$

where  $a$ ,  $b$ ,  $c$  are empirical coefficients given in table 2.4 and  $N_{Fr}$  is mixture Froude number

$$N_{Fr} = \frac{v_m^2}{gd} \dots\dots\dots(2.83)$$

<b>Table 2.4:</b> <i>Empirical coefficients for calculating liquid holdup</i>			
<b>Flow Pattern</b>	<b>a</b>	<b>b</b>	<b>c</b>
Segregated	0.980	0.4846	0.0868
Intermittent	0.845	0.5351	0.0173
Distributed	1.065	0.5824	0.0609

Liquid holdup for horizontal flow should be greater or equal to the no-slip liquid volume fraction. The inclination correction factor is given by,

$$\psi = 1.0 + C[\sin(1.8\theta) - 0.333\sin^3(1.8\theta)], \dots\dots\dots(2.84)$$

where  $\theta$  is actual angle of pipe from the horizontal, and  $C$  is liquid holdup parameter. The liquid holdup parameter is defined as

$$C = (1.0 - \lambda_L) \ln(e\lambda_L^f N_{LV}^g N_{Fr}^h), \dots\dots\dots(2.85)$$

with a restriction,  $C \geq 0$ .  $e, f, g, h$  are empirical coefficients. They vary with flow regime and flow direction and should be determined from table 2.5. Only uphill flow direction is included here. For the distributed flow pattern no correction is needed.  $C$  will be zero, giving  $\psi$  equal to one. If the flow falls in the transition regime, an interpolation should be carried out.

<b>Table 2.5: Empirical coefficients for calculating liquid holdup parameter</b>				
<b>Flow Pattern (Uphill)</b>	<b>e</b>	<b>f</b>	<b>g</b>	<b>h</b>
Segregated	0.011	-3.7608	3.5390	-1.6140
Intermittent	2.960	0.3050	-0.4473	0.0978

Values for the two phase friction factor were found by solving the pressure-gradient equation, Eq. 2.78. The two-phase friction factor was normalized by dividing it by a no-slip friction factor ( $f_n$ ). This may be found from a Moody diagram, see figure 2.1 or by using no-slip values in Reynolds-number and equations for smooth pipe friction factor. Based on these values, Beggs and Brill proposed the following equation for two phase friction factor,

$$\frac{f}{f_n} = e^S, \dots\dots\dots(2.86)$$

where

$$S = \frac{\ln y}{-0.0523 + 3.182 \ln y - 0.8725(\ln y)^2 + 0.01853(\ln y)^4}, \dots\dots\dots(2.87)$$

and

$$y = \frac{\lambda_L}{[H_{L(\theta)}]^2} \dots\dots\dots(2.88)$$

To ensure that the correlation degenerates to single phase flow when  $y = 1$ , Beggs and Brill proposed that  $S$  should be calculated as,

$$S = \ln(2.2y - 1.2), \dots\dots\dots(2.89)$$

when  $1 < y < 1.2$ .

*2.4.7 Petroleum Experts' Correlations (Petroleum Experts 2010)*

Petroleum Experts correlations are a combination off different correlations. It is developed by the company Petroleum Experts. Papers describing the correlations have not been found, only a brief description in the Prosper manual. It is believed that the correlations are used as described earlier. Flow regimes are determined using Gould et al. (1974) flow map. See table 2.6 for correlations used in the various flow regimes. Liquid holdup and frictional factors are found using the respective flow correlations.

<b>Table 2.6: Correlations used by Petroleum Experts' correlations</b>	
<b>Flow regime</b>	<b>Correlation</b>
Bubble Flow	Wallis and Griffith
Slug Flow	Hagedorn and Brown
Transition	Duns and Ros
Annular Mist Flow	Duns and Ros

It is stated that by using the physical properties of vapor and liquid phases determined in situ, the individual flow rates, pipe geometry and pressure level, one can predict the flow regime likely to occur at that particular point. Gould et al. (1974) have developed a flow regime map for vertical flow, see figure 2.15. It was developed on the basis of results from observations on literature data and laboratory experiments.

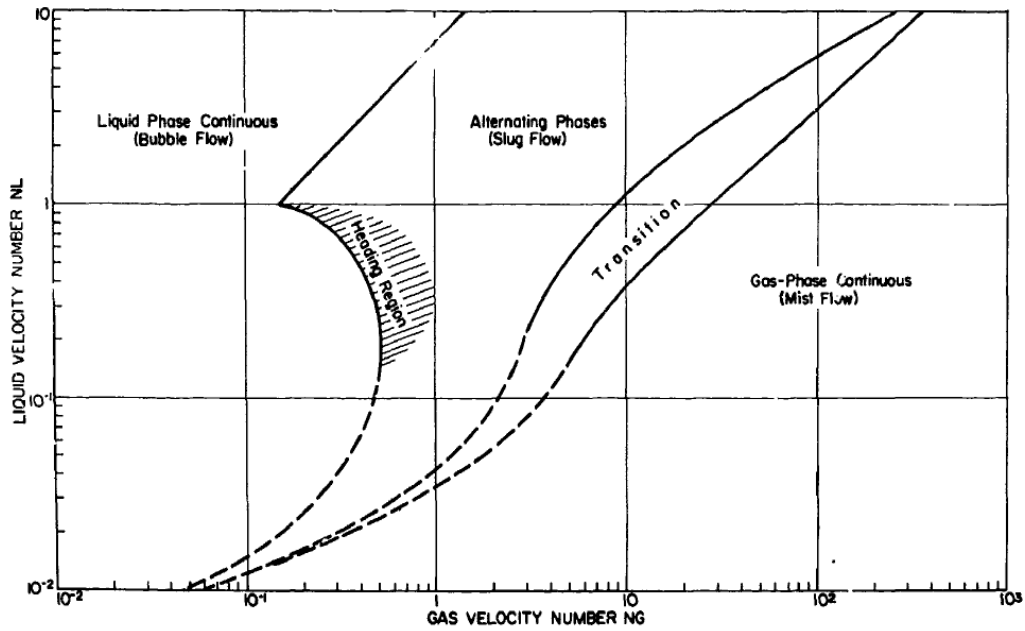


**Figure 2.15:** Flow regime map (Gould et al. 1974)

The regimes are discriminated into liquid-phase continuous (bubble flow), alternating phases (slug flow), gas-phase continuous (mist flow), transition (between slug and mist) and a heading region (both phases continuous). It is important to recognise that the location of the flow regime boundaries only is approximated (Gould et al. 1974).

### 3 Study of Pressure-Drop Prediction in Liquid and Gas-Condensate Wells

Conceptual test data describing liquid and gas wells are manually generated to study prediction of pressure drop, using the different multiphase-flow correlations available in Prosper. Prosper is developed by the company Petroleum Experts, and is a well performance, design and optimisation program (Petroleum Experts 2010). Well configuration is the same for all generated tests, only flow data changes. A description of the well configuration is given in table A.1 and A.3 and figure A.1 in Appendix A. Test data given to Prosper is; tubing head pressure (THP) and temperature (THT), water cut (WCT), liquid rate and gas-oil ratio (GOR). From these data, pressure profiles may be calculated. To help in analysing results, gas-liquid ratios,

$$GLR = \frac{q_G}{q_o + q_w} = GOR \left( 1 - \frac{WCT}{100} \right), \dots\dots\dots(3.1)$$

and gas rates

$$q_G = GOR \times q_L \left( 1 - \frac{WCT}{100} \right), \dots\dots\dots(3.2)$$

are calculated based on the input data. The objective of studying conceptual test data is to see if there are major differences in predicted pressure drops and identify main contributions to the pressure drops without bias from measure data. Furthermore it is attempted to find the correlations that best fit the various production scenarios. Uncertainties regarding real test data are eliminated and generated tests may be used for studying specific effects. No measured pressure drops are available for comparison; hence the average predicted pressure drop will be used as reference when comparing the different correlations. To reveal correlations standing out, the correlations deviation ( $\Delta$ ) from average pressure drop was calculated:

$$\Delta = dP_{Cor} - dP_{Avg}, \dots\dots\dots(3.3)$$



where  $dP_{Cor}$  is pressure drop from a given correlation and  $dP_{Avg}$  is the average pressure drop from all correlations.

### 3.1 Liquid Wells

Five tests describing typical liquid wells were manually generated. They are named Liquid wells A to E. Input data as well as GLR and gas rates are given in table 3.1. Calculations are performed for two liquid rates, 4000 Sm<sup>3</sup>/day and 2000 Sm<sup>3</sup>/day. GOR is kept constant while WCT, and thereby GLR, is varied.

**Table 3.1: Data for conceptual liquid wells**

Liquid well	q <sub>L</sub> [Sm <sup>3</sup> /day]	q <sub>G</sub> [Sm <sup>3</sup> /day]	GOR [Sm <sup>3</sup> /Sm <sup>3</sup> ]	GLR [Sm <sup>3</sup> /Sm <sup>3</sup> ]	THP [Bar]	THT [°C]	WCT [%]
A	4000	640000	160	160	100	60	0
B	4000	320000	160	80	100	60	50
C	4000	64000	160	16	100	60	90
D	2000	320000	160	160	100	60	0
E	2000	32000	160	16	100	60	90

Figure 3.1 clearly shows that the hydrostatic term gives the main contribution to the total pressure drop for Liquid well A. This is true for all the liquid wells as shown in figures B.1 to B.5 in Appendix B. The hydrostatic gradient contributes with ~85 to 98 % of the total pressure drop, depending on water cut and liquid rate. Remaining pressure drop comes from friction, 2 to 15 %. The highest contribution from acceleration was 0.2 %. Pressure drop due to acceleration is thereby negligible for all liquid wells, and will not be discussed any further.

It is worth noticing that Hyro-3P (H3P) stands out regarding split between hydrostatic and frictional contribution, see figure 3.1. It gives a high contribution from the frictional term compared to the other correlations, when water cut is zero. This is most pronounced for liquid well A. At higher water cut a more similar split compared to the other correlations is shown, see figures B.1 to B.5 in Appendix B. This may imply that H3P behaves poorly when only two phases are present; giving too high contribution from friction and low contribution from the hydrostatic term. The split

between hydrostatic and frictional pressure drop may also be a result of how Prosper splits the contribution to the total pressure drop. OLGAS 3P (O3P) and OLGAS 3P Extended (O3PE) are also three-phase correlations. They do not show the same deviation as H3P.

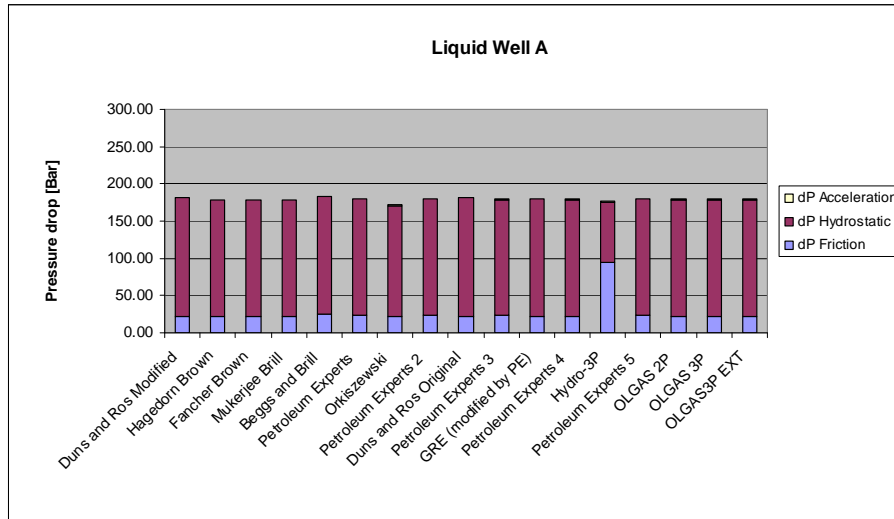


**Figure 3.1:** Pressure drop by various correlations

Predicted pressure drops for Liquid wells A to C are shown in figures 3.2 to 3.4. (Total, hydrostatic and frictional respectively). As expected there is a correlation between GLR and hydrostatic pressure drop. The increased density of the fluid column results in higher pressure drop. The effect is enlarged because GLR is varied by increasing WCT and not oil rate. Water has a higher density than oil, giving an even heavier column. A negative correlation between GLR and frictional pressure drop is observed in figure 3.4. Lower gas rate leads to lower friction. Same trends were observed for liquid well D and E. Again H3P is standing out, giving large frictional pressure drops compared to the other correlations.

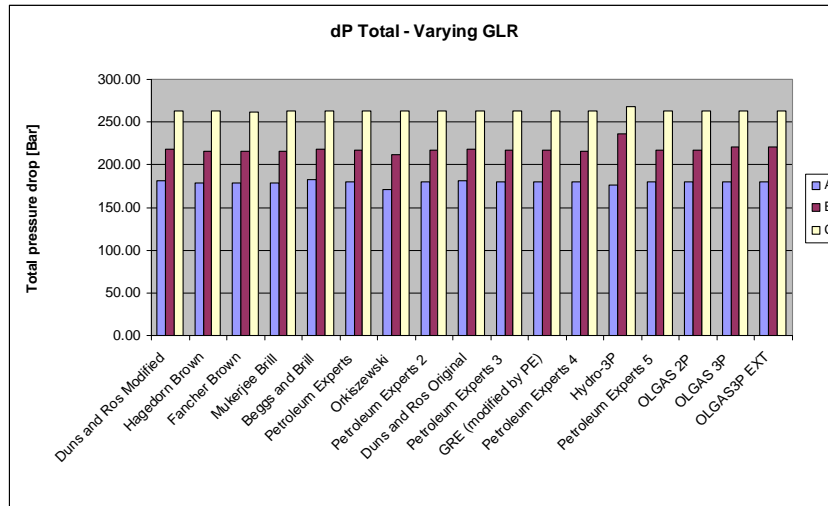


**Figure 3.2:** Total pressure drop by various correlations and varying GLR

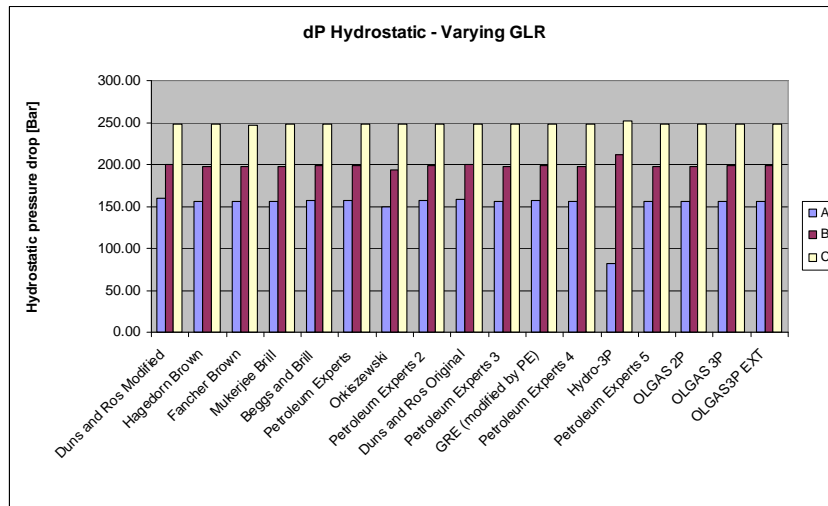


**Figure 3.3:** Hydrostatic pressure drop by various correlations and varying GLR

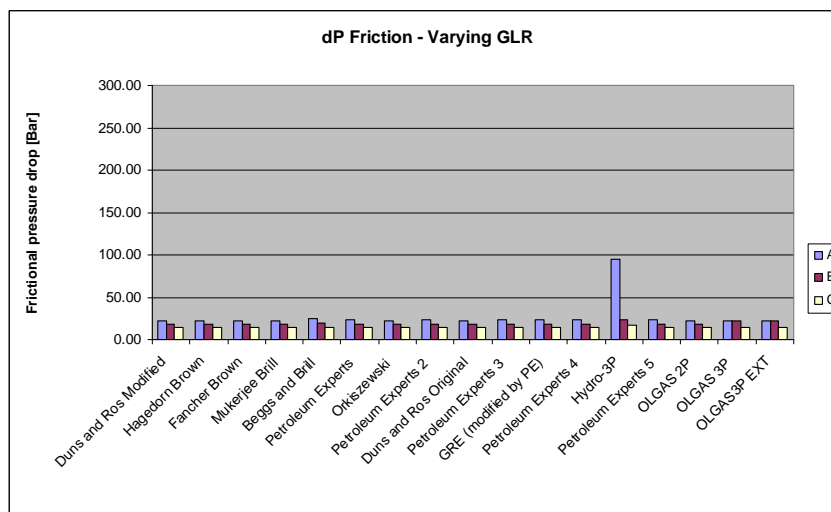


**Figure 3.4:** Frictional pressure drop by various correlations and varying GLR

Each correlation's deviation from the average predicted pressure drop is shown in figures 3.5 to 3.9. Deviation is found by Eq. 3.3. Most of the correlations show little deviation, +/- 2 bar. Some of the correlations stand out, giving larger negative or positive deviation from the average. Duns and Ros Modified (DRm) shows a positive deviation from the average for all tests, due to high predicted pressure drops. The deviation decreases with decreasing GLR. Orkiszewski (O) shows the same trend, less deviation as GLR decreases, but is always negative compared to the average. Beggs and Brill (BB) gives a positive deviation from the average at zero water cut, and seems to perform more in line as water cut is increased. As mentioned above, H3P stands out, giving the highest frictional pressure drop for all tests. There might be an error in how Prosper estimates hydrostatic versus frictional contribution to the total pressure drop for H3P. For high GLR it gives a total pressure drop close to the average. For low GLR, H3P predicts high total pressure drop compared to the average. In general it is observed that the best agreement between the correlations is found at low GLR.

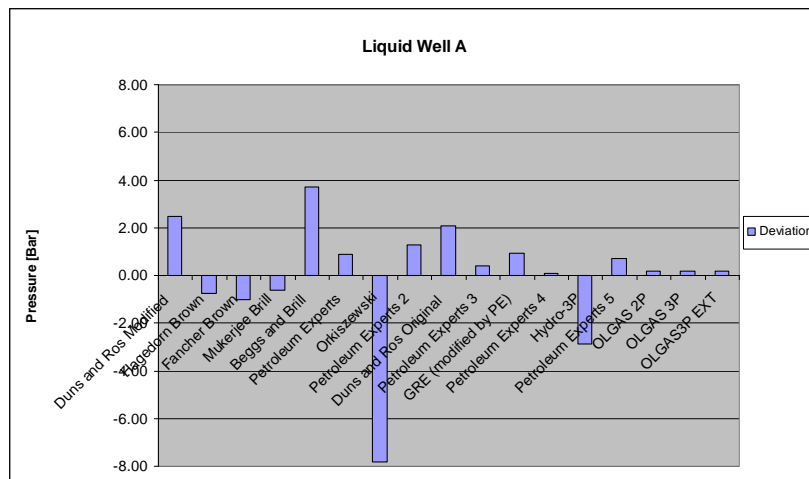


**Figure 3.5:** Correlations deviation from average predicted pressure drop

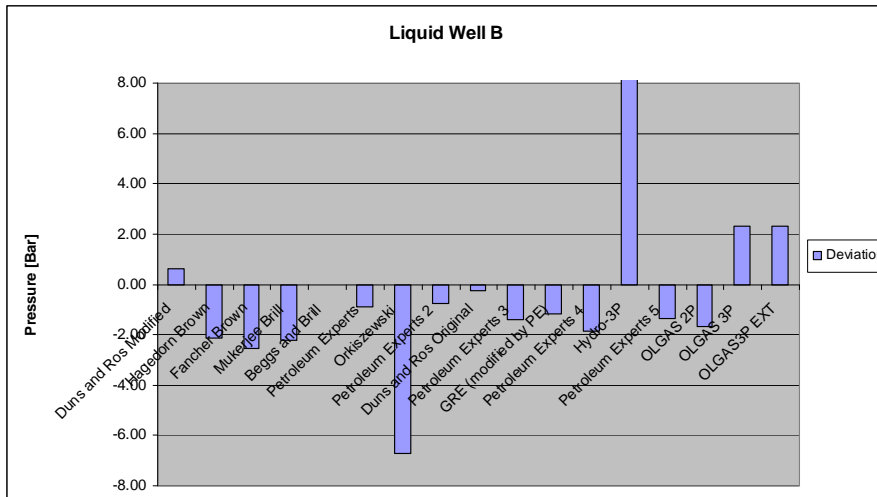


**Figure 3.6:** Correlations deviation from average predicted pressure drop

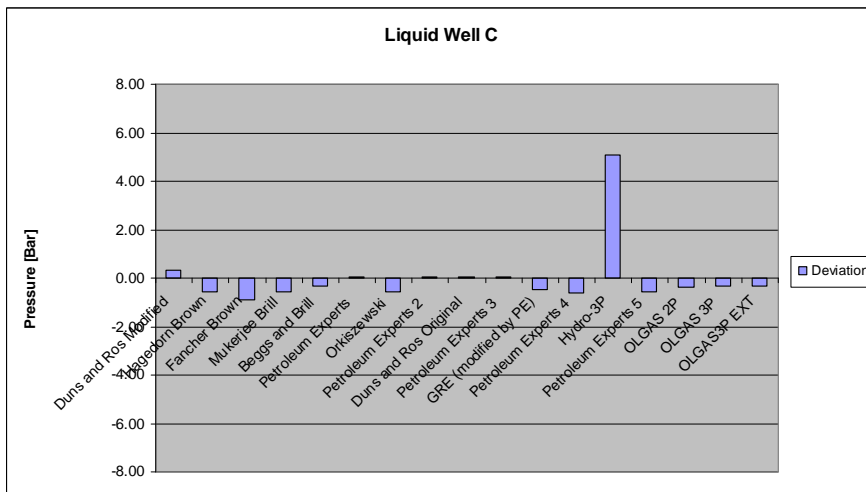


**Figure 3.7:** Correlations deviation from average predicted pressure drop

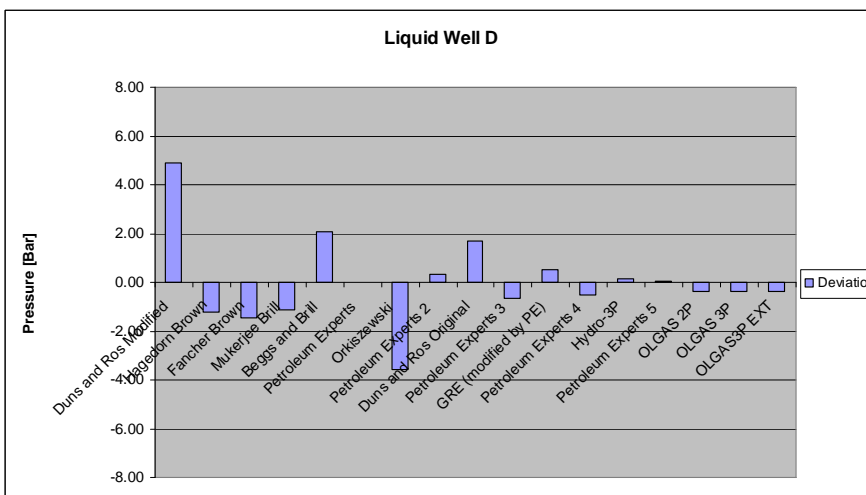


**Figure 3.8:** Correlations deviation from average predicted pressure drop

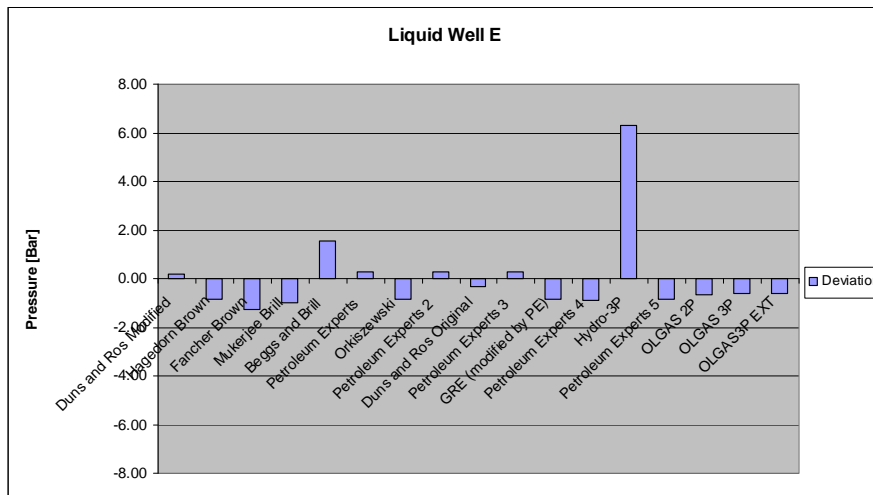


**Figure 3.9:** Correlations deviation from average predicted pressure drop

Fancher and Brown (FB) is a no-slip correlation. Due to this it was expected that it would give low pressure drops compared to the other correlations. This is true when excluding the outliers. FB is always showing the largest negative deviation from the average in the +/- 2 bar range.

Hydrostatic pressure drop gives the main contribution for all liquid wells studied. The lack of variation between the correlations may thereby be explained by similar estimations of liquid holdup. The hydrostatic pressure drop is sensitive to holdup, because it gives the mixture density. This is the only parameter in the hydrostatic term which is not the same for all the correlations. Test data are describing liquid wells which seem to give little room for error when calculating holdup. In addition modifications done by Prosper seems to give similar estimations of liquid holdup. Petroleum Experts (PE), Petroleum Experts 2 (PE2), Petroleum Experts 3 (PE3) and DRm use the same flow regime map. Liquid holdup estimations from Beggs and Brill are used in Hagedorn and Brown (HB) and DRm. Small variations between correlations are believed to originate from the friction term. As GLR decreases, even more similar liquid holdups are estimated. This explains less variation in predicted pressure drop for liquid wells C and E.

## 3.2 Gas-Condensate Wells

### 3.2.1 Effects of Increasing Gas-Rate on Pressure-Drop Prediction

Tests describing typical gas-condensate wells were generated, as described in table

3.2. They were set up to study the effect of gas rate on pressure- drop prediction.

GOR was varied, while liquid rate was constant and WCT was kept constant to zero.

**Table 3.2: Data for conceptual gas-condensate wells**

<b>Gas- condensate well</b>	<b>q<sub>L</sub> [Sm<sup>3</sup>/day]</b>	<b>q<sub>G</sub> [Sm<sup>3</sup>/day]</b>	<b>GOR [Sm<sup>3</sup>/Sm<sup>3</sup>]</b>	<b>GLR [Sm<sup>3</sup>/Sm<sup>3</sup>]</b>	<b>THP [Bar]</b>	<b>THT [°C]</b>	<b>WCT [%]</b>
A	500	500000	1000	1000	100	60	0
B	500	1000000	2000	2000	100	60	0
C	500	2000000	4000	4000	100	60	0
D	500	4000000	8000	8000	100	60	0
E	500	8000000	16000	16000	100	60	0

As expected, total pressure drop is largest for high gas rate. Frictional pressure drop gets more and more pronounced as the gas-rate increases, see figures 3.10 to 3.14. Notice the difference in scale on figure 3.14. By increasing gas rate, hydrostatic pressure drop will decrease while frictional pressure drop will increase. For  $q_G > 4 \times 10^6$  Sm<sup>3</sup>/day, contribution from friction term exceeds the hydrostatic term and total pressure drop is increased. Pressure drop due to acceleration is small. Even at a gas-rate of  $8 \times 10^6$  Sm<sup>3</sup>/day, it contributes with no more than 3% of the total pressure drop.

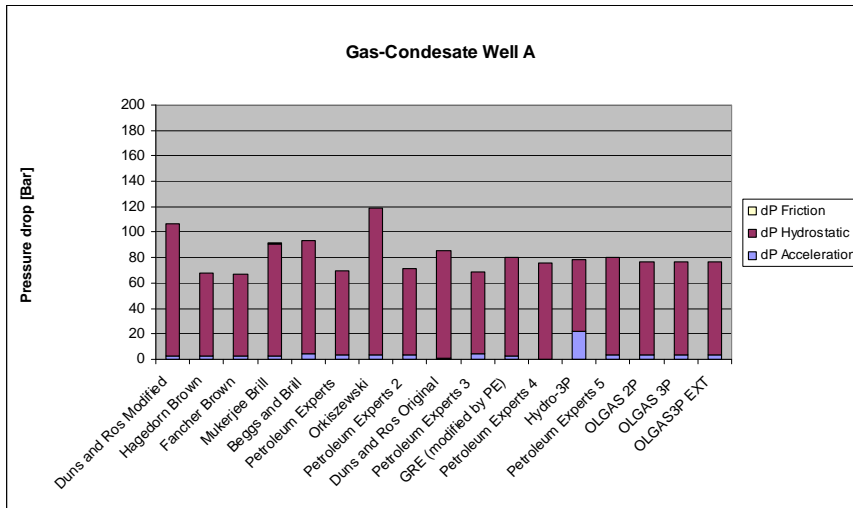


**Figure 3.10:** Pressure drop by various correlations

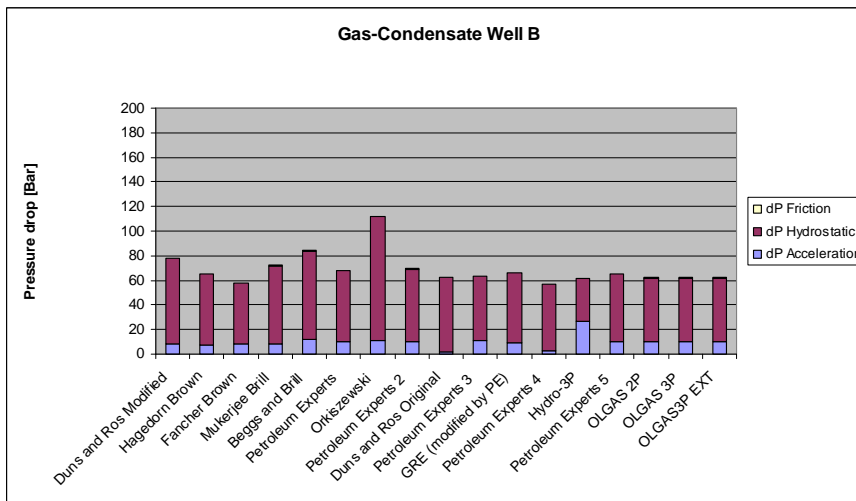


**Figure 3.11:** Pressure drop by various correlations

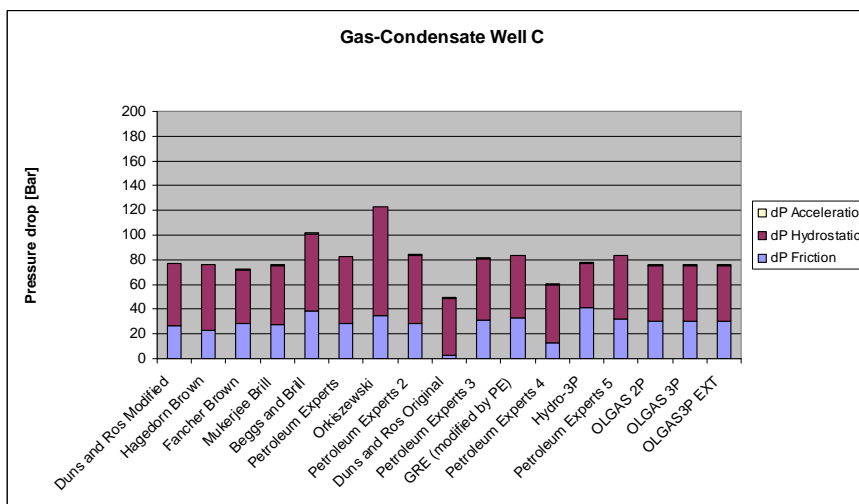


**Figure 3.12:** Pressure drop by various correlations



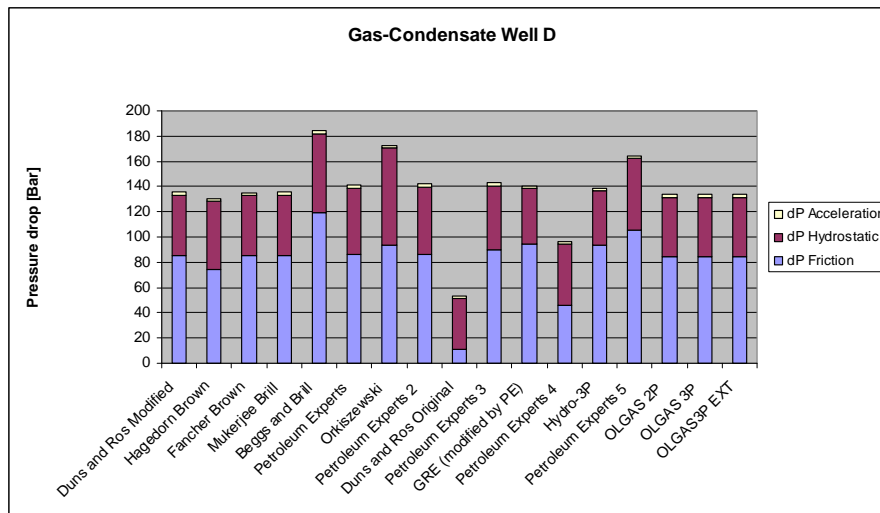


**Figure 3.13:** Pressure drop by various correlations

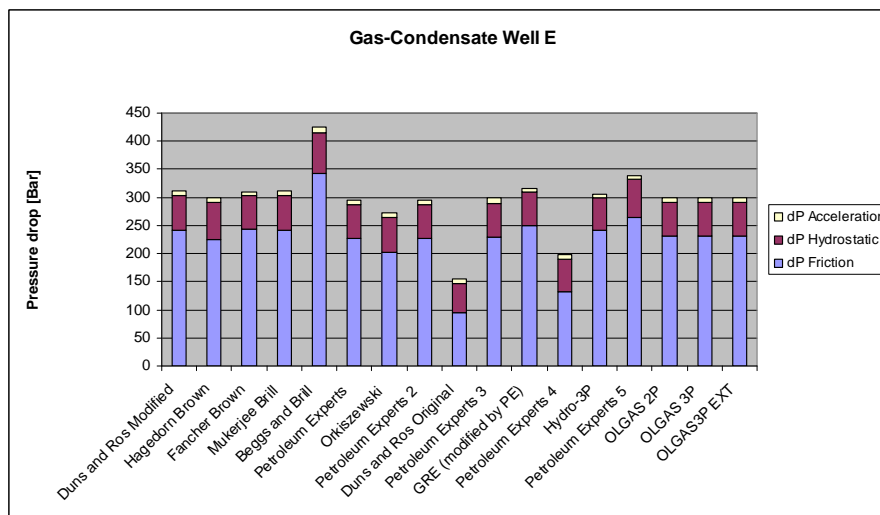


**Figure 3.14:** Pressure drop by various correlations

It is worth noticing that H3P is standing out regarding the contribution percentage, as described in section 3.1. For wells A, B and C it gives high contribution from the frictional term compare to the other correlations. The water cut is zero for all wells, still H3P perform more in line with the other correlations for wells D and E with higher GLR. There might be an error in calculation algorithm for Hydro-3P, or in Prosper's split between hydrostatic and frictional contribution. H3P seems to give too high contribution from the frictional term when only two phases are flowing at low GLR. Regarding total pressure drop, H3P performs in line with the other correlations.

For test E, BB correlation gives the highest frictional pressure drop while Duns and Ros Original (DRo) predict the lowest. In turn the same is observed for the total pressure drop. Except Orkiszewski, all correlations predicts lowest hydrostatic pressure drop for test C, where both hydrostatic and frictional pressure drops are low.

The correlations give a large spread in predicted pressure drops, see figures 3.15 to 3.19. By looking at deviation from average predicted pressure drop, it is observed that some of the correlations stand out. In general DRo and Petroleum Experts 4 (PE4) predict low values for friction compared to the other correlations. This results in large negative deviation from the average. Orkiszewski gives high pressure drops at low gas rates, it seems to over predict the hydrostatic contribution compared to the other correlations. At higher gas rates Orkiszewski deviates less from the average. DRm also gets more in line with the other correlations at high gas-rates. BB and Petroleum Experts 5 (PE5) predicts pressure drop close to the average for low gas rate. Deviation increases as gas rate increases as a result of high friction predicted compared to the other correlations. It was expected that BB should give high pressure drop, because it is in general a pipeline correlation (Beggs and Brill 1973).

HB, FB, PE, PE2, PE3 and the OLGAS correlations give little deviation regardless of gas rate, and are believed to be the most accurate correlations for gas-condensate wells.

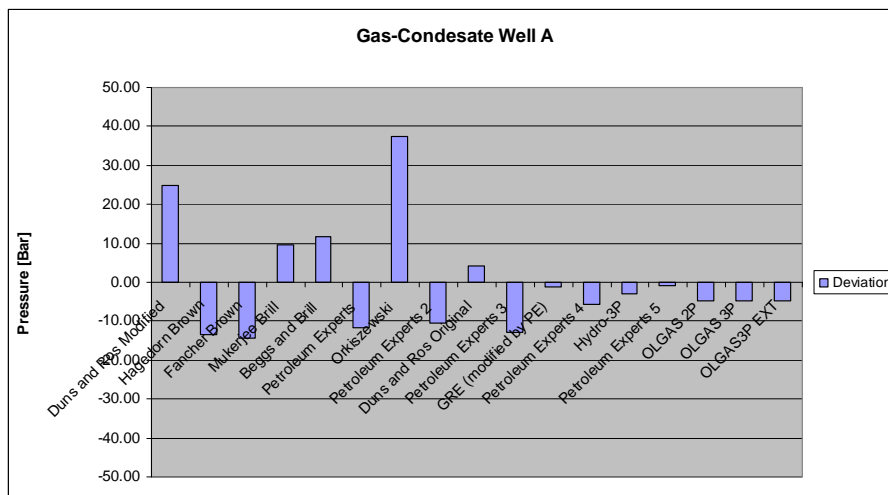


**Figure 3.15:** Correlations deviation from average predicted pressure drop

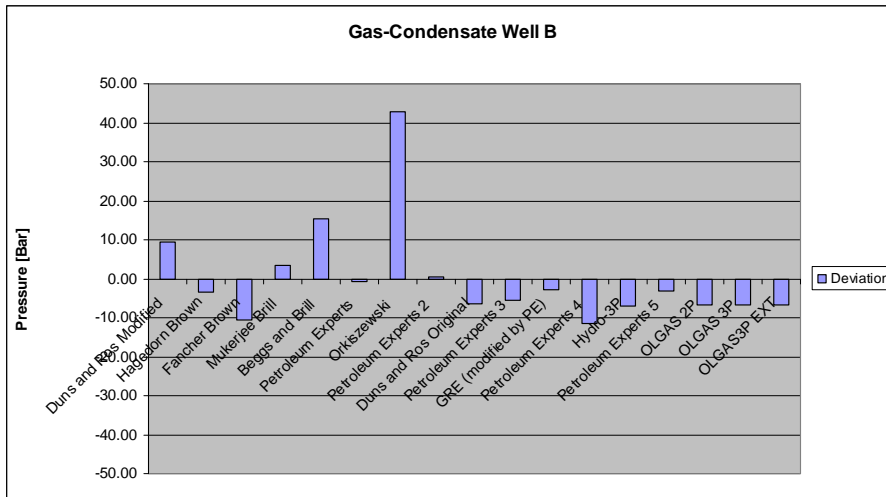


**Figure 3.16:** Correlations deviation from average predicted pressure drop

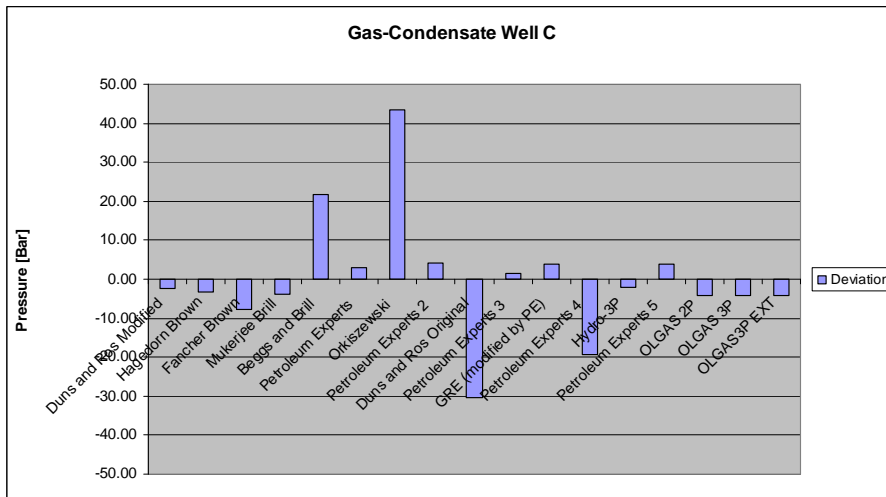


**Figure 3.17:** Correlations deviation from average predicted pressure drop

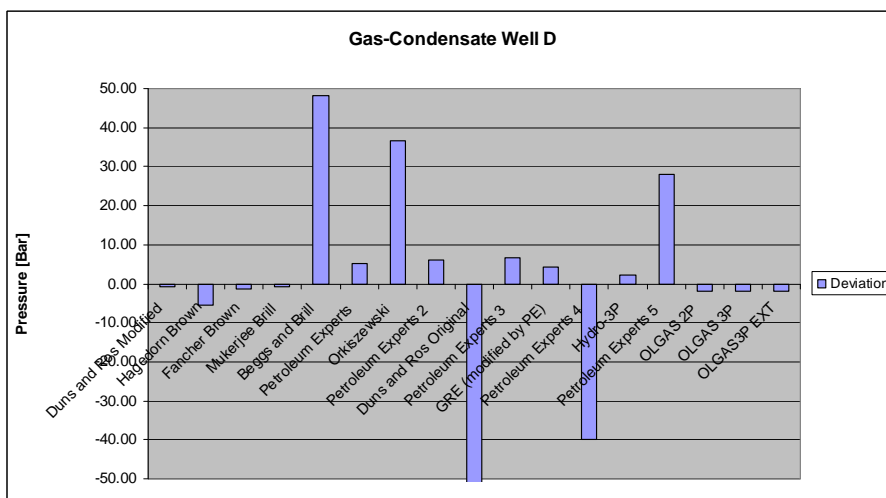


**Figure 3.18:** Correlations deviation from average predicted pressure drop

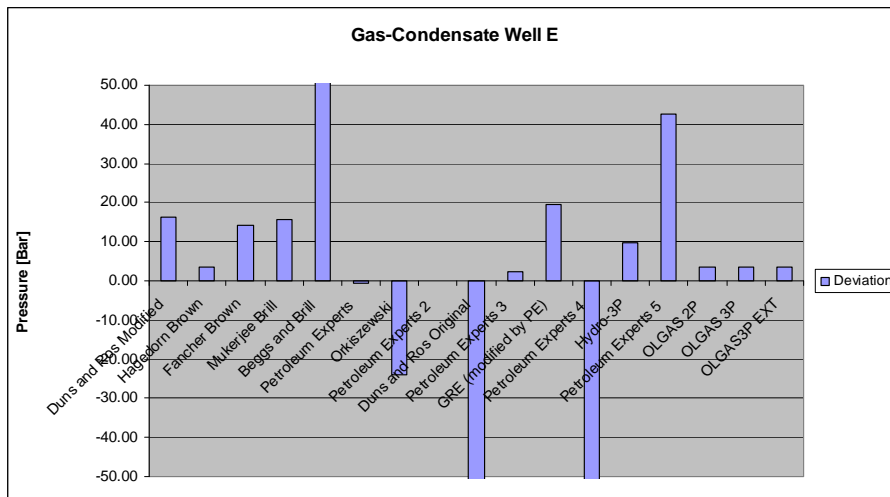


**Figure 3.19:** Correlations deviation from average predicted pressure drop

Variation in flow regimes predicted increases as gas-rate increases. It is observed that the different correlations predict various pressures in the same flow regime. For gas-condensate wells A-C, slug flow is the main regime. For these wells, hydrostatic pressure drop is highest and deviations are believed to originate from estimations of liquid holdup. At higher gas-rates, well D and E, there is larger variation in flow regimes predicted along the wellbore. As expected, slug, transition and mist flow are in general predicted from bottom to top. In turn larger deviation for predicted frictional pressure drops are observed and thereby for the total pressure drop. There can be various factors resulting in deviation amongst the correlations. Friction factor correlation, estimation of holdup, and which mixture density is used in the friction gradient will give deviation amongst the correlations.

### 3.2.2 Effects of Varying Oil-Water Ratio on Pressure-Drop Prediction

To study the effect of varying oil-water ratio, gas-condensate tests A and D was repeated. WCT and GOR were increased, while GLR and gas rate was kept constant, as described in table 3.3. Results of predicted pressure drops are shown in figures 3.20 to 3.25. Hydrostatic pressure drop is the main contribution while friction gives a small contribution in comparison for tests A. For tests D, frictional pressure drop gives the main contribution due to high gas rate. Acceleration is regarded negligible for all tests.

<b>Table 3.3: Data for conceptual gas-condensate wells</b>							
<b>Gas-condensate well</b>	<b>q<sub>L</sub> [Sm<sup>3</sup>/day]</b>	<b>q<sub>G</sub> [Sm<sup>3</sup>/day]</b>	<b>GOR [Sm<sup>3</sup>/Sm<sup>3</sup>]</b>	<b>GLR [Sm<sup>3</sup>/Sm<sup>3</sup>]</b>	<b>THP [Bar]</b>	<b>THT [°C]</b>	<b>WCT [%]</b>
A	500	500000	1000	1000	100	60	0
A2	500	500000	2000	1000	100	60	50
A3	500	500000	5000	1000	100	60	80
D	500	4000000	8000	8000	100	60	0
D2	500	4000000	16000	8000	100	60	50
D3	500	4000000	40000	8000	100	60	80

Even though the correlations give a large variation in predicted pressure drops, a trend is evident for A, A2 and A3 tests. Hydrostatic pressure drop increase with increased WCT. Water has a higher density than oil, making the hydrostatic column heavier. For tests with higher GLR, D wells, this trend is not observed. At higher GLR (>2-3000 Sm<sup>3</sup>/Sm<sup>3</sup>) it seems immaterial whether the liquid phase is oil or water. Differences in pressures observed when increasing water cut is less than differences between the correlations.

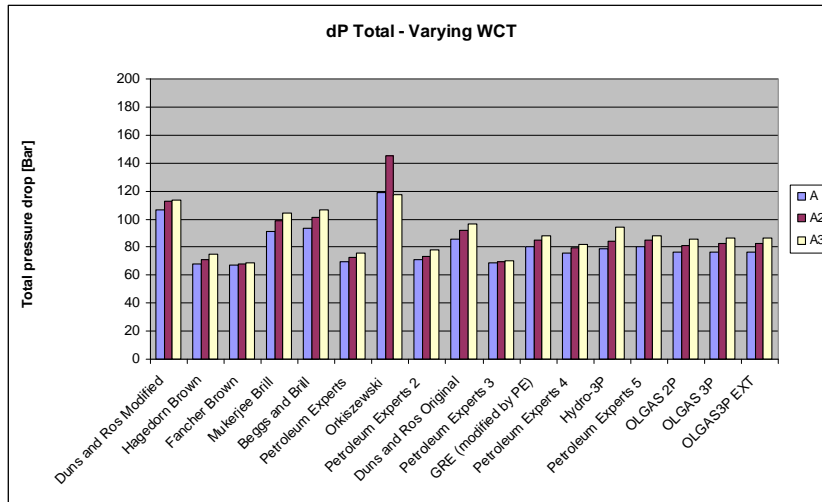


**Figure 3.20:** Total pressure drop from various correlations with varying WCT

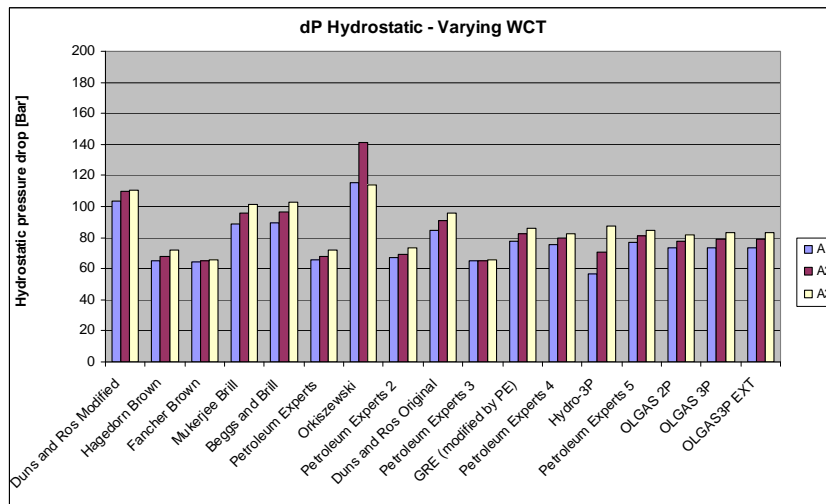


**Figure 3.21:** Hydrostatic pressure drop from various correlations with varying WCT

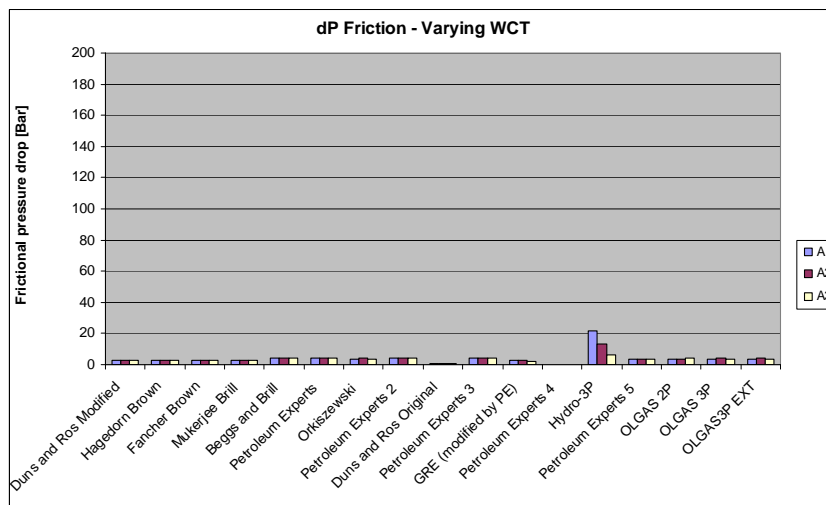


**Figure 3.22:** Frictional pressure drop from various correlations with varying WCT

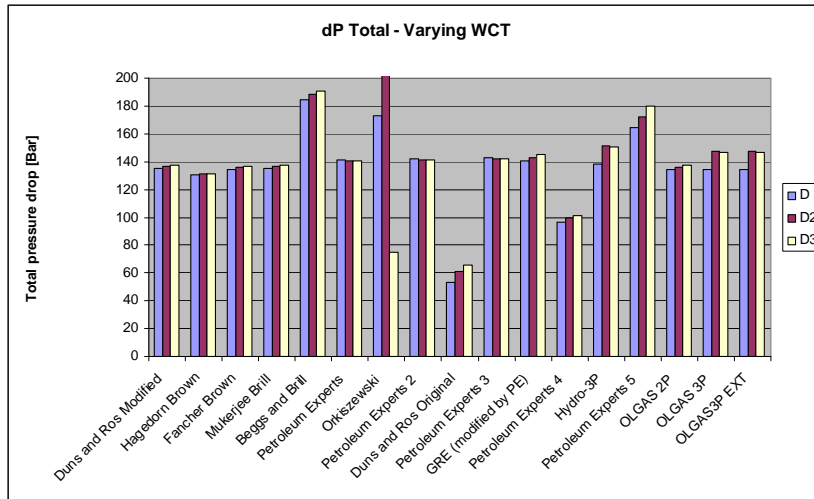


**Figure 3.23:** Total pressure drop from various correlations with varying WCT

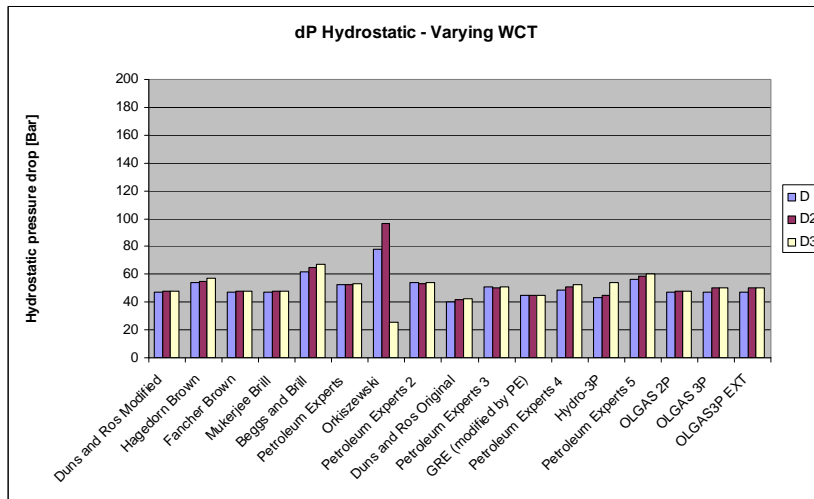


**Figure 3.24:** Hydrostatic pressure drop from various correlations with varying WCT

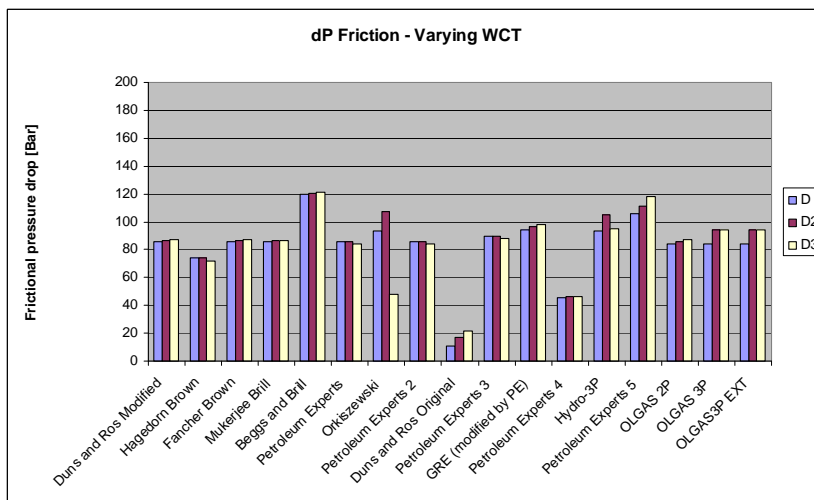


**Figure 3.25:** Frictional pressure drop from various correlations with varying WCT

Orkiszewski stands out the most. It deviates from the trend of higher hydrostatic pressure loss with increasing water cut, observed for A wells. It predicts the lowest hydrostatic pressure drops for a water cut of 80%. Furthermore Orkiszewski predicts the lowest pressured drop of all correlations in test D3, but the highest of all for A3. This may imply that Orkiszewski is sensitive to GLR. It predicts low pressure drops for liquid wells and high for gas-condensate wells. For liquid wells it performs more in line at low GLR, whereas for gas-condensate wells it deviates less from the average as gas rate increases. This may be explained by pressure discontinuities between flow regimes.

For wells with low GLR, DRm, Mukerjee and Brill (MB), BB and Orkiszewski predict the highest pressure drops. Also for high GLR, BB and Orkiszewski are predicting high pressure drops. High predicted total pressure drops derives from high predicted hydrostatic pressure drop. DRm and MB is more in line at high GLR, while DRo and PE4 predict low pressure drops.

With regards to frictional pressure drop for A wells, DRo, PE4 and H3P stands out. H3P gives the highest values where DRo and PE4 predict the lowest. The variation in predicted frictional pressure drop is not pronounced in total pressure drop, because contribution from the hydrostatic term is considerably larger.

As expected, WCT has little effect on predicted frictional pressure drops, see figures 3.22 and 3.25. Larger deviation amongst the correlations is observed for D wells. At higher GLR friction gets more pronounced. DRo and PE4 stand out predicting low frictional pressure drops. Hence low total pressure drops are predicted for these correlations.



### 3.3 Conclusions

From studying prediction of pressure drop in conceptual liquid and gas-condensate wells it was found that:

- For liquid wells main contribution to total pressure drop comes from the hydrostatic term.
- Hydrostatic pressure drop decrease with GLR and increase with WCT.
- Frictional pressure drop is highly dependent on gas rate.
- Contribution from the acceleration term was found negligible for all realistic cases (small contribution at very high gas rate).
- Frictional pressure drop may exceed hydrostatic pressure drop at high gas rates.
- The correlations in Prosper give similar pressure drops for liquid wells. Larger variation in predicted pressure drops were observed for the gas-condensate wells.
- Orkiszewski correlation seems to give pressure discontinuities between flow regimes and is not recommended to be used for pressure prediction.
- H3P is not recommended to be used when predicting pressure drop. It seems to overestimate frictional pressure drop.
- DRo and PE4 predicts low frictional pressure drop for gas-condensate wells.
- BB is mainly a pipeline correlation, and is not recommended to be used for pressure prediction.
- FB is not recommended to be used for pressure prediction, because it is a no-slip correlation.
- HB, FB, PE, PE2, PE3 and the OLGAS correlations are considered to give acceptable pressure predictions for all the scenarios studied, regardless of input data.

## 4 Comparison of Measured and Predicted Bottomhole Pressures

Data used in this analysis are gathered from six different wells located in the Statfjord Field. A total of 203 approved production tests were analysed. All data are from deviated wells with properties as described in table 4.1. A more detailed description of the wells is found in figures A.1 to A.6 and tables A.1 to A.8 in Appendix A. Calculations are performed using Prosper. The aim for this analysis was to quantify accuracy of the correlations when predicting bottomhole pressures. An effort was made to see if the percentage error correlated with properties like GLR, GOR, WCT and production rates.

Property	Range	Units
Gas-liquid ratio	0 - 10000	Sm <sup>3</sup> /Sm <sup>3</sup>
Water cut	0 - 100	%
Liquid rate	70 - 2900	Sm <sup>3</sup> /day
Gas rate	0 - 1270000	Sm <sup>3</sup> /day
Depth DHPG TVD	1702 - 2581	m
Depth DHPG MD	1908 - 3628	m
Tubing size	5 - 7	inch
Deviation inclination	24 - 85	degrees

To quantify the accuracy of each correlation the percentage error was calculated,

$$\%Error = \left( \frac{\Delta P_{\text{predicted}} - \Delta P_{\text{measured}}}{\Delta P_{\text{measured}}} \right) \times 100. \dots\dots\dots(4.1)$$

Each correlation's mean error for all tests was calculated. To reveal errors cancelling each other, the absolute error and standard deviation were included. Results were grouped by high and low GLR, where high GLR is defined above or equal to 1000 Sm<sup>3</sup>/Sm<sup>3</sup> and low GLR less than 1000 Sm<sup>3</sup>/Sm<sup>3</sup>. Tests including gas lift were treated as an independent group. Results were analyzed as a total and by well, to ensure that results were consistent for all well configurations. Analyze by well is found in Appendix B, figures B.9 to B.50.

#### 4.1 Accuracy of Correlations

Figure 4.1 shows average percentage error for all 17 correlations using all 203 tests. It shows that HB, FB, PE, PE2 and PE3 give the lowest percentage error. The standard deviation is also smallest for these correlations, meaning they are consistent. They all lie within 10 % error, which is regarded an acceptable error. BB and MB give the highest percentage error. This is consistent with earlier work (Persad 2005; Pucknell et al. 1993; Trick 2003). As mentioned earlier, BB is primarily a pipeline correlation. It was developed based on gas-water data, and seems to over predict pressure drops (Beggs and Brill 1973).

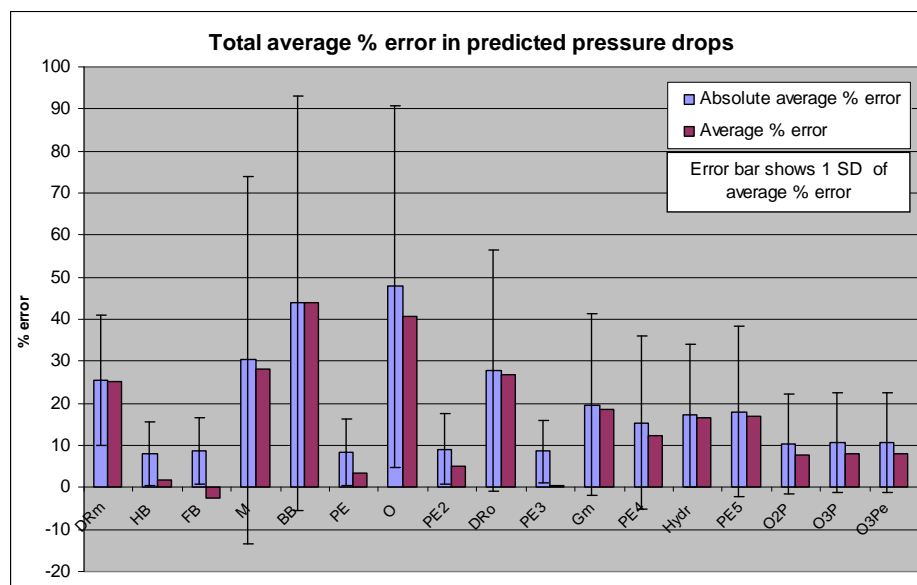


**Figure 4.1:** Average percentage error in predicted pressure drop when analysing all tests

As expected FB gives the lowest pressure drops for all the tests, giving negative percentage error in figure 4.1. This is a no-slip correlation. It is stated by Petroleum Experts (2010) that predicted pressures from FB always should be less than measured. This is not the case here. Results show that FB predicts both to high and to low pressure drops compared to the measured values, but is always low compare to the other correlations. Further FB is not recommended to use for quantitative work, even if it gives a good mach to measured data (Petroleum Experts 2010; Brill and Mukherjee 1999). FB is recommended to be used only as a quality control. Pressures lower than predicted from FB should not be trusted.

HB shows good accuracy to measured pressure drop, still it should be used with caution. Petroleum Experts (2010) do not recommend the use of HB for condensates and whenever mist is the main flow regime because pressure drop will be under predicted.

Results grouped by GLR and gas-lift are shown in figure 4.2. Results by grouping shows same trend as the total. Again HB, FB, PE, PE2 and PE3 give low percentage error for all groups. It is worth mentioning that low GLR group includes 99 tests, high GLR 77 tests and gas lift only 27 tests.

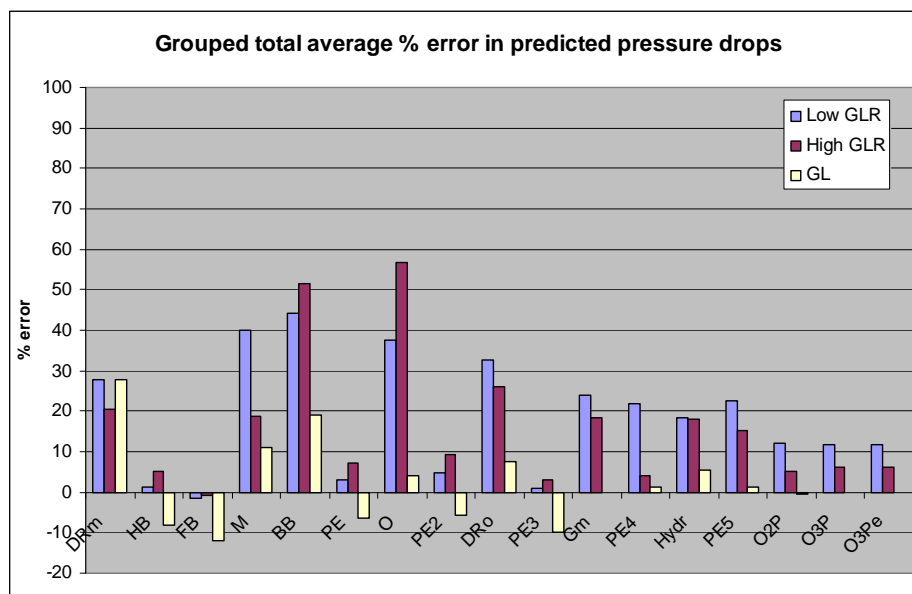


**Figure 4.2:** Average percentage error in predicted pressure drop when analysing all tests divided in high and low GLR, and tests including gas-lift

Large variation in accuracy amongst the correlations is observed both for high and low GLR. This was unexpected, based on results from fictitious tests. For the fictitious tests a large spreading in predicted pressure drops were observed for gas-condensate wells, whereas for liquid wells all correlations gave similar results. A comparable range of GLR was used in the fictitious tests. Still higher gas rates for the gas-condensate wells and higher liquid rates for the liquid wells were used. Lack of variation amongst the correlations at low GLR observed for fictitious test, is believed to originate from similar estimations of liquid holdup. This is clearly not the case here. Higher gas rates for the conceptual gas-condensate wells gives a more pronounced

frictional pressure drop. Due to lower gas rate, this is not observed when analysing real tests.

Many of the correlations seem to be more accurate for higher GLR. A possible explanation for more accurate prediction at high GLR is given by Persad (2005). He proposes that less liquid holdup and gas slippage in the tubing gives more accurate predicted pressure drops. Even so, the correlations predicting most accurate pressure drops, show lowest percentage error for low GLR, which is consistent with the analysis in chapter 3.

In general, lower pressure drops are predicted for test including gas lift. This was expected because gas-lift will make the hydrostatic column lighter. HB, FB, PE, PE2 and PE3 predict too low pressure drops when gas lift is included. This is shown as negative percentage errors in figure 4.2. Some of the less accurate correlations, regarding high and low GLR, give reasonable errors for tests including gas-lift. There is high uncertainty in gas-lift rate, and correlations seem to give a relative shift in pressure with gas-lift rate. In addition it is worth noticing that a close to perfect match may be the result of cancelling errors. This was observed especially for Gray Modified (Gm), PE5 and the OLGAS correlations, for tests including gas lift. Both too high and too low pressures were predicted, giving a close to zero percentage error in figure 4.2. For high and low GLR cancelling of errors was not observed.

It was found that hydrostatic pressure drop gave the largest contribution to the total pressure drop for all tests. Hence, the crucial factor for accuracy will be the estimation of liquid holdup. This compares favourably with the fictitious tests. Figures 4.3 and 4.4 show how hydrostatic and frictional pressure drops vary with GLR for well A-2. As expected, hydrostatic pressure drop decreases, while frictional pressure drop increases with increasing GLR. The same was observed for all the wells. Higher frictional pressure drop at low GLR is an effect of gas lift.

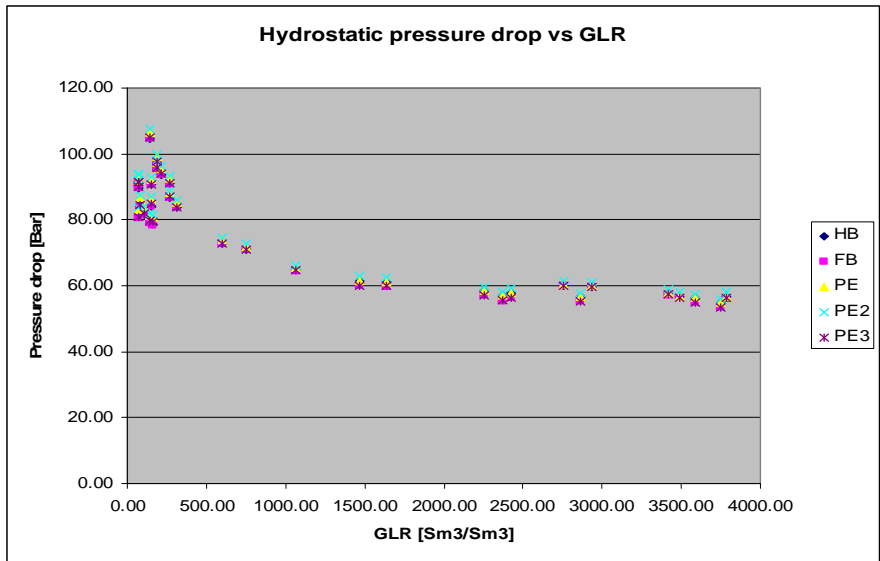


**Figure 4.3:** *Hydrostatic pressure drop versus GLR*

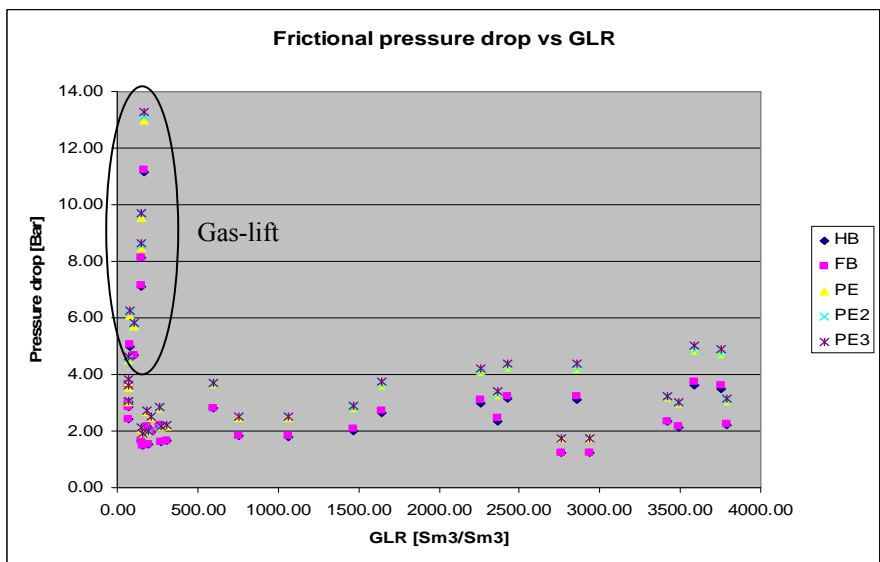


**Figure 4.4:** *Frictional pressure drop versus GLR*

Deviation between predicted and measured pressure drops are believed to originate from differences in the estimation of liquid holdup. As figures 4.3 and 4.4 show, frictional pressure drop is very small compared to the hydrostatic pressure drop. Differences in estimating the friction gradient will henceforth have less influence on accuracy.

## 4.2 Effect of Input Data on Accuracy of Correlations

It was attempted to find a correlation between percentage error and input data.

Percentage error plotted against GLR is shown in figure 4.5. Remaining results are found as figures B.51 to B.54 in Appendix B. Only the correlations giving lowest percentage error is included; HB, FB, PE, PE2 and PE3.

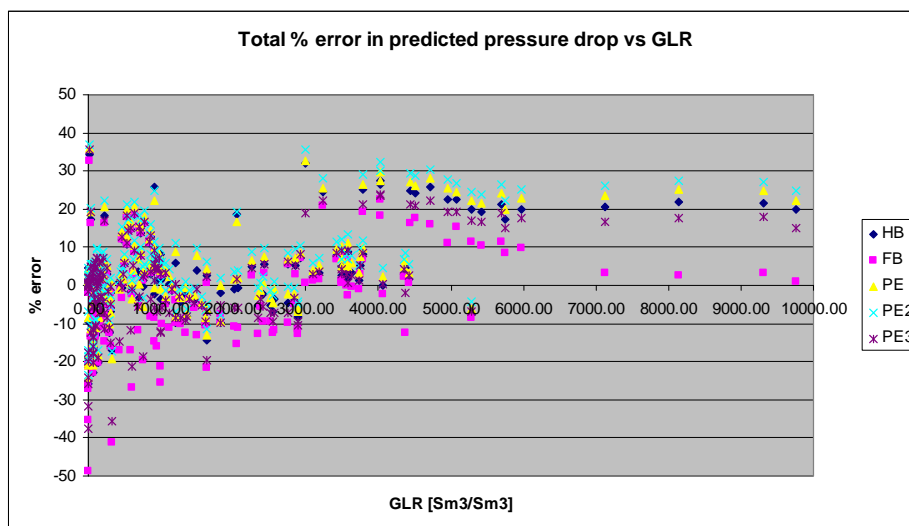


**Figure 4.5:** *Percentage error versus GLR*

Percentage error seems to correlate with GLR. Too low pressure drops are predicted at low GLR, and for higher GLR too high pressure drops are predicted, see figure 4.5. It is observed a collection of points giving high percentage error compared to the rest. These points are a result of too large pressure drop predicted in well C-12, see figure B.39 in Appendix B. This is the only well with GLR in the range 4000 – 10000 Sm<sup>3</sup>/Sm<sup>3</sup>. In this range, all the correlations give higher percentage error and the trend of higher percentage error as GLR increase is less evident. The high percentage errors from C-12 may be explained by high gas rates. Percentage error increases with gas rate, see figure B.43 in Appendix B. At higher gas rates, friction will become more evident and the friction term will introduce higher possibilities of error as described in chapter 3. Regarding WCT and percentage error, a reversed trend is found, see figure 4.6. Low WCT gives too high pressure drops while high WCT gives too low pressure drops. This observation was expected as there is a strong correlation between GLR and WCT at low oil rates.

The trends observed may imply that the correlations are sensitive to GLR and thereby WCT. At low GLR it is believed that liquid holdup is underestimated, and at high GLR liquid holdup is overestimated. This could be a result of insufficient flow regime boundaries, or in the various equations for estimating liquid holdup. In addition, the correlations used do not consider slippage between oil and water. Hence uncertainty in liquid density may influence hydrostatic pressure drop.

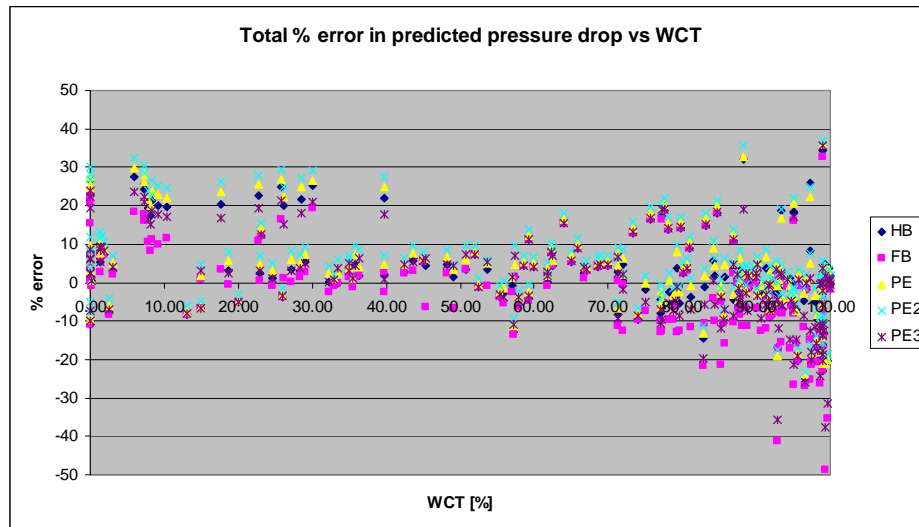


**Figure 4.6:** *Percentage error versus WCT*

Pucknell et al. (1993) observed a decrease in accuracy with GOR above  $200 \text{ Sm}^3/\text{Sm}^3$ . For the majority of the test analysed in this thesis, the GOR range exceed  $200 \text{ Sm}^3/\text{Sm}^3$ . No clear trend regarding GOR was observed; see figure B.51 in Appendix B. To some degree, correlations seem to perform more accurately as gas rate increases, as discussed briefly above. The same is true regarding oil rate, see figures B.53 and B.54 in Appendix B. This may originate from uncertainty in rate measurements. High rates give less uncertainty. Accuracy of predicted pressure drops will naturally depend on quality of input data.



### 4.3 Conclusions

From comparing predicted pressures from various correlations with measured pressures it was found that:

- HB, FB, PE, PE2 and PE3 gives highest accuracy for all tests studied.
- PE, PE2 and PE3 are recommended to be used for pressure drop prediction.
- FB can be included for quality control.
- HB is not recommended due to recommendations given by Petroleum Experts (2010).
- Liquid holdup is the most important factor for accuracy here, because main pressure drop comes from the hydrostatic term.
- A correlation between percentage error and GLR was observed; at low GLR correlations predict too low pressures whereas too high pressures are predicted at higher GLR. Reversed trend is found regarding WCT, because WCT and GLR correlates at low oil rate.
- A modification in estimation of liquid holdup or flow regime boundaries could result in higher accuracy for the correlations.

## 5 Modification of Correlations to Match Measured Bottomhole Pressures

An analysis of modifying correlations by tuning to measured data was performed. Prosper was used for tuning the correlations (VLP matching). The main objective was to see if correlations could be modified in a way giving even higher accuracy for a wider range of GLR. In chapter 4, it was observed that correlations predict low pressures at low GLR, and high pressures at high GLR compared to the measured pressures. For wells in the Statfjord Field, GLR will increase as reservoir pressure depletes. When predicting future performance of the field, VLP curves are based on multiphase correlations. Hence correlations should preferably give accurate pressure prediction for all flow conditions.

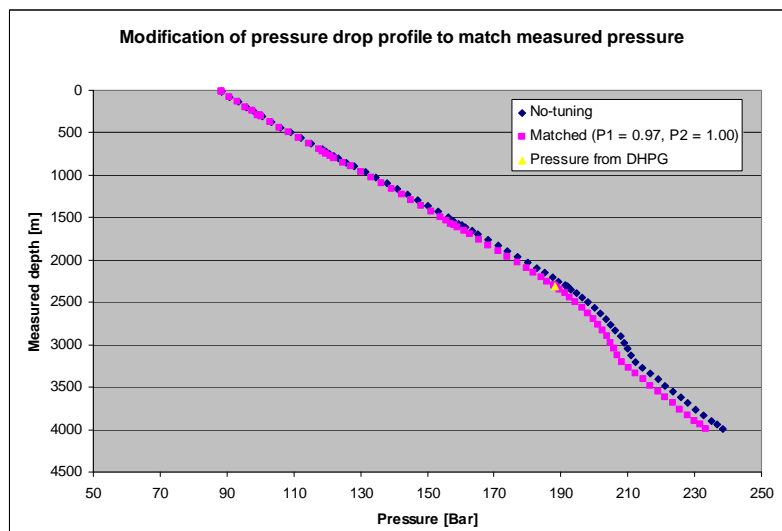


**Figure 5.1:** *Pressure-drop profile from no-tuning and tuned correlation*

### 5.1 VLP Matching Method with Prosper (Petroleum Experts 2010)

To tune a correlation in Prosper, at least one measured bottomhole pressure for the corresponding test data is needed. Both automatic and manual tuning is possible, and one can use one or more pressure point when tuning a correlation. If automatic tuning is chosen, the bottomhole pressure is first calculated using the unadjusted correlation. Then error between measured and calculated pressures is determined using the chi-squared error. A non-linear regression is used to modify the pressure drop profile so it passes through the measured data point, see figure 5.1. The gravity and/or friction

terms in the pressure-loss equation are adjusted. Errors between measured and calculated pressures are determined again. The process is repeated until error between measured and calculated pressures is less than 1 psi, or 50 iterations have been completed.

Parameter 1 (P1) and parameter 2 (P2) are multipliers for the hydrostatic and frictional term respectively. The tuning parameters are given by iterations described above, or as manual input. If the pressure profile needs to be shifted to the left, P1 and/or P2 will be a number lower than one, as figure 5.1 shows. Reversed, if pressure profile needs to be shifted to the right, P1 and/or P2 will be a number greater than one. P1 and P2 should be equal to one if the correlation had a perfect match to the measured data. If the parameters need to be adjusted more than +/- 10 %, a warning will be given. If P1 is adjusted much, Prosper gives a warning stating that there probably is an inconsistency in fluid density, and it is recommended to check PVT data and rates/pressures. In the case of correct PVT, the largest source of error for liquid wells lies in the estimation of liquid holdup. Prosper will first try to make a match by adjusting estimation of liquid holdup. If this results in adjusting parameter 1 more than 5 %, the density is adjusted. If P2 is adjusted more than +/- 10 % it is stated that the roughness factor (RF) or flow rates may be incorrect. No good explanation of how two parameters can be tuned, when only one measured point is available, was found. It is believed that Prosper tunes by emphasizing the term that gives highest contribution to the total pressure loss.

## **5.2 Effect of Tuning Correlations to Test Data**

To study effect of tuning correlations, test data from two different wells have been chosen, namely A-2 and B-1. The wells are described in Appendix A, tables A.1, A.3 and A.5 and figures A.1 and A.3. Test data including gas-lift was excluded, because of high uncertainty in gas-lift rates and to reveal the effect of tuning more easily. The correlations HB, FB, PE, PE2 and PE3 were modified. Pressure traverse from one set of test data was tuned to match the measured bottomhole pressure. The modified correlations, with respective tuning parameters calculated by Prosper, were then used to predict pressures for all the remaining tests. Percentage error was calculated using equation 4.1. Accuracy of the modified correlations for variable GLR may thereby be

compared to the case of no-tuning. Test data giving high, intermediate and low GLR was tuned, one each run, see table 5.1. Average percentage error was plotted as shown in figure 5.2 and 5.3. They show accuracy for tuned correlations when used on data it was not tuned for. The correlation tuned to high GLR was used on tests with intermediate and low GLR. Correlation tuned to intermediate GLR was used on high and low GLR and correlation tuned to low GLR was used to predict pressures for tests with intermediate and high GLR.

**Table 5.1: GLR from test data used in tuning**

<b>Well</b>	<b>High GLR</b> <b>[Sm<sup>3</sup>/Sm<sup>3</sup>]</b>	<b>Interm. GLR</b> <b>[Sm<sup>3</sup>/Sm<sup>3</sup>]</b>	<b>Low GLR</b> <b>[Sm<sup>3</sup>/Sm<sup>3</sup>]</b>
A-2	2760	750	190
B-1	1505	850	75

For A-2, the case of no-tuning and tuning on intermediate GLR gives the lowest percentage error. Tuning on high GLR gives the highest percentage error for all correlations, see figure 5.2. All data used when tuning gave originally too high pressures, meaning tuning parameters will be lower than one for all cases. There is little variation in accuracy, and all cases except tuning on high GLR, gives less than 5 % error.

For B-1, tuning on low GLR gives largest percentage error for all correlations except FB, see figure 5.3. This is an effect of tuning a test where the correlations initially predicted too low pressures, and tuning parameters are greater than one. Applying these parameters to other test data, where pressure initially was too high, will result in worsening errors. As mentioned earlier, FB is a no-slip correlation. Hence it will predict the lowest pressures. When the other correlations give close to zero percentage error, FB will give a negative error. FB predict to low pressures for many of the tests. Pressures will be increased when tuning a correlation to test data giving too low pressures, making FB more accurate. This explains the behavior of FB compared to the other correlations in figure 5.3 for low GLR.

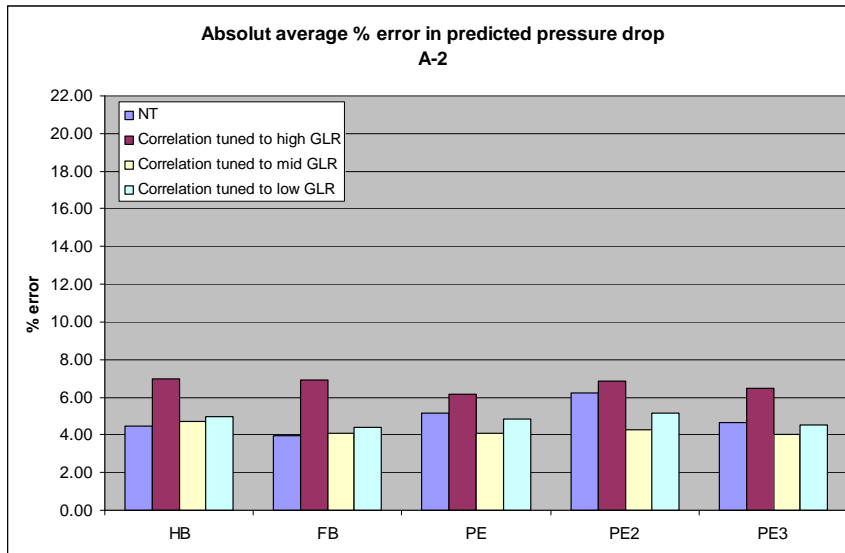


**Figure 5.2:** Results from tuning for well A-2

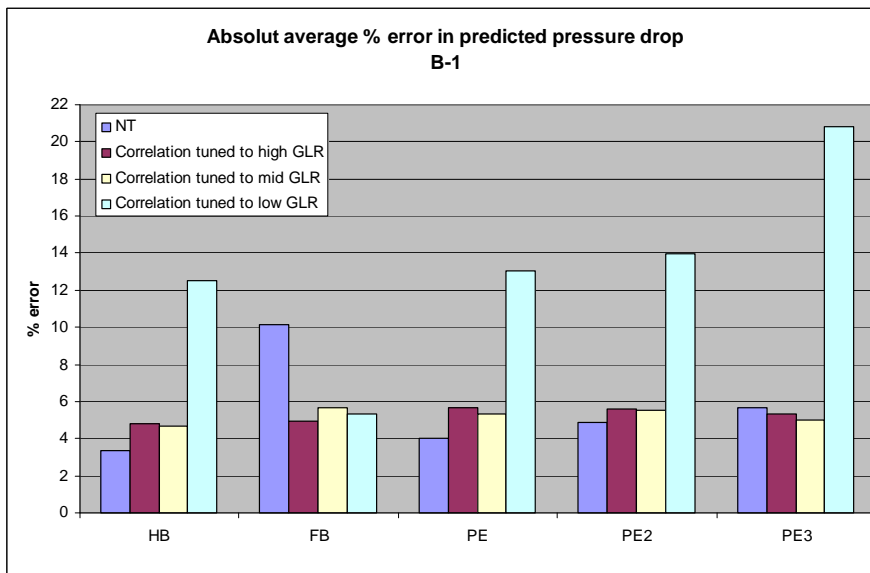


**Figure 5.3:** Results from tuning for well B-1

The effect of tuning tests with high, low and intermediate GLR for PE2 is shown in figures 5.4 and 5.5. Percentage error versus GLR is plotted for PE2. This correlation was chosen based on previous analysis and a historical study. The correlations PE, PE2 and PE3 have shown good accuracy. Historically PE2 is the most common used correlation for Statfjord wells. It has shown a good match to measured pressures for a large range of tests, from many wells. It is believed that the study of tuning PE2 will apply for PE and PE3 as well, because they behave similar to PE2 and the procedure of tuning in Prosper is independent on correlation.

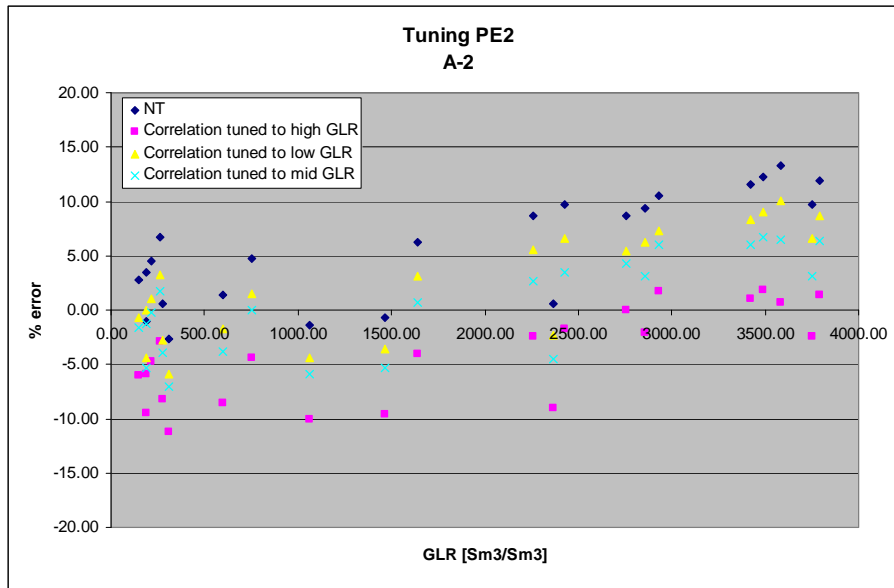


**Figure 5.4:** Results from tuning on PE2 for well A.2

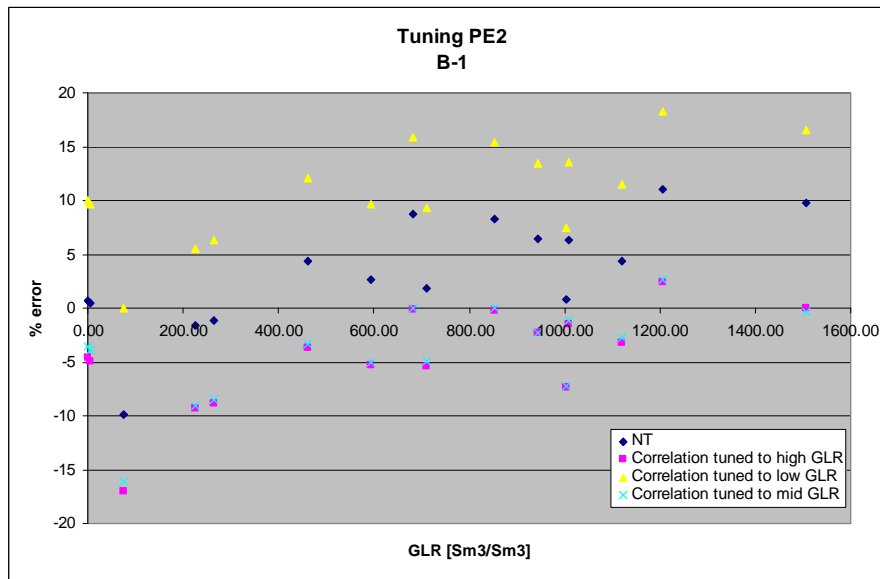


**Figure 5.5:** Results from tuning on PE2 for well B-1

The trend of higher error with GLR is not changed by tuning. Data points are rather shifted upwards or downwards as tuning parameters are increased or decreased. Some tests deviate from the others giving lower percentage errors. No logical explanation for this was found by studying input data. Still, they show the same trend as the others, giving too low pressures for low GLR and too high pressures for higher GLR.

Tuning a correlation to test data with high GLR makes the correlation more accurate for tests with high GLR, but less accurate for tests with low GLR, see figures 5.4 and 5.5. This is an effect of P1 and P2. Correlations need a larger adjustment to match test data with high GLR than low GLR. Using tuning parameters gained from tuning on test data with high GLR on test data with low GLR, will give too low predicted pressures and reduce the accuracy of the correlation.

Tuning a correlation to test data with low GLR will improve accuracy both for high and low GLR when tuning parameters are reduced, see figure 5.4. Still the tuning is too small to give significant improvement for the test with higher GLR. If tuning parameters are increased, accuracy of the correlation will be less for all tests originally giving too high pressures, see figure 5.5. This is the same effect as discussed earlier.

Tuning on a test with intermediate GLR gives the most accurate correlation both for A-2 and B-1. Tuning parameters gained will reduce errors at high GLR and slightly worsen errors at low GLR. Difference between high and intermediate GLR for B-1 is less than for A-2. Hence the effect of tuning on test with high or low GLR gets more similar for B-1.

**Table 5.2:** *Tuning parameters obtained by tuning PE2*

<b>Tuning</b>	<b>Parameter 1</b>	<b>Parameter 2</b>
No tuning	1.00	1.00
High GLR	0.94	0.34
Mid GLR	0.97	0.59
Low GLR	0.97	1.00
All selective tests	0.95	0.29

A selective range of results are plotted for PE2, see figure 5.6. The selection is based on previous analysis. Tests showing a clear trend regarding percentage error with GLR were chosen, to more easily study effect of tuning parameters. Well A-2 was used because it has the widest range of GLR. Tuning parameters for PE2 are given in table 5.2. For all cases studied, pressure profiles need to be shifted to the left because

predicted pressure was originally too high. Tuning parameters will thereby be less than one. High GLR gives highest percentage error, and needs to be changed the most. Both hydrostatic and frictional terms are tuned. For intermediate GLR, less tuning is necessary, giving parameters closer to one. Test with low GLR demands least tuning and only the hydrostatic term is altered.

It was attempted to tune on all the selected tests simultaneously. This can be a good way of modifying correlations. In this case, result is close to the once by tuning on test with high GLR as most of the selected tests are in the range of high GLR. If test data gave more similar GLR, it is believed that tuning on many tests simultaneously may give the most accurate correlation. It is recommended to do this analysis, for quantifying the most accurate correlation to be used in qualitative work (such as prediction of future performance of a well or field). The analysis of tuning should include trial of tuning on high, intermediate and low GLR and a trial where many tests are tuned simultaneously. Test data covering expected GLR range in predictions should be emphasized.

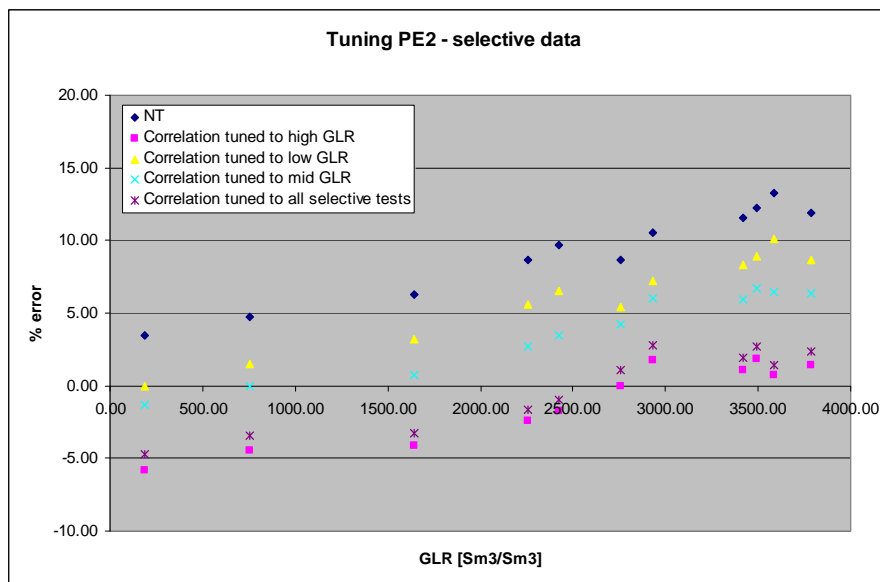


**Figure 5.6:** Results from tuning on PE2 from well A-2, showing only selective tests.

In chapter 3 it was shown that frictional pressure drop gets more evident as gas rate increases. Hence tuning with parameter 2 is reasonable at high GLR. Still, regarding percentage contribution to total pressure losses, friction gives low contribution (3 %) for all cases. Consequently, tuning on the friction terms is questionable.



### 5.3 Studying Manual Tuning in Prosper

Manual tuning was performed to study the effect of each tuning parameter by itself. Main objective was to see if one set of tuning parameters could make a correlation more accurate for both high and low GLR. If this is a possibility, changing parameter 1 and 2 should not have the same effect on test data with high and low GLR respectively. In addition roughness factor was changed for the last two runs, to see if it would give a noticeable effect. Selected tests from A-2 were used. Test data are actual measured data and tuning parameters used to modify correlations are chosen.

First manual tuning on the hydrostatic term with P1 was performed. P2 was held constant whereas P1 was varied as described in table 5.3. Afterwards P1 was kept constant while P2, multiplier for the friction term, was varied. Results are shown in figures 5.7 and 5.8.

<b>Table 5.3: Manual tuning parameters and roughness factor</b>			
<b>Manual tuning no.</b>	<b>Parameter 1</b>	<b>Parameter 2</b>	<b>Roughness factor</b>
1	0.98	1.00	$1.52 \times 10^{-5}$
2	0.96	1.00	$1.52 \times 10^{-5}$
3	0.94	1.00	$1.52 \times 10^{-5}$
4	0.92	1.00	$1.52 \times 10^{-5}$
5	1.00	0.90	$1.52 \times 10^{-5}$
6	1.00	0.80	$1.52 \times 10^{-5}$
7	1.00	0.70	$1.52 \times 10^{-5}$
8	1.00	0.50	$1.52 \times 10^{-5}$
9	1.00	1.50	$1.52 \times 10^{-5}$
10	1.00	1.00	$1.60 \times 10^{-5}$
11	1.00	1.00	$0.08 \times 10^{-5}$

A large effect by changing P1 is observed. By shifting it from 1.00 to 0.98, percentage error is altered approximately 2.5 %. It was expected a larger effect of changing P1 for the tests with low GLR than for tests with high GLR, due to a heavier hydrostatic column. This is observed, but the difference is small. Delta percentage error for highest and lowest GLR is no more than 0.6 % and is considered negligible.

Lack of variation is believed to be an effect of contribution percentage. For all tests, both high and low GLR, the hydrostatic term gives the main contribution (97 %).

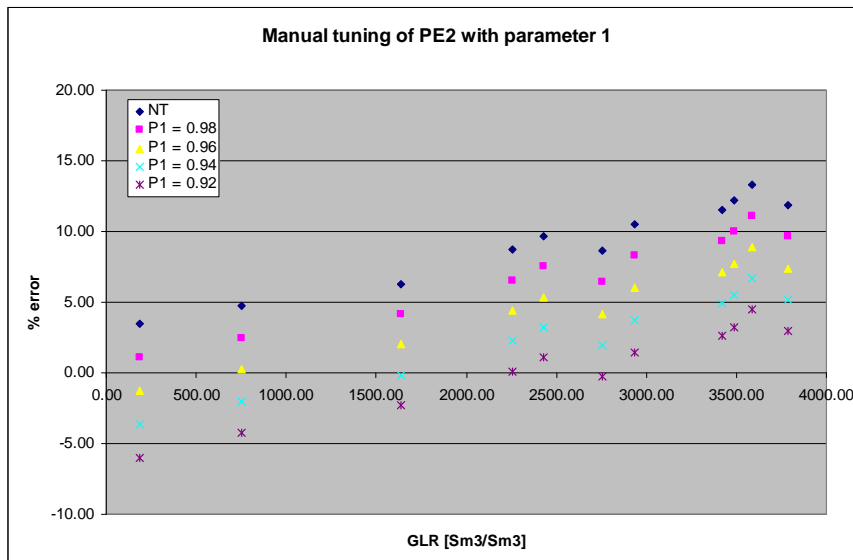


**Figure 5.7:** Results from manual tuning on hydrostatic term.

Changing P2 gives a very small alternation of percentage error. This was expected due to the low contribution from the frictional term to the total pressure loss (3 %). By changing P2 from 1.00 to 0.50, percentage error is only altered by 3 % for high GLR and 2 % for low GLR. This shows little difference between effects on high versus low GLR. Same explanation as for hydrostatic tuning yield, same percentage contribution at low and high GLR gives similar effect of tuning.

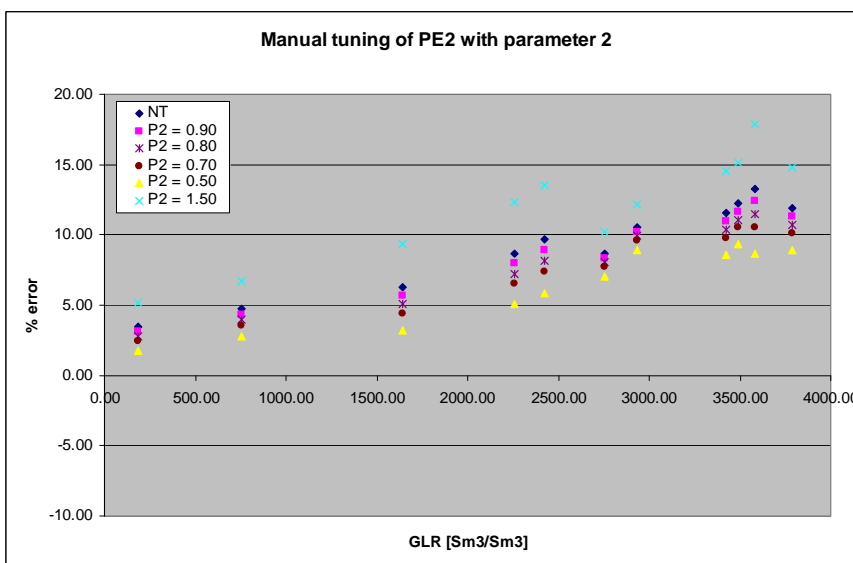


**Figure 5.8:** Results from manual tuning on friction term

By changing either P1 or P2, all test data gave the same relative shift. Hence it is not possible to get reasonable results for all tests by one set of tuning parameters when such a large range of GLR is evident. It is believed that a larger potential of improvement lies in modifying equations for estimating liquid holdup or flow regime boundaries. Percentage error increases with GLR, implying that pressures predicted is too high. A reduction of liquid holdup would improve the accuracy. This could be done by modifying equations for estimation of liquid holdup, or by changing flow regime boundaries. Petroleum Experts correlations uses different correlations for the different flow regimes. A change in flow regime boundaries would give another correlation to be used for estimation of liquid holdup. A temporary workaround can be to modify densities, use artificial values. By reducing liquid and gas density the hydrostatic column will be lighter, and more accurate pressures may be predicted for a wider GLR range. This workaround should be tested out, and one should be sceptic when using artificial densities.

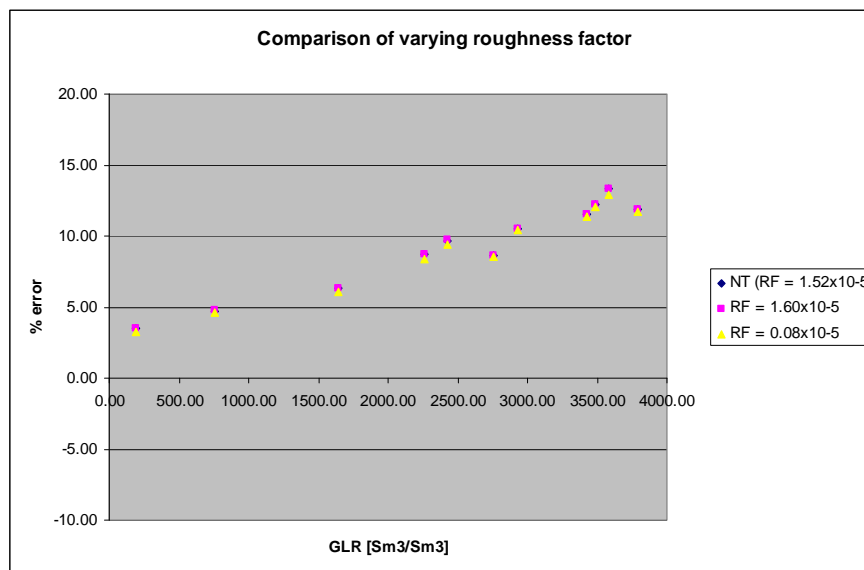


**Figure 5.9:** Effect of changing roughness factor on percentage error.

The roughness factor was increased by 5 % and decreased to only 5 %. All runs give approximately the same results regarding percentage error versus GLR, see figure 5.8. Consequently, effects of changing the roughness factor seem negligible. A decrease in the roughness factor is needed to obtain lower pressures. When a large friction correction is given, Petroleum Experts (2010) encourages reducing the roughness

factor to 0.00015 inch ( $3.81 \times 10^{-6}$  m) or less if stainless steel tubing is used. There seems to be little benefit by doing so in this case.

It will be physically impossible to correct the percentage error of pressure by changing the roughness factor. Still, the roughness factor may be important if friction has a larger contribution; at higher gas rate, or when the pipe is rough. Such conditions are not expected for wells in the Statfjord Field. Thereby effect of changing roughness factor is considered negligible for this study.

#### **5.4 Conclusions**

From studying modifications of correlations with tuning in Prosper it was found that:

- Matching correlations to one set of data does not necessarily improve accuracy of the correlations for other test data.
- Tuning will improve accuracy of correlations for a respective GLR range.
- It is recommended to carry out an analysis on tuning to verify accuracy of correlations before using correlations in quantitative work.
- Parameter 1 will be the essential tuning parameter when main contribution to pressure loss comes from the hydrostatic term.
- Changing parameter 2 will give little effect on accuracy of a correlation when frictional pressure drop is low.
- One set of tuning parameters will not give reasonable results for a large GLR range when main contribution to pressure loss comes from the hydrostatic term.
- No evident effect was proven by changing the roughness factor.
- Modification of equations for estimating liquid holdup or flow regime boundaries is believed to improve accuracy for correlations over a wider GLR range.

## 6 Effect of Using Tuned Correlations in Simulations

Adequate modelling of vertical lift performance will be important at many stages regarding development of a field. As described earlier, the Statfjord Field has changed drainage strategy from pressure maintenance to depletion. Gas will be liberated from the remaining oil in the reservoirs. Most of the gas is expected to come from the Brent Group. In order to make a realistic study of future performance, adequate modelling of VLP will be an important factor.

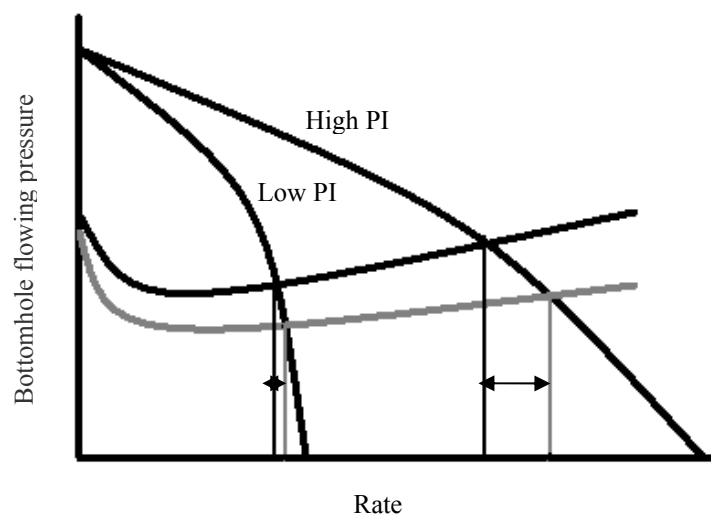


**Figure 6.1:** *Sketch of VLP and IPR curves*

Production rates are given by the intersection of VLP and inflow performance relationship (IPR) curves, see figure 6.1. Changing either VLP or IPR will result in new rates. VLP curves are calculated based on multiphase flow correlations. For this analysis PE2 will be the correlation used when creating lift curves. In previous sections it was found that PE2 in general give too high pressures, especially at high GLR. To account for this one may modify the correlation so that the pressure profile fits the measured bottom-hole pressure as described in chapter 5. Errors that might be introduced by using a tuned correlation, to create VLP curves when predicting future performance, will be studied in this section.

A brief sensitivity analyse of how input parameters may change the effect of tuning will also be discussed. The objective is to give a recommendation of how correlations

should be used for generating VLP curves for modelling performance of the Statfjord Field. Normally, correlations will be tuned to the last production test, and used to predict future production. Is this good practise? The correlation might be accurate at the beginning, but will errors increase with time?

### **6.1 Simulation with ProdPot**

Simulations will be performed using ProdPot. A tool which is developed internally in Statoil for generating production profiles. ProdPot enable systematic prediction of production profiles using Prosper. Input data such as listed below are given to Prosper:

- Reservoir pressure
- Productivity Index (PI)
- Gas-liquid ratio (GLR)
- Water cut (WCT)
- Wellhead pressure (WHP)
- Gas lift injection rate (optional)

VLP and IPR curves are calculated in Prosper, and the intersection between them reported as production rates. In ProdPot, a development for the input data can be added. Input data will then vary with time. Prosper will calculate new VLP and IPR curves whenever time-dependant input data is updated. Input data, and development with time, is based on production experience and simulations with full field model in Eclipse. ProdPot does not include material balance in calculations. If ProdPot is used for predicting field performance, iteration between input data from Eclipse and rates from ProdPot should be carried out.

In this analysis, only single well production is studied. Furthermore, the objective of this analysis is to see how prediction of production rates may be affected by using tuned correlations. By controlling input data, it will be easier to study effects encountered by using different correlations. This was the main reason for choosing ProdPot as simulation tool in this thesis. Only one well profile is used for all the simulations, to ensure that only the desirable parameters are changed. The well used is A-2, which is described in figure A.1, table A.1 and A.3 in Appendix A.

## 6.2 Simulations with Tuned Correlations

### 6.2.1 Low GLR Development

A simulation case was set to describe a realistic scenario for the Brent Group, with increasing GLR as pressure depletes, see figure 6.2. Table 6.1 also describes input parameters that change with time. It is worth noticing that both input and output data are simulated and not real data. No measured data are available when predicting future performance. Simulation is believed to be the best option when predicting future performance for the Statfjord Field.

When no other is pointed out, GLR is referred to as production GLR. Well GLR describes GLR with included gas-lift. Both predicted GLR and pressure development for the Brent Group are collected from the full field simulation model and used as input to the ProdPot simulation. GLR and reservoir pressure development will be the same for all simulations. WCT was kept constant at 95 %, WHP to 20 bar, and gas-lift injection rate to 100 kSm<sup>3</sup>/d. Only the correlation used to calculate VLP curves is varied. Manual tuning on PE2 was used, and one Prosper file for each tuning was set up. Only P1 (hydrostatic term) was changed. Input data describes scenarios where contribution from the friction will be low and tuning with P2 was found negligible. Values of P1 for the various GLR ranges are chosen based on historically values observed when tuning correlations with production tests data.

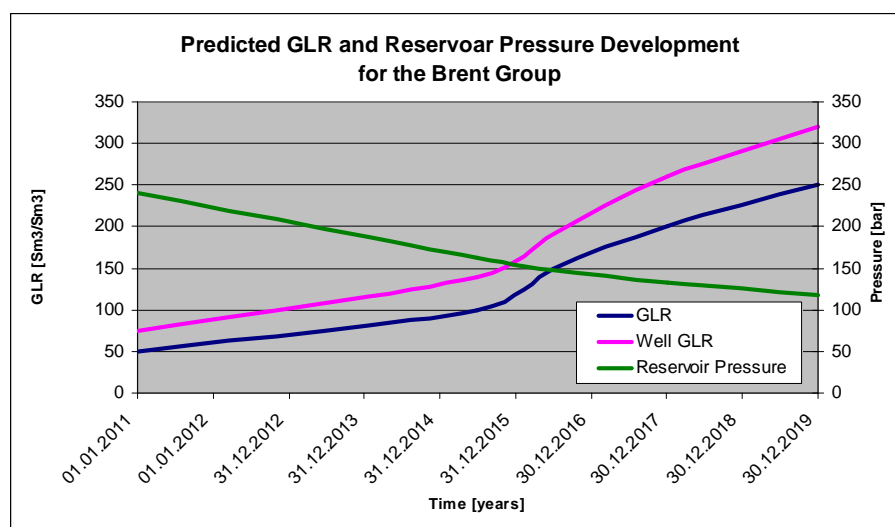


**Figure 6.2:** Predicted GLR and reservoir pressure development from full field model

Start date	01.01.2011	01.07.2015	01.07.2016	01.01.2018
End date	01.07.2015	01.07.2016	01.01.2018	01.01.2020
GLR range [Sm <sup>3</sup> /Sm <sup>3</sup> ]	50 - 100	100 - 150	150 - 200	200 - 250
Well GLR range [Sm <sup>3</sup> /Sm <sup>3</sup> ]	75 - 140	140 - 190	190 - 260	260 - 320
Reservoir pressure [Bar]	241 - 163	163 - 148	148 - 132	132 - 117
P1	1.01	0.99	0.98	0.97
P2	1.00	1.00	1.00	1.00

First a base case (BC) was run. In simulation, the most trusted tuning of PE2 was used for the respective GLR range as described in table 6.1. Consequently the correlation used in simulation was changed as GLR develop with time. Hence BC will be considered as the most accurate simulation. The same simulation was run again, without changing the correlation as GLR increase. One set of tuning parameters for PE2 was then used for the entire time range. This was done to see how production profiles may be affected using tuned correlations. In a more practical sense; study effects of tuning a correlation to test data with low GLR and use this tuned correlation when predicting future performance, and inversely. The same case-study was simulated for three different productivity indexes (PI); 10, 100 and 300 m<sup>3</sup>/d/bar, to see if effects of using tuned correlations change with PI.

Figures 6.3 and 6.4 shows results when PI = 100 m<sup>3</sup>/d/bar. For GLR range studied in this simulation, similar rates are observed for all the correlations. 5 % error bars are plotted for BC. All the correlations are close to the 5 % error, and are within a 10 % error from BC. Still, a trend of increasing rates with lowering P1 is evident. Same trend regarding highest and lowest rates are observed for both gas and liquid. As expected, the lowest value of P1 gives the highest rate. By lowering P1, the hydrostatic gradient will decrease. In turn this gives a lighter hydrostatic column and fluids will be easier to lift. The opposite is true for increasing P1. Hence, the case of P1 = 0.97 will always give the highest rates, and P1 = 1.01 always the lowest. For



liquid rates, the largest deviation amongst the correlations is observed in the beginning. Liquid rates will decrease with time, giving more similar predictions from the correlations, see figure 6.2. The opposite is observed for gas rate, see figure 6.3. As gas rates increase with time, larger deviation is observed between the correlations.

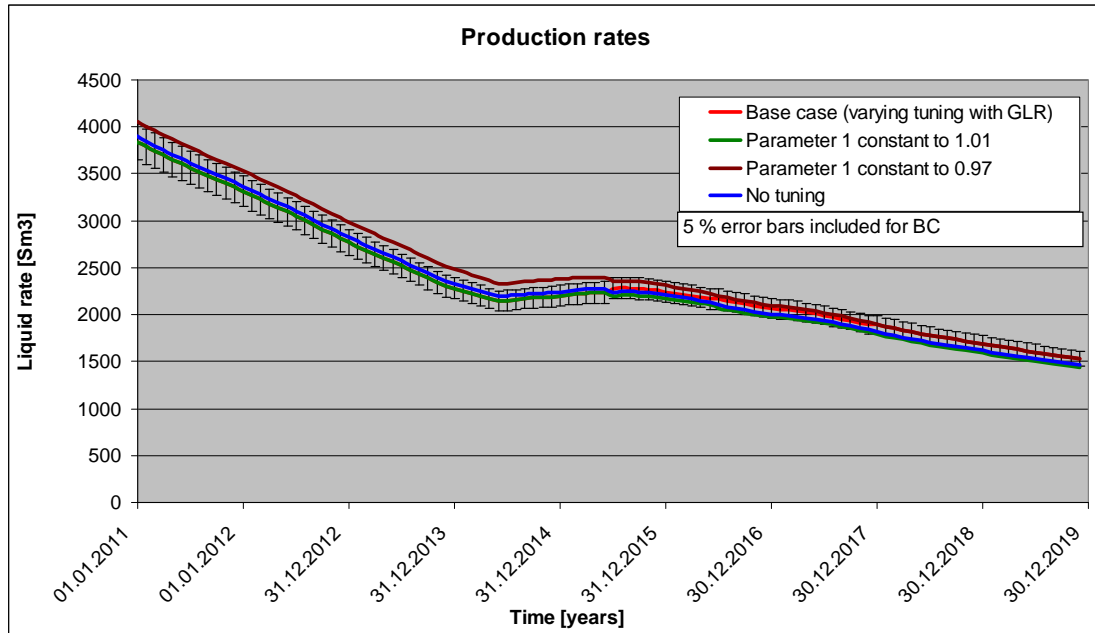


**Figure 6.3:** Liquid rates from simulation with GLR development for the Brent Gp.

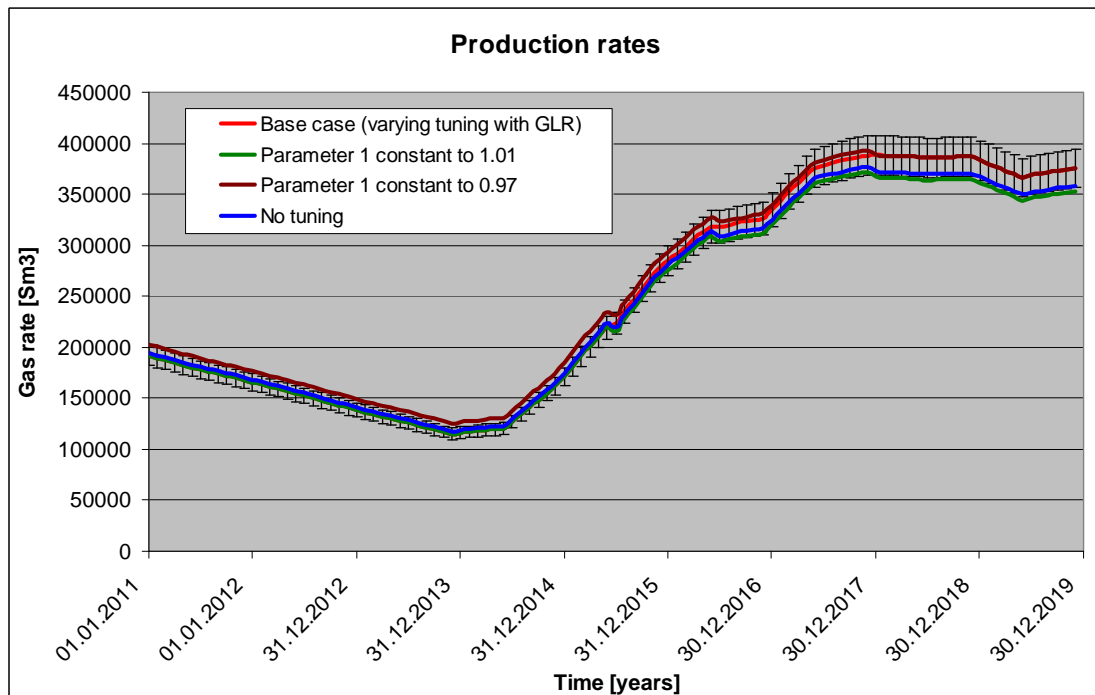


**Figure 6.4:** Gas rates from simulation with GLR development for the Brent Gp.

By tuning a test with low GLR, in this case with  $P1 = 1.01$ , conservative rates will be predicted. It will give a good match in the beginning and too low rates as GLR increase with time. The error will to some degree increase with time, because  $P1$  should have been decreased with increasing GLR. Still, the correlation with  $P1 = 1.01$  lies within or close to the 5 % error the entire time range. If a correlation tuned to a higher GLR is used, the rates will be too high in the beginning and more accurate as GLR increase. Correlation with  $P1$  constant to 0.97 is slightly above 5 % error in the beginning, but gives a perfect match at the end. For predictions, it is generally more accepted to be accurate in the beginning and a bit off later in time. Hence, it will be better to tune on a test with low GLR and use this correlation when predicting future performance than using a correlation tuned to higher GLR. Still, one should be aware of the errors introduced. In figures 6.3 and 6.4, the case of no-tuning lies within the 5 % error from base case for the entire time range. This implies that no-tuning could be a better choice of correlation when creating VLP curves.

The same trends are observed regardless of  $PI$ . Lowest values of  $PI$  give highest rates and highest value of  $PI$  give lowest rates. The deviation between highest and lowest rates, namely the effect of tuning, is affected by  $PI$ , see figures 6.5 and 6.6.

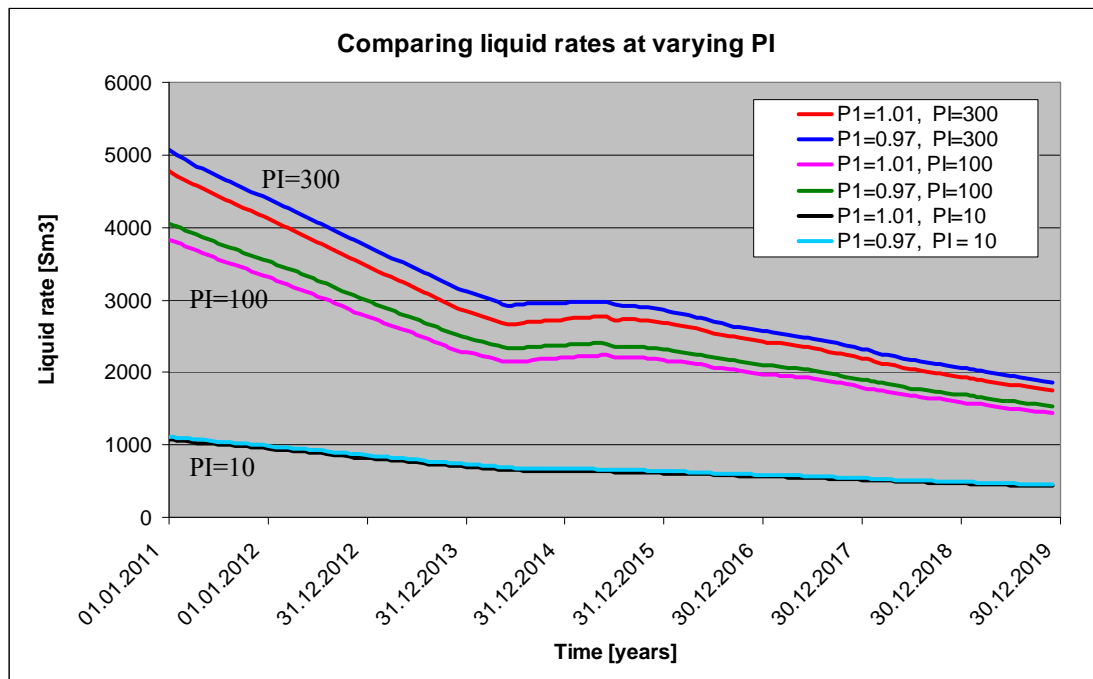


**Figure 6.5:** Liquid rates from simulation at varying  $PI$

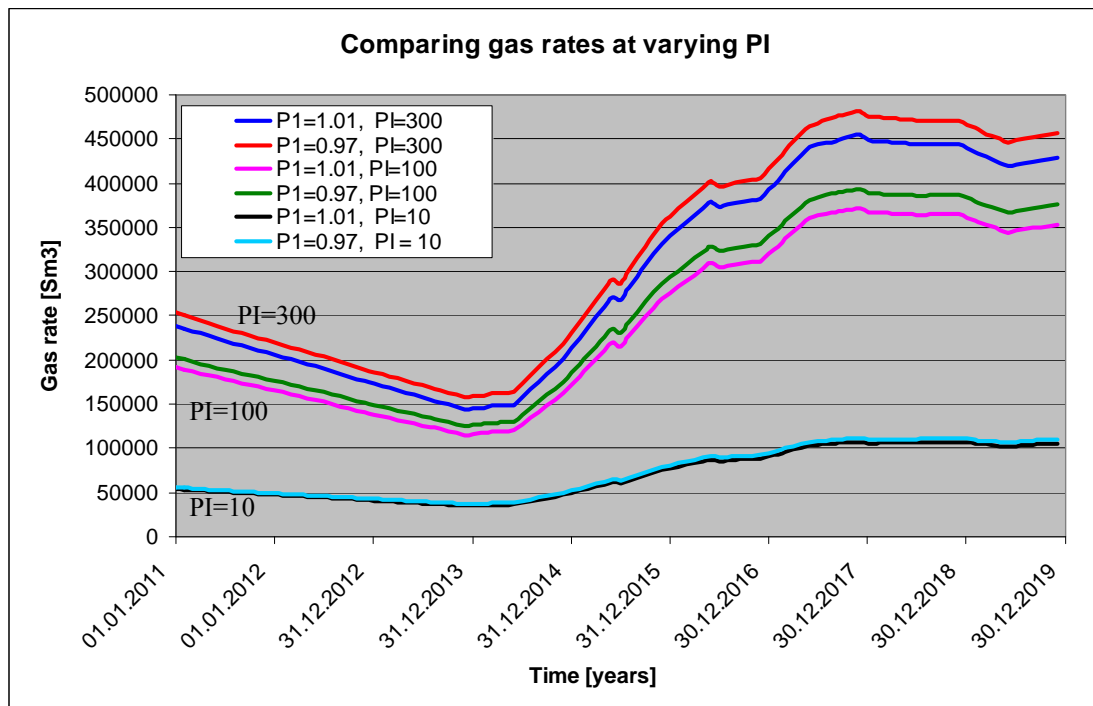


**Figure 6.6:** Gas rates from simulation at varying PI

Increasing PI gives higher deliverability from the reservoir, resulting in higher production rates. The opposite is true by lowering PI. This is expressed graphically in figure 6.1. Intersection for high PI gives a higher rate than intersection for low PI. Figure 6.1 also shows that a change in the VLP curve will have larger effect on rates when PI is high.

Using tuned correlations, less deviation is observed when  $PI = 10 \text{ m}^3/\text{d}/\text{bar}$ , and larger deviation is observed when  $PI = 300 \text{ m}^3/\text{d}/\text{bar}$ , see figure 6.5 and 6.6. At higher rates a larger effect of tuning will be evident, because of larger pressure loss in the tubing. Very low PI will give reservoir limited production, and the production rates will be low. Hence, the effect of pressure loss in the tubing will be very small if not negligible. As PI increase, total pressure loss in tubing will be larger and production will be tubing limited. Tuning the hydrostatic gradient will have a larger effect when production is tubing limited, because main pressure loss will be in the tubing.

### 6.2.2 High GLR Development

A similar study to the one described above was performed with a more radical GLR development. All input data except GLR development are the same as above, and PI was kept constant to 100 m<sup>3</sup>/d/bar. GLR was set to increase from 50 Sm<sup>3</sup>/Sm<sup>3</sup> to 2850 Sm<sup>3</sup>/Sm<sup>3</sup> in a time frame of 10 years, see figure 6.7. This scenario is more relevant for wells in the Statfjord Formation than in the Brent Group. Real production tests in corresponding GLR range was tuned in Prosper and the correlations obtained used in simulations. Table 6.2 describes GLR development and tuning parameters.

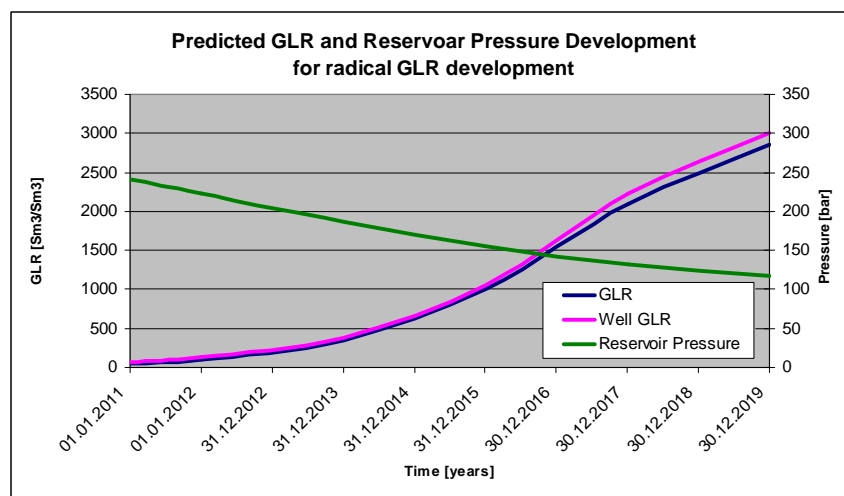


**Figure 6.7:** Radical GLR development and reservoir pressure from full field model

	01.01.2011	01.01.2012	01.01.2014	01.01.2016	01.01.2018
Start date	01.01.2011	01.01.2012	01.01.2014	01.01.2016	01.01.2018
End date	01.01.2012	01.01.2014	01.01.2016	01.01.2018	01.01.2020
GLR range [Sm <sup>3</sup> /Sm <sup>3</sup> ]	50 - 100	100 - 350	350 - 1000	1000 - 2100	2100 - 2850
Well GLR range [Sm <sup>3</sup> /Sm <sup>3</sup> ]	70 - 140	140 - 380	380 - 1060	1060 - 2225	2225 - 3000
Reservoir pressure [Bar]	241 - 223	223 - 187	187 - 155	155 - 132	132 - 117
P1	1.01	0.97	0.97	0.97	0.94
P2	1.00	1.00	0.59	0.50	0.34

The result of changing correlation with GLR range versus using one correlation for the entire prediction is shown in figures 6.8 and 6.9. The same trend regarding tuning and rates are observed as for simulation case for the Brent Group. However, a larger deviation between the correlations is evident with a more radical GLR development. Hence, tuning has a larger effect on production rates in this case. The increased effect of tuning is believed to be a result of both higher gas rates, and tuning on both hydrostatic and friction gradients.

Notice that increasing GLR will lower the hydrostatic gradient but at the same time friction will increase. Consequently, this leads to a larger source of error when using tuned correlations in simulations. 5 % error bars are included on the graph representing production forecast when changing correlation with GLR. None of the simulations with constant correlation are within the 5 % error for the entire time range.

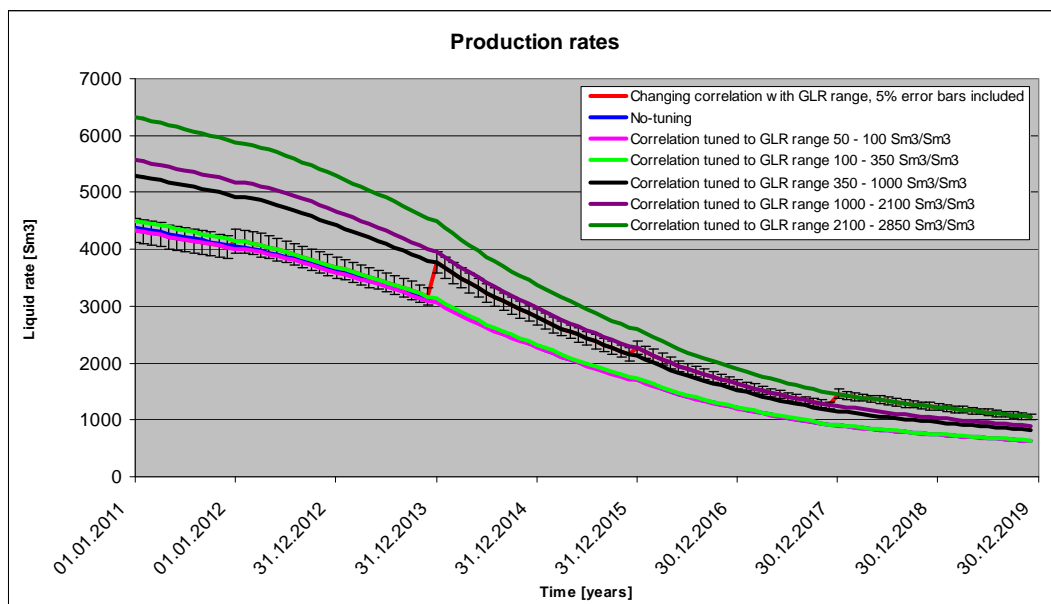


**Figure 6.8:** Liquid rates from simulation with larger GLR development

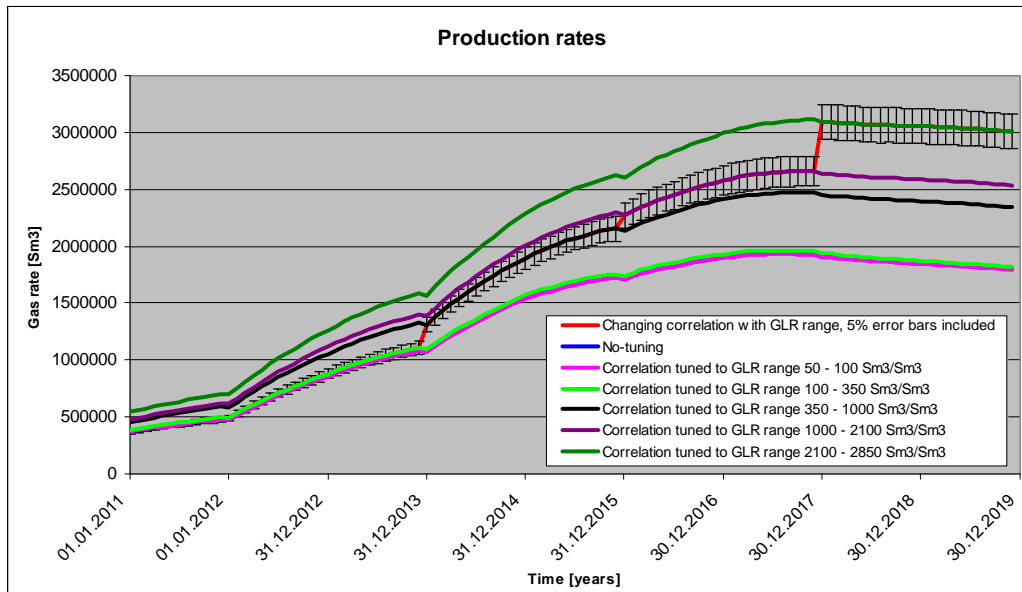


**Figure 6.9:** Gas rates from simulation with larger GLR development

No-tuning and the correlations tuned to GLR ranges of 50 – 350  $\text{Sm}^3/\text{Sm}^3$  give the same results. This implies that increasing parameter 1 to 1.01 or reducing it to 0.97 has little effect on production rates. There is a larger deviation between correlations tuned to GLR range 50 – 350  $\text{Sm}^3/\text{Sm}^3$  and 350 – 1000  $\text{Sm}^3/\text{Sm}^3$ . Only P2 is changed between these correlations, still larger production rates are observed. This shows that friction is important at higher GLR, and changing P2 gives an effect. The highest rates are observed by tuning on highest GLR range because both P1 and P2 are reduced.

Results from simulations support previous analysis on tuning in chapter 5. Tuning a correlation will improve the accuracy for the correlation for a respective GLR range. In chapter 4 it was found that too low pressure drops were predicted for tests with low GLR and especially those including gas-lift. This will be the scenario for most of the wells in the Statfjord Field. Tuning a correlation to such production tests will give conservative rates when predicting future performance. This will give larger error than not tuning when GLR increase, because generally P1 needs to be reduced as GLR increase. Using a correlation tuned with slightly reduced P1 and P2 are believed to give the most accurate production forecast. If a very low GLR is observed, and it is believed to increase with time, no-tuning could be a better option than tuning on test data giving low GLR. Using a correlation tuned to high GLR will give optimistic production rates and is not recommended.

### 6.3 Sensitivity Analysis

To study the effect of tuning a correlation more thoroughly a set of simulations was run with varying input parameters, as described in table 6.3. All the simulation cases were run for various tuning of the hydrostatic term (P1 was varied). Input data studied are typical for the Brent Group. P2 was kept constant to one, because the GLR will be in a range generating little friction. Water cut was kept constant at 80 %, reservoir pressure at 241 bar, PI at 100 m<sup>3</sup>/d/bar and time frame was one year for all simulations. By this, only the desirable input data are changed respectively.

**Table 6.3: Setup for sensitivity analyse when tuning with P1**

Simulation	GLR [Sm <sup>3</sup> /Sm <sup>3</sup> ]		WHP [Bar]		Diameter [inches]		Gas-lift rate [kSm <sup>3</sup> /d]	
	50	200	20	40	7	5	100	0
1	x		x		x		x	
2		x	x		x		x	
3	x			x	x		x	
4		x		x	x		x	
5	x		x			x	x	
6		x	x			x	x	
7	x			x		x	x	
8		x		x		x	x	
9	x		x		x			x
10		x	x		x			x
11	x			x	x			x
12		x		x	x			x
13	x		x			x		x
14		x	x			x		x
15	x			x		x		x
16		x		x		x		x

One Prosper file for each tuning was set up and only one input parameter was changed at the time. To study how tuning on the hydrostatic term is affected by various input data, percentage change in liquid rate was calculated as

$$\%q_{L_{change}} = \frac{q_{L_{tuned}} - q_L}{q_L} * 100 . \dots\dots\dots(6.1)$$

Percentage change in liquid rate will describe change in liquid rate, from no-tuning, when altering P1. Only liquid rates are presented. Relative changes will be the same for the gas phase, due to constant production GLR.

Figure 6.10 shows that effect of tuning is dependent on input data, and that magnitude of errors introduced by tuning P1 will change with input data. Some of the simulations give high percentage change in rate by tuning, while others show less. Regardless of input data used in this analysis, liquid rates change less than 10 % if P1 is changed +/- 3 % (marked with dashed lines on figure 6.10). For the Statfjord Field, this range will cover most of the historical tuning parameters, when tuning correlation to production tests.

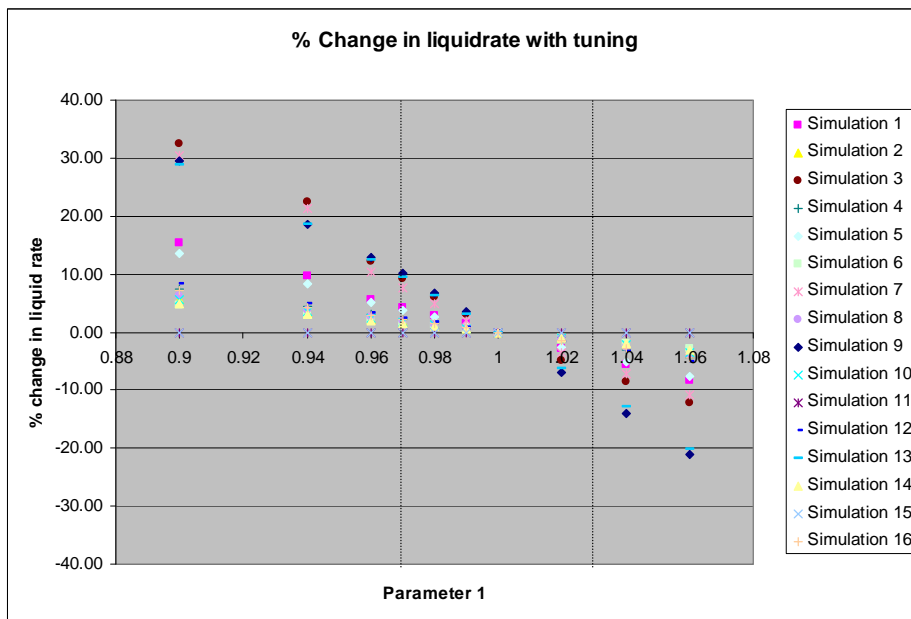


**Figure 6.10:** Percentage change in liquid rate with varying input parameters and correlations

Little effect on tuning was observed by changing tubing size. Altering 400 m of 7 inch tubing to 5 inch tubing gave reduced rates, but the effect on tuning is regarded negligible, see figure B.55 in Appendix B. Changing WHP, GLR and if the well is on



gas-lift has an effect on tuning. Figure 6.11 shows how GLR and WHP affect tuning with P1.

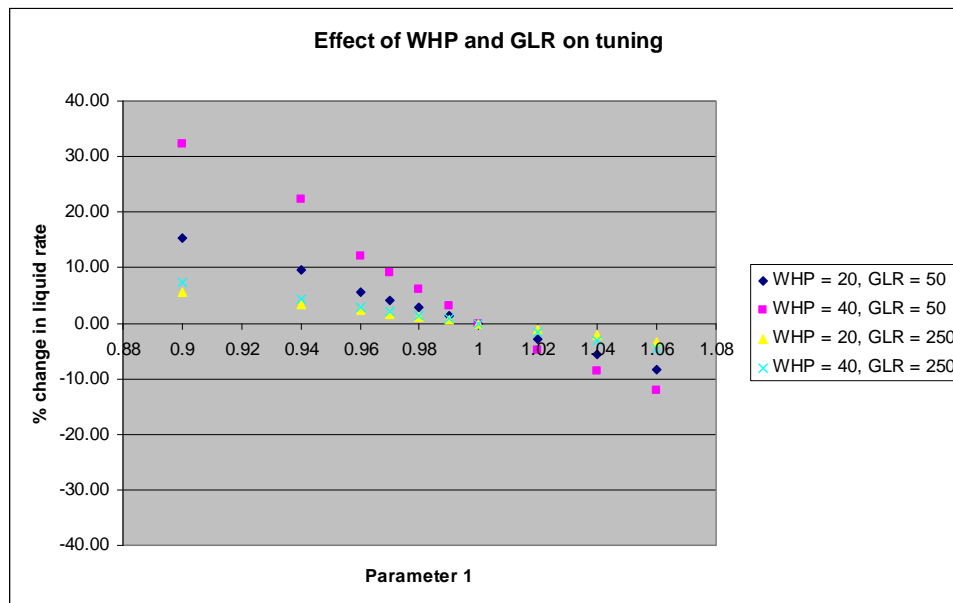


**Figure 6.11:** Percentage change in liquid rate, the effect of WHP and GLR on tuning

The effect of tuning is higher for the case of higher WHP. When  $P1 = 0.9$ , and WHP = 40 bar, the liquid rate is increased by more than 30 % compared to the case of no-tuning. When WHP = 20 bar, liquid rate is increased by 15 %. This is believed to be a result of a lighter hydrostatic column in the tubing when WHP is low. Evaporation from the liquid phase into the gas phase may happen deeper in the tubing, giving a lighter column. Tuning on P1 will thereby have a larger effect when WHP is high, because the hydrostatic contribution to the pressure drop will be higher. This effect is most pronounced when  $GLR = 50 \text{ Sm}^3/\text{Sm}^3$ , because the hydrostatic contribution will be highest with low GLR.

Figure 6.11 also shows that tuning has a larger effect when GLR is low, because of a heavier hydrostatic column. Increased GLR reduces the hydrostatic contribution, giving a lighter column. Hence, changing P1 will give a smaller effect when  $GLR = 200 \text{ Sm}^3/\text{Sm}^3$  compared to the case of  $GLR = 50 \text{ Sm}^3/\text{Sm}^3$ . Tuning on tests with high GLR normally results in lowering P1. This lowering will have a larger effect to the pressure loss when GLR is low and hydrostatic pressure losses higher. Using a correlation tuned to high GLR when predicting rates at lower GLR should thereby not

be trusted. If P1 is slightly reduced when tuning on lower GLR, errors will not increase with GLR. By using this correlation to predict rates as GLR increase the error will not increase because effect of tuning will decrease as GLR increase. Still, the rates predicted at higher GLR will be conservative, because higher GLR will demand further lowering of P1. Gas-lift gives the same effect on tuning as GLR. Gas injected into the tubing gives a lighter column making the fluids easier to lift. A lighter column will be less affected by changing P1.

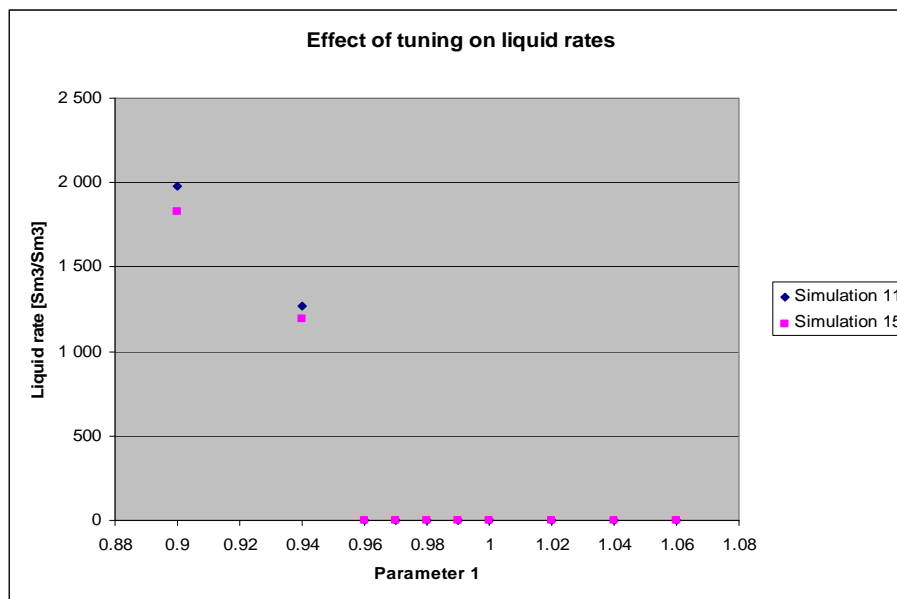


**Figure 6.12:** *Liquid rate from simulations with  $GLR = 50 \text{ Sm}^3/\text{Sm}^3$ ,  $WHP = 40 \text{ bar}$  and no artificial gas-lift*

For simulations 11 and 15, only the lowest values of P1 gave production, see figure 6.12. For those simulations both WHP and GLR was low, and they were run without gas-lift. Such low values of P1 are not suspected to be used when creating VLP curves. Still, one should be aware of this effect regarding lifetime prediction for a well or field. If low values of parameter 1 is used an optimistic prediction will result, and lifetime may be overestimated. This will be true regardless of input parameters.

## 6.4 Conclusions

From studying errors that might be introduced when using tuned correlations in simulations, and sensitivity of input data on tuning it was found that:

- Production will be reservoir limited at low productivity index, and effects of using tuned correlations are very small.
- High productivity index gives larger effect of tuned correlations because production will be tubing limited
- Errors introduced by tuned correlations give little effect on simulation results with GLR development expected for the Brent Gp. ( $50 - 300 \text{ Sm}^3/\text{Sm}^3$ ). Only a small effect of changing correlation with GLR was observed. Hence, one correlation may be used for the entire time frame.
- If a more radical GLR development is believed to arise, caution should be paid to how correlations are tuned. It is recommended to change tuning parameters as a function of GLR. Correlations to be used in respective GLR ranges should be based on an analysis of tuning.
- No-tuning is recommended to be used for predictions if tuning to test data results in increasing tuning parameters.
- If tuning to test data result in a small reduction of tuning parameters, this correlation is preferred over no-tuning when predicting future performance.
- It is not recommended to use a correlation where tuning parameters are increased, if GLR is predicted to increase.
- Errors introduced by tuning correlations to a test with low GLR will not increase with time. Effect of tuning will be less evident as GLR increase. (Still, rates will be conservative because P1 probably should be lowered as GLR increase)
- It is not recommended to use a correlation tuned to a higher GLR range than expected with time. Rates will be optimistic, especially in the beginning as tuning parameters will have a larger effect on lower GLR.

## 7 Main Conclusions and Recommendations

From studying differences in multiphase-flow correlations, and their accuracy when predicting bottomhole pressures it was found that PE, PE2 and PE3 are the most accurate and consistent correlations in Prosper. For liquid wells the hydrostatic gradient will be the main contribution to total pressure loss, and estimations of liquid holdup will be the important factor for accuracy. As gas-rate increase, hydrostatic pressure loss will decrease and frictional pressure drop increase. Largest deviation between correlations is observed at high gas-rate. A correlation between accuracy of correlations and GLR was observed. At low GLR and tests including gas-lift correlations give too low pressures. At higher GLR too high pressures are predicted.

It was done a study on tuning correlations to see if correlations could be modified in a way giving higher accuracy for a wider GLR range. By tuning in Prosper, it seems impossible to tune a correlation in a way giving increased accuracy for a wide GLR range. Modification to the liquid holdup, either by modifying equations for estimating liquid holdup or by modifying flow regime boundaries, is believed to enable higher accuracy for a wider range of GLR.

Little effect of using tuned correlations in simulation was observed for a GLR development of 50 to 300  $\text{Sm}^3/\text{Sm}^3$  in 10 years. By increasing GLR development (50 to 2850  $\text{Sm}^3/\text{Sm}^3$ ) a larger effect of using tuned correlations are observed. In addition, the effect of tuning will depend on input data. At low production index production will be reservoir limited, and effects of using tuned correlations small. For higher productivity indexes where production is tubing limited, effect of using tuned correlations will be larger. A heavier column will be more influenced by changing the hydrostatic gradient. Using a correlation tuned to tests data with high GLR will give optimistic rates at lower GLR, because pressure will be underestimated. Using a correlation tuned to low GLR is believed to give conservative production rates. No-tuning is believed to give more accurate prediction of production rates as GLR increase, compared to a correlation where parameter 1 is increased.

## 7.1 Recommendations

When generating VLP curves for the Statfjord full field model, the following is recommended:

- Use one of the following multiphase-flow correlations, PE, PE2 or PE3.
- Take all tests of high quality into consideration when choosing correlation and tuning of it to use in prediction. Emphasise on tests covering the expected GLR range with time.
- Evaluate tuning parameters given by tuning with Prosper. Tuning on the friction term will have little impact at low GLR. As GLR increase, tuning on the friction term will give larger impact.
- Use tuning parameters fit for purpose. For a narrow GLR range (as for the Brent Group, 50 – 300 Sm<sup>3</sup>/Sm<sup>3</sup>) one correlation may be used for the entire time range. If GLR is expected to cover a wider range, change tuning parameters as a function of GLR development.
- Create VLP curves based on GLR range expected in prediction, given it is only possible to use one sett of tuning parameters in Prosper when creating VLP curves. For the full field model in Eclipse, use the keyword ACTION to pick the relevant lift curve.

## 8 Sources of Error

Listed below are possible sources of error, effect and presence may vary.

- Errors while testing due to;
  - Rate measurements
  - Testing procedure
  - Well stability
  - Operator error
- Error in gauge measurements of temperature and pressure
- Error in assumed parameters
  - Roughness factor
  - Temperature profile
  - GLR development
  - Pressure development
- Errors in PVT data
- Human error when handling large quantities of data
- Errors in Prosper calculations
- Errors in the correlations

## 9 References

Beggs, H.D. and Brill, J.P. 1973. A Study of Two-Phase Flow in Inclined Pipes. *J Pet Technol*:607-617; *Trans.*, AIME, **255**. SPE 4007-PA.

Brennen, C.E. 2005. *Fundamentals of Multiphase Flow*. Cambridge University press. ISBN 0-521-84804-0.

Brill, J.P. 1987. Multiphase Flow in Wells. *J Pet Technol*: 15-21. Distinguished Author Series. SPE 16242-PA.

Brill, J.P. and Mukherjee, H. 1999. *Multiphase Flow in Wells*. Monograph series, SPE, Richardson, Texas **17**: 2-69.

Duns, H.Jr. and Ros, N.C.J. 1963. Vertical Flow of Gas and Liquid Mixtures in Wells. Section II – Paper 22 – PD 6, Netherlands. WPC 10132.

Ellul, I.R., Saether, G. and Shippen, M.E. 2004. *The Modeling of Multiphase Systems under Steady-State and Transient Conditions – A Tutorial*. PSIG 0403 presented at the PSIG Annual Meeting, Palm Springs, California, 20-22 October.

Fancher, JR.G.H and Brown, K.E. 1963. Prediction of Pressure Gradients for Multiphase Flow in Tubing. *SPE J*: 59-69. SPE 440-PA.

Gould, T.L., Tek, M.R. and Katz, D.K. 1974. Two-Phase Flow Through Vertical, Inclined, or Curved Pipe. *J Pet Technol*: 915-926. SPE 4487-PA.

Gray, H.E. 1974. Vertical Flow Correlation in Gas Wells. In *User manual for API 14B, Subsurface controlled safety valve sizing computer program*, Appendix B. Washington, DC: API.

Hagedorn, A.R. and Brown, K.E. 1965. Experimental Study of Pressure Gradients Occuring During Continuous Two-Phase Flow in Small-Diameter Vertical Conduits. *J Pet Technol*: 475-484. SPE 940-PA.

Orkiszewski, J. 1967. Predicting Two-Phase Pressure Drops in Vertical Pipe. *J Pet Technol*: 829-938. SPE 1546-PA.

Persad, S. 2005. Evaluation of Multiphase-Flow Correlations for Gas Wells Located Off the Trinidad Southeast Coast. Paper SPE 93544 presented at the 2005 Latin American and Caribbean Petroleum Engineering Conference, Rio de Janeiro, Brazil, 20-23 June.

Petroleum Experts 2010. *User Manual for IPM Prosper*, version 11.5

Poettmann, F.H. and Carpenter, P.G. 1952. *The Multiphase Flow of Gas, Oil, and Water Through Vertical Flow Strings with Application to the Design of Gas-lift Installations*. API 52-257.

Pucknell, J.K., Manson, J.N.E. and Vervest, E.G. 1993. An Evaluation of Recent “Mechanistic” Models of Multiphase Flow for Predicting Pressure Drops in Oil and Gas Wells. Paper SPE 26682 presented at the Offshore European Conference, Aberdeen, 7-10 September.

Reinicke, K.M., Remer, R.J. and Hueni, G. 1987. Comparison of Measured and Predicted Pressure Drops in Tubing for High-Water-Cut Gas Wells. *SPE Prod Eng*: 165-177. SPE 13279-PA.

Time, R.W. 2009. *Two-Phase Flow in Pipelines*. Course compendium, University of Stavanger.

Trick, M.D. 2003. *Comparison of Correlations For Predicting Wellbore Pressure Losses in Gas-Condensate and Gas-Water Wells*. PETSOC 2003-019.



Yahaya, A.U. and Gahtani, A.A. 2010. A Comparative Study Between Empirical Correlations & Mechanistic Models of Vertical Multiphase Flow. Paper SPE 139631 presented at the 2010 SPE/DGS Annual Technical Symposium and Exhibition, Al-Khobar, Saudi Arabia, 04-07 April.

Zavareh, F., Hill, A.D. and Podio, A.L. 1988. Flow Regimes in Vertical and Inclined Oil/Water Flow in Pipes. Paper SPE 18215 presented at the SPE 63<sup>rd</sup> Annual Technical Conference and Exhibition, Houston, Texas, 02-05 October.

## Appendix A Description of Wells

<b>Table A.1: Description of wells and test data</b>						
<b>Property</b>	<b>A-2</b>	<b>A-40</b>	<b>B-1</b>	<b>B-11</b>	<b>C-12</b>	<b>C-41</b>
<b>Max inclination above DHPG [Degrees]</b>	46.5	85	46.6	66.7	60.5	24-37
<b>Depth DHPG m MD</b>	2311	3406	1908	3628	2527	2234
<b>Depth DHPG m TVD</b>	2025	2081	1702	2581	1929	2126
<b>Tubing size [inch]</b>	7.0 - 5.5	7.0 - 5.5	7.0 - 5.5	7.0 - 5.5	7.0 - 5.5	7.0 - 5.5
<b>Roughness factor [m]</b>	1.524*10 <sup>-5</sup>	1.524*10 <sup>-5</sup>	1.524*10 <sup>-5</sup>	1.524*10 <sup>-5</sup>	4.500*10 <sup>-5</sup>	4.500*10 <sup>-5</sup>
<b>Overall Heat Coefficient [W/m<sup>2</sup>/K]</b>	16.5	12.1013	10	10	25.8541	71.0649
<b>Temperature profile in Prosper</b>	Rough Approximation	Rough Approximation	Rough Approximation	Rough Approximation	Rough Approximation	Rough Approximation
<b>Number of tests</b>	33	29	28	25	31	57
<b>GLR range [Sm<sup>3</sup>/Sm<sup>3</sup>]</b>	70-3800	20 - 5395	0 - 1500	0 - 4070	205 - 9760	25 - 1825
<b>WCT range [%]</b>	0-95	0 - 100	85 - 100	20 - 100	0 - 100	0 - 85
<b>Gas rate range [kSm<sup>3</sup>]</b>	105-1250	16 - 1210	0 - 800	0 - 1150	70 - 1265	20 - 275
<b>Liquid rate range [Sm<sup>3</sup>]</b>	240 - 2840	145 - 1070	370 - 1220	235 - 1324	70 - 620	90 - 865
<b>WHP range [Bar]</b>	35 - 215	25 - 220	20 - 140	60 - 205	40 - 210	35 - 185

<b>Table A.2: PVT data (for all wells)</b>	
<b>Solution GOR [Sm<sup>3</sup>/Sm<sup>3</sup>]</b>	154.7
<b>Oil Gravity [Kg/m<sup>3</sup>]</b>	837.7
<b>Gas Gravity [sp. Gravity]</b>	0.8483
<b>Water Salinity [ppm]</b>	20023.3
<b>Mole Percent H<sub>2</sub>S [%]</b>	0
<b>Mole Percent CO<sub>2</sub> [%]</b>	0.36
<b>Mole Percent N<sub>2</sub> [%]</b>	0.59

**Table A.3: Deviation survey for A-2 (in Prosty)**

Measured Depth [m]	True Vertical Depth [m]	Cumulative Displacement [m]	Angle [degrees]
0	0	0	0
200	200	0	0
310	309.99	1.48247	0.7722
500	499.92	6.6397	1.55539
700	699.51	19.4397	3.66944
900	896.08	56.3209	10.6265
1100	1083.34	126.561	20.5608
1300	1256.75	226.205	29.8824
1500	1422.4	338.277	34.0806
1700	1580.36	460.95	37.8331
1900	1731.72	591.679	40.8171
2100	1881.67	724.024	41.4313
2300	2019.25	869.185	46.5359
2500	2127.22	1037.54	57.3265
2700	2213.83	1217.81	64.3387
2900	2279.38	1406.76	70.8677
3200	2348.51	1698.69	76.6774
4157.67	2831.54	2525.62	59.7097

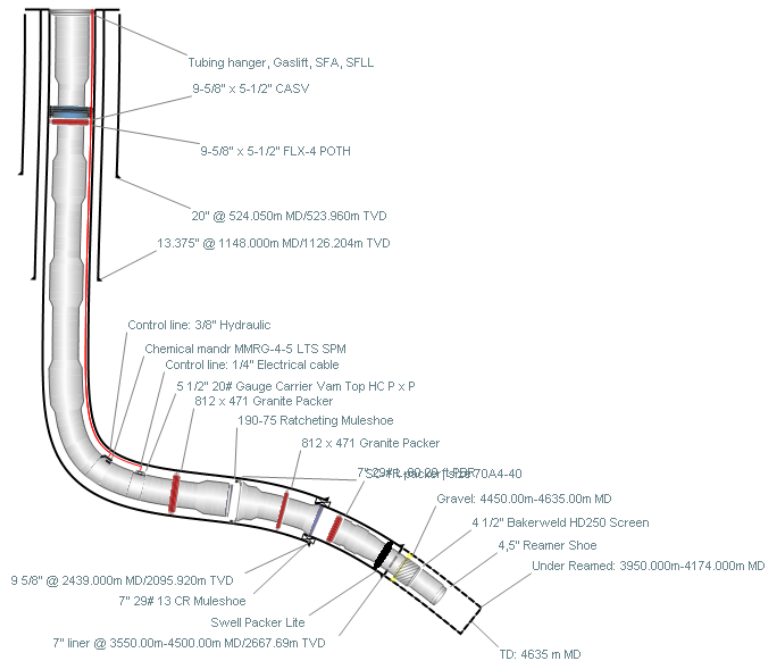


**Figure A.1: Completion schematic for A-2**

**Table A.4: Deviation survey for A-40 (in Prosty)**

Measured Depth [m]	True Vertical Depth [m]	Cumulative Displacement [m]	Angle [degrees]
0	0	0	0
450	449.59	19.2046	2.44595
600	597.75	42.6271	8.9835
770	760.35	92.2381	16.9675
870	853.17	129.446	21.844
900	881.49	139.345	19.2653
1000	977.71	166.579	15.8038
1070	1043.99	189.095	18.7631
1380	1298.88	365.535	34.6917
2160	1849.56	917.94	45.0896
2340	1948.67	1068.2	56.591
2570	2001.6	1292.02	76.6952
3200	2063.59	1918.97	84.3531
3600	2098.22	2317.46	85.0334
3888.08	2206.34	2584.49	67.9563
4146.77	2400.03	2755.96	41.5192
4539.63	2694.52	3015.99	41.4437
4631	2759.48	3080.25	44.6874

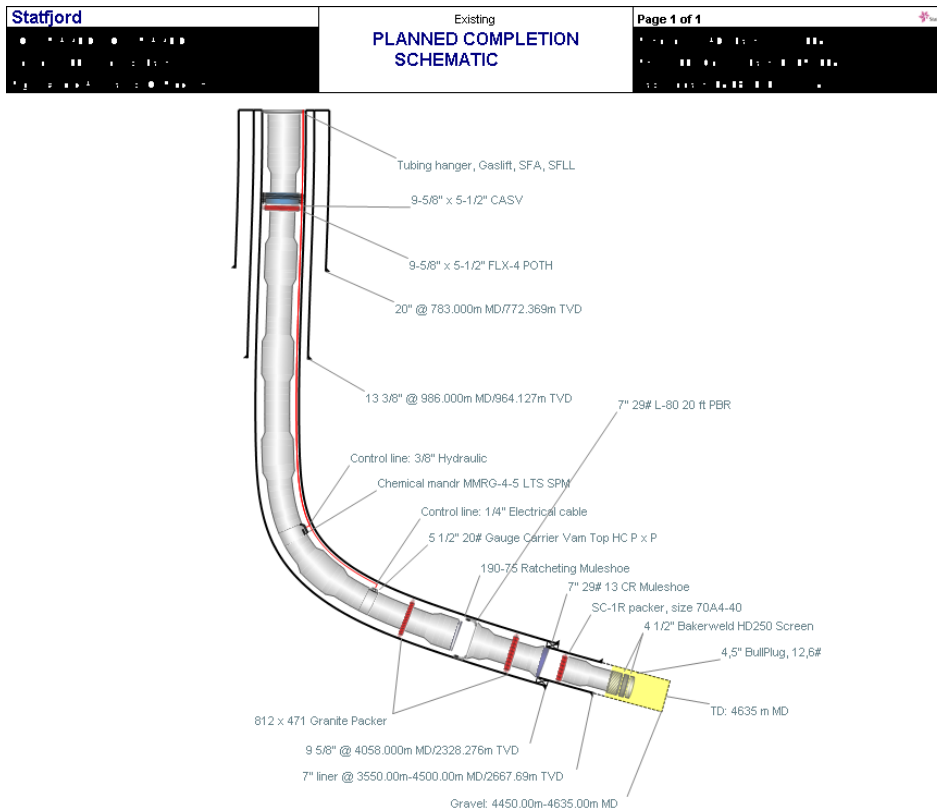


**Figure A.2: Completion schematic for A-40**

Measured Depth [m]	True Vertical Depth [m]	Cumulative Displacement [m]	Angle [degrees]
-----	-----	-----	-----
0	0	0	0
23	23	0	0
600	596.02	67.6541	6.7335
850	836.98	134.275	15.455
1100	1068.98	227.42	21.8748
1500	1422.48	414.603	27.9019
1820	1642.55	646.916	46.5502
2100	1831.61	853.45	47.5292
2250	1931	965.796	48.5015
2480	2091.45	1130.59	45.7645
2640	2183.91	1261.17	54.6988
2870	2295.11	1462.5	61.0872
3195.6	2449.24	1749.31	61.7466
3367.43	2545.68	1891.52	55.8575
3549	2667.03	2026.58	48.0611
3650	2753	2079.59	31.6589
3765	2844.14	2149.73	37.5782

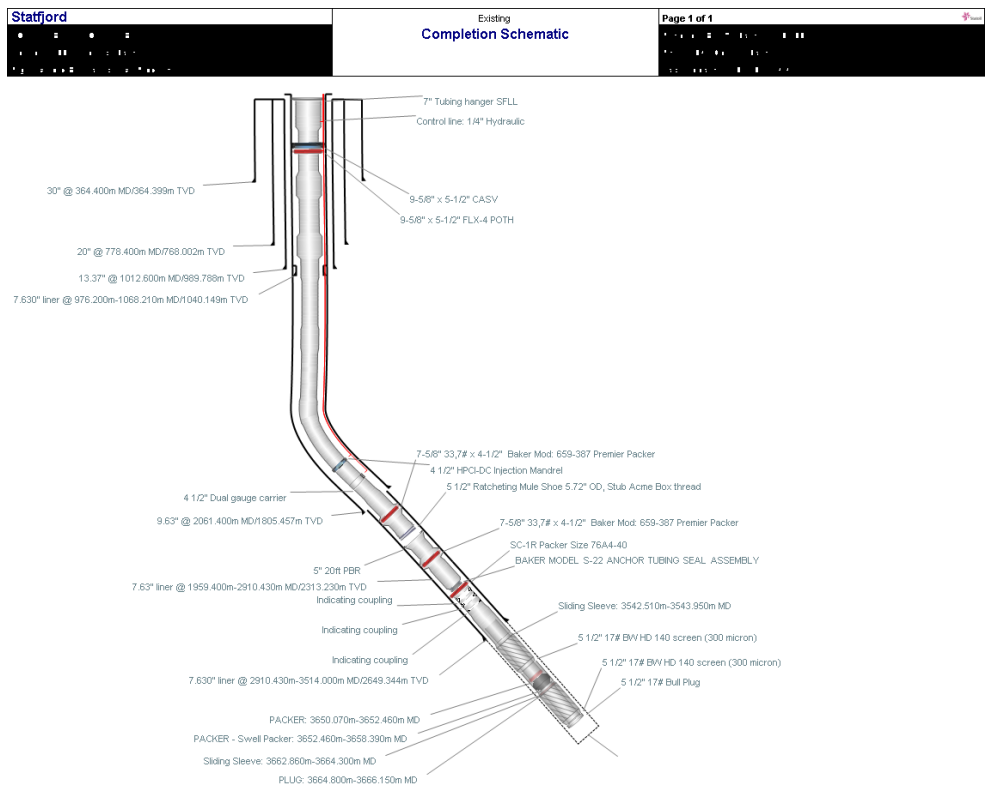


**Figure A.3: Completion schematic for B-1**

**Table A.6: Deviation survey for B-11 (in Prosty)**

Measured Depth [m]	True Vertical Depth [m]	Cumulative Displacement [m]	Angle [degrees]
-----	-----	-----	-----
0	0	0	0
513	513	0	0
696	692	38.0525	12.0015
1018	973	195.288	29.2295
1144	1064	282.437	43.7617
1454	1306	476.179	38.6803
2024	1783	788.223	33.1918
2594	2142	1230.96	50.9628
3380	2453	1952.82	66.6919
4017	2781	2498.88	59.0083

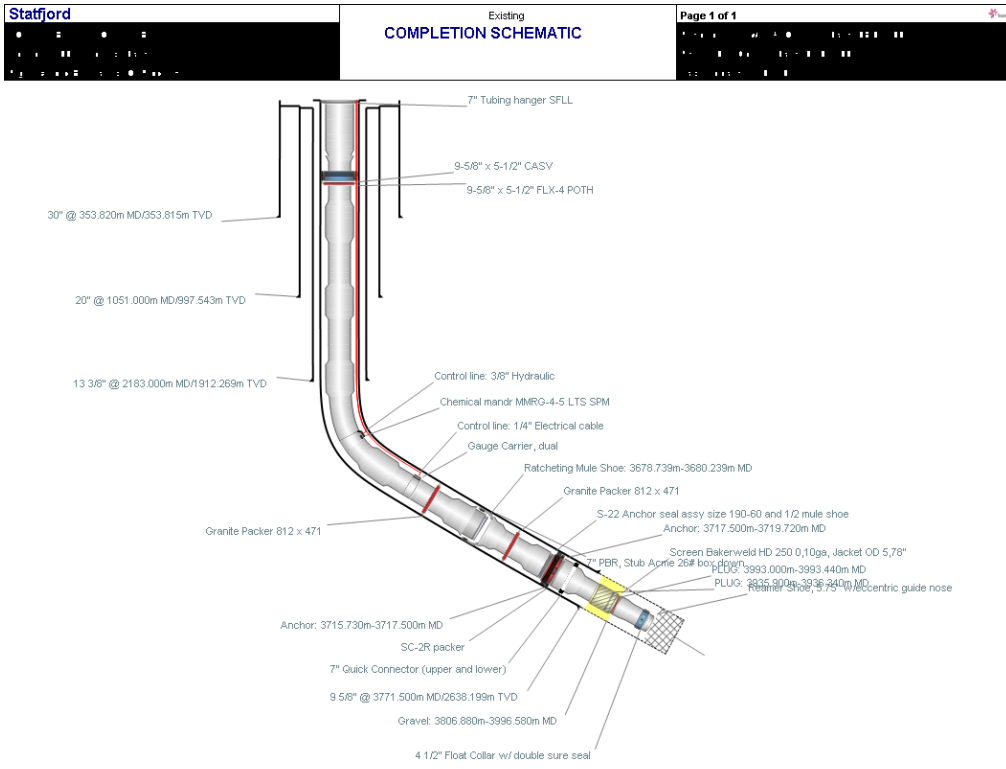


**Figure A.4: Completion schematic for B-11**

**Table A.7: Deviation survey for C-12 (in Prosty)**

Measured Depth [m]	True Vertical Depth [m]	Cumulative Displacement [m]	Angle [degrees]
-----	-----	-----	-----
0	0	0	0
490	490	0	0
540	539.95	2.23551	2.56256
800	792.53	63.9068	13.7212
1080	1061.87	140.431	15.8608
1290	1255.8	220.999	22.5603
1400	1344.4	286.191	36.3458
1630	1488.5	465.454	51.206
1900	1620.5	700.987	60.7324
2526.6	1929	1246.38	60.5055
2760	2044	1449.48	60.4807
3014.08	2152.3	1679.33	64.7706
3187.45	2232.8	1832.88	62.3334
3245.37	2267.06	1879.58	53.7361
3418.19	2395.96	1994.69	41.7667
3504.73	2469.76	2039.89	31.4841
3619.06	2576.29	2081.39	21.2865
3706.4	2660.7	2103.83	14.8829

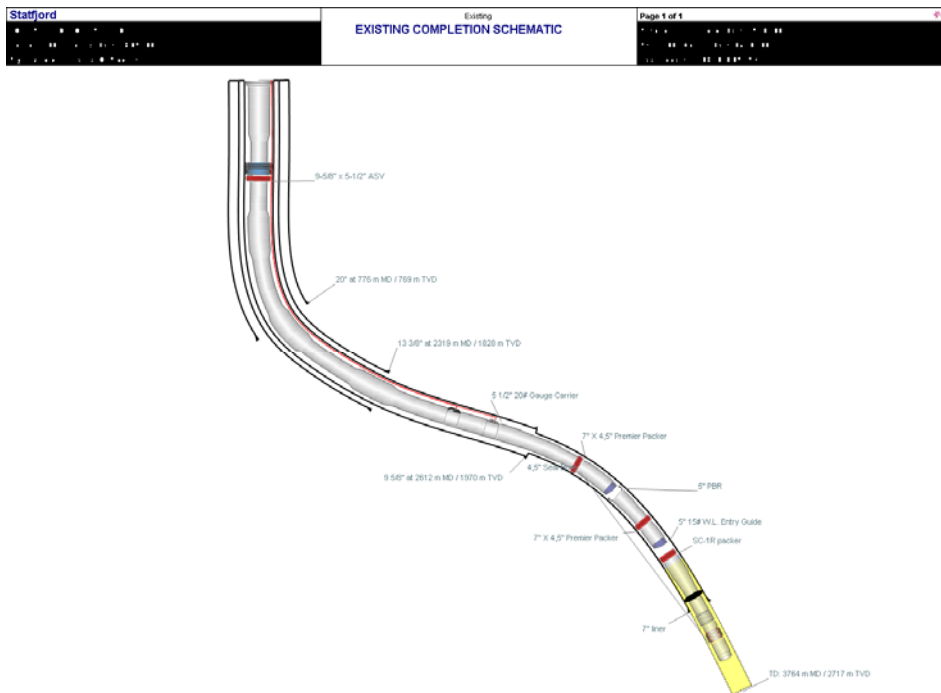


**Figure A.5: Completion schematic for C-12**

**Table A.8: Deviation survey for C-41 (in Prosty)**

Measured Depth [m]	True Vertical Depth [m]	Cumulative Displacement [m]	Angle [degrees]
0	0	0	0
430	430	0	0
719	715.3	46.0967	9.17812
834.7	822.9	88.6259	21.5665
1124.5	1083	216.423	26.1666
2020.6	1925.6	521.415	19.8985
2222.3	2109.5	604.263	24.2517
2313.9	2182.2	659.988	37.4703
2798.6	2539.1	987.946	42.5801
2886.3	2587.3	1061.21	56.6603
2971.9	2624.5	1138.31	64.2414
3058.5	2646.3	1222.12	75.4199
3233.2	2667.4	1395.54	83.0629
3290.8	2671.3	1453.01	86.1176
3404	2679	1565.94	86.0996
3550	2718	1706.64	74.5068
3662.5	2756.9	1812.2	69.7707
3790	2801	1931.83	69.7643

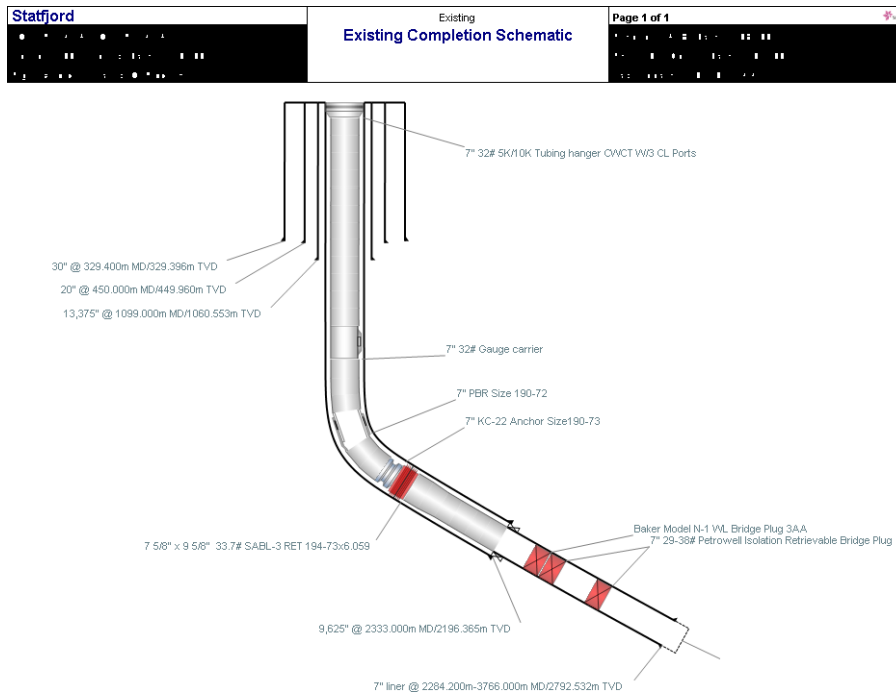


**Figure A.6: Completion schematic for C-41**



## Appendix B Figures

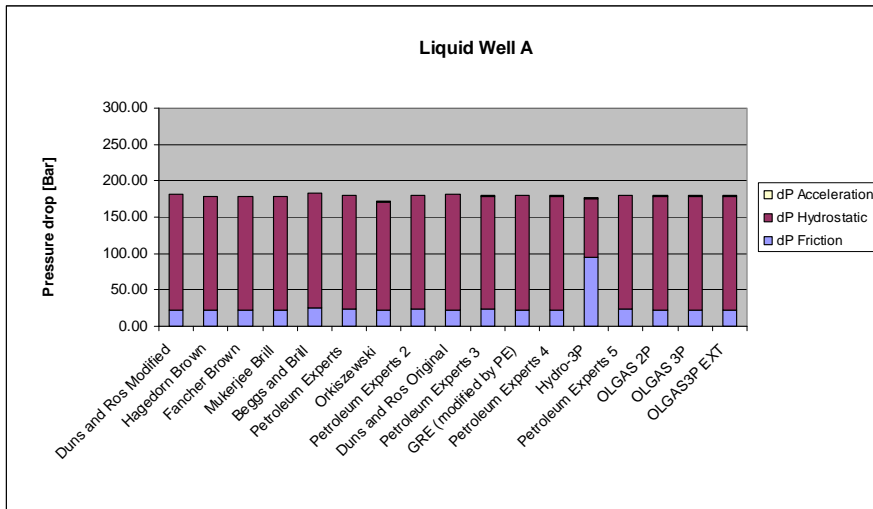


**Figure B.1:** Pressure drop by various correlations

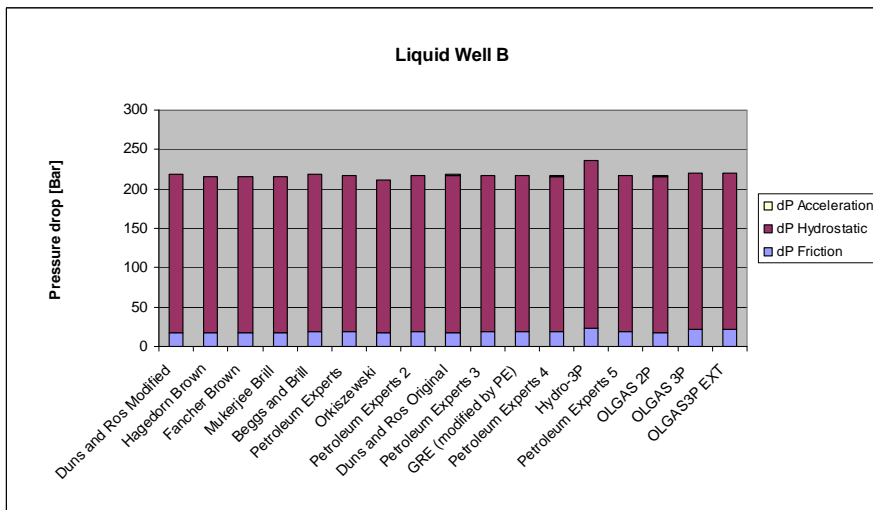


**Figure B.2:** Pressure drop by various correlations

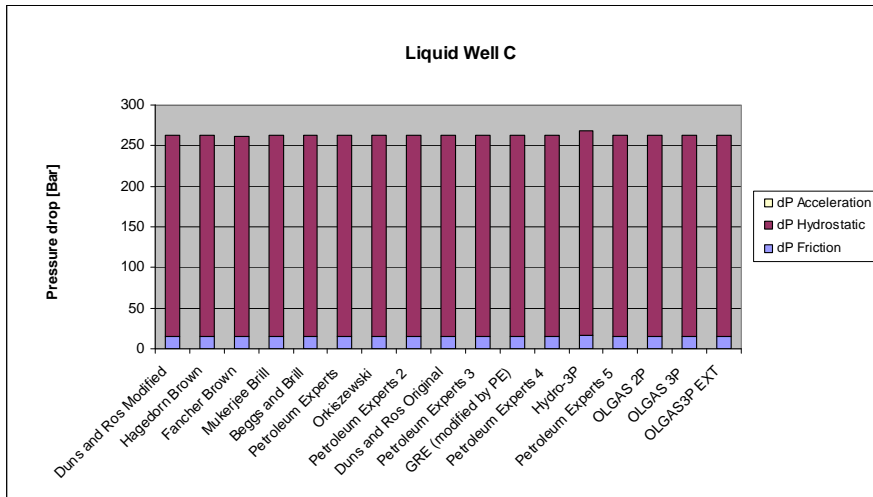


**Figure B.3:** Pressure drop by various correlations

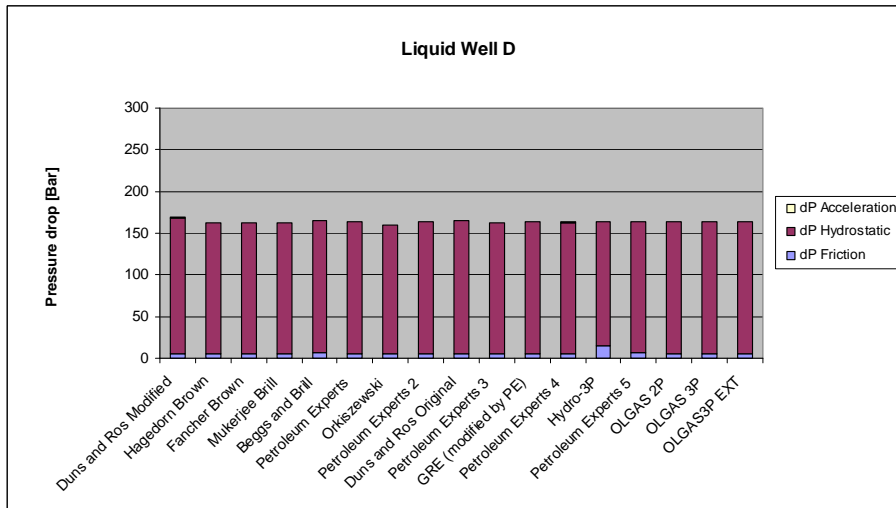


**Figure B.4:** Pressure drop by various correlations

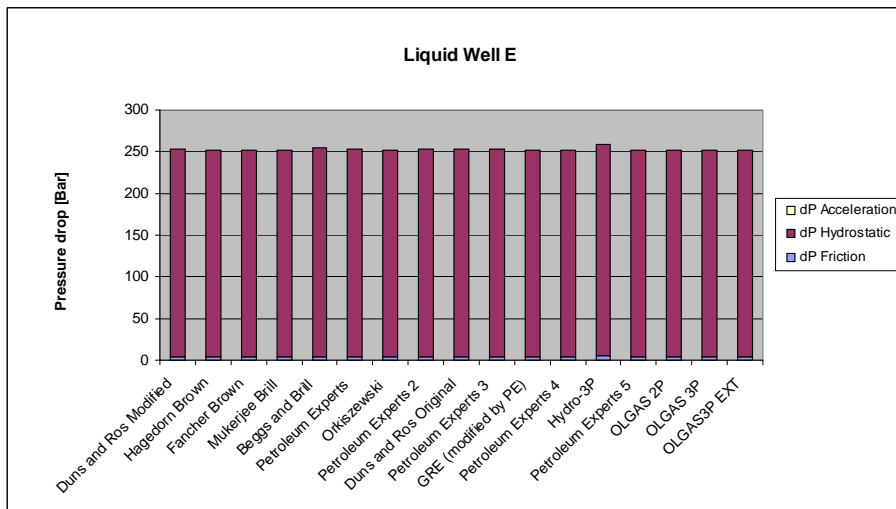


**Figure B.5:** Pressure drop by various correlations

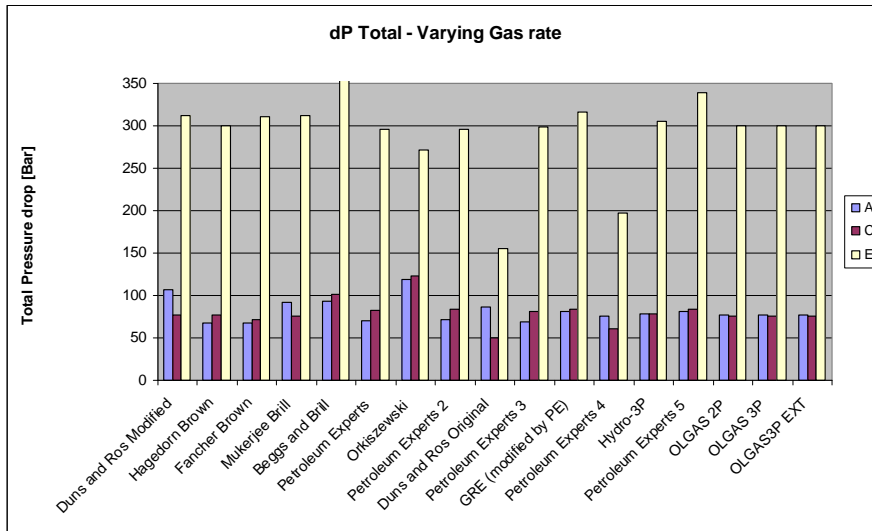


**Figure B.6:** Total pressure drop by various correlations and varying gas-rate

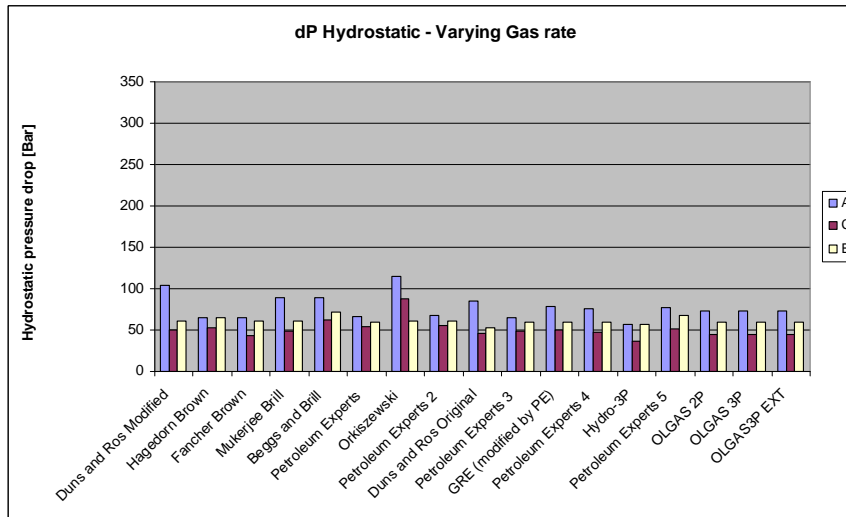


**Figure B.7:** Hydrostatic pressure drop by various correlations and varying gas-rate

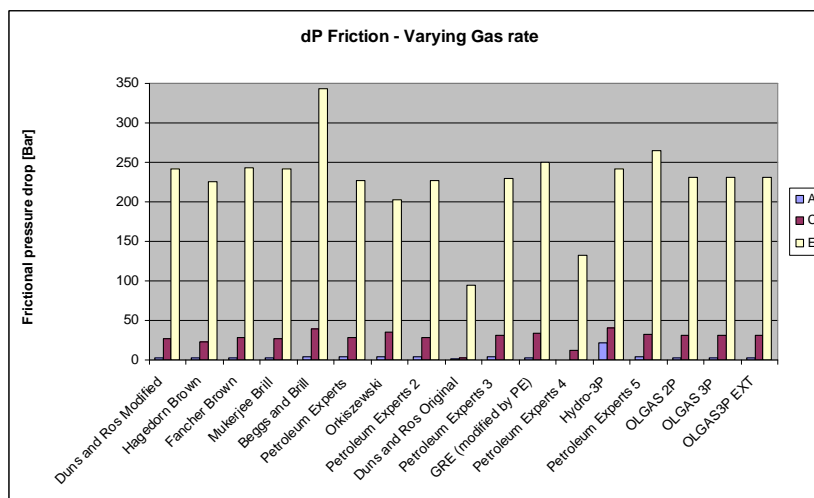


**Figure B.8:** Frictional pressure drop by various correlations and varying gas-rate

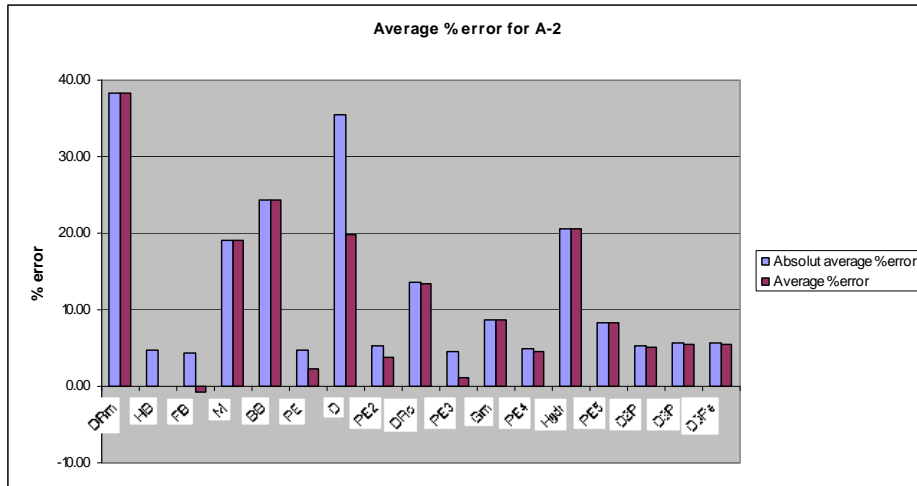


**Figure B.9:** Average percentage error in predicted pressure drop for A-2

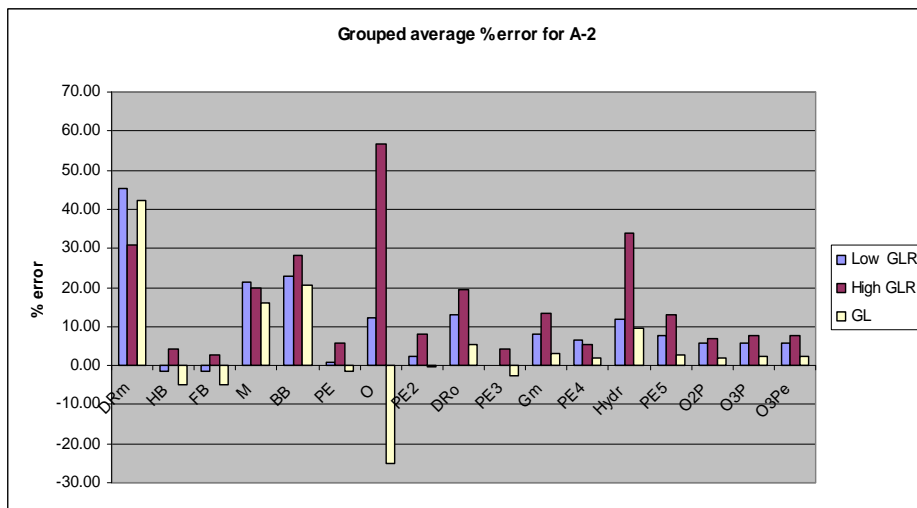


**Figure B.10:** Average percentage error for A-2, divided in groups of high and low GLR and tests including gas-lift

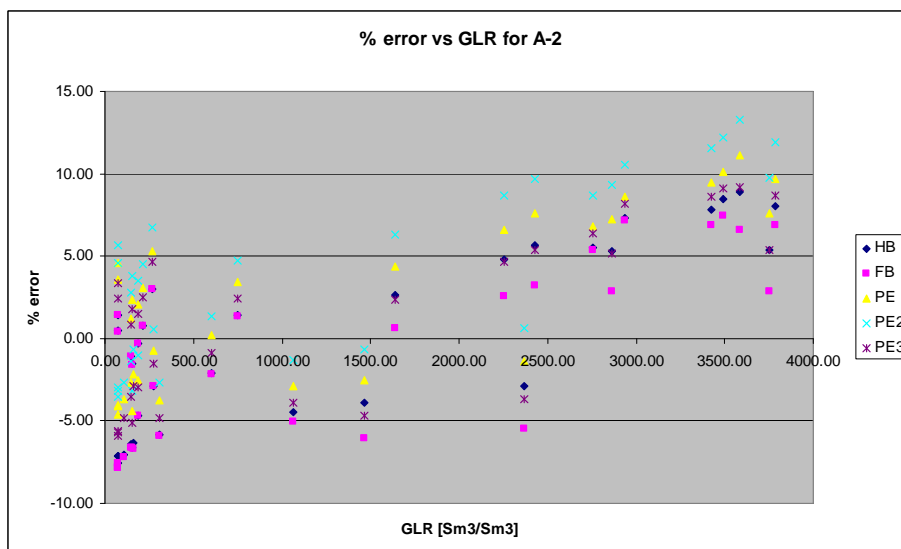


**Figure B.11:** Percentage error in predicted pressure drop versus GLR for A-2

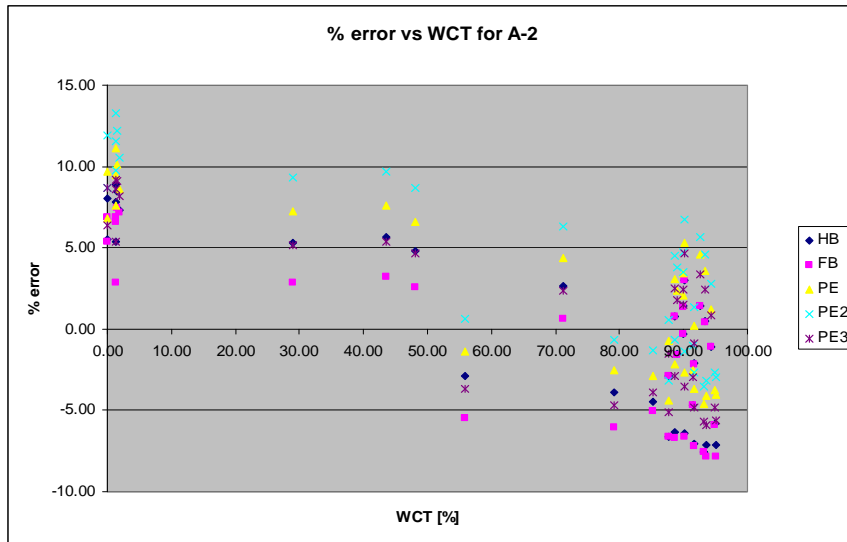


**Figure B.12:** Percentage error in predicted pressure drop versus WCT for A-2

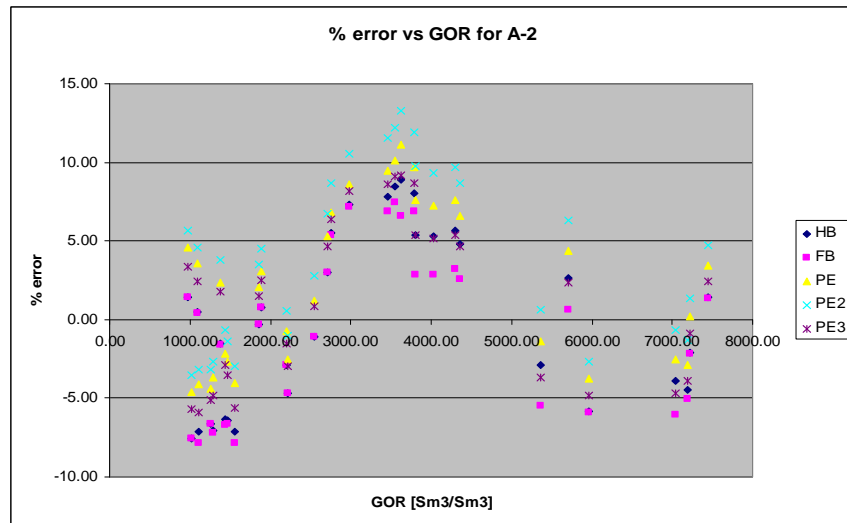


**Figure B.13:** Percentage error in predicted pressure drop versus GOR for A-2

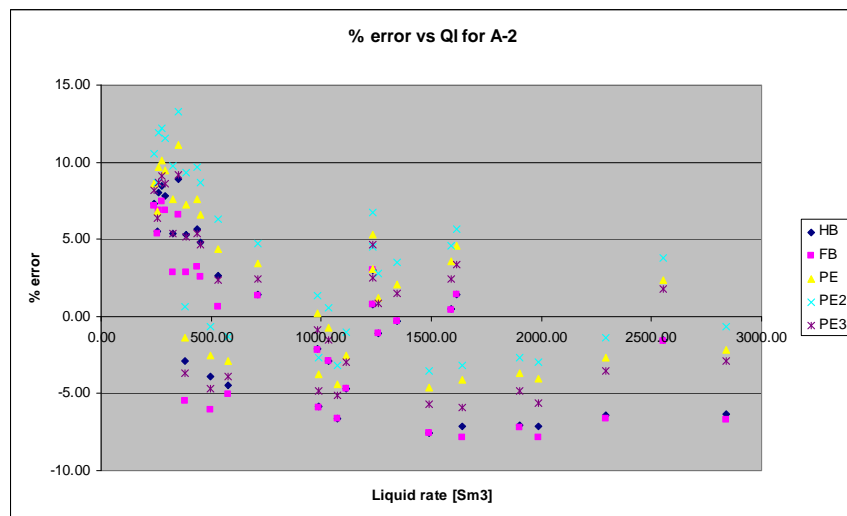


**Figure B.14:** Percentage error in predicted pressure drop versus liquid rate for A-2

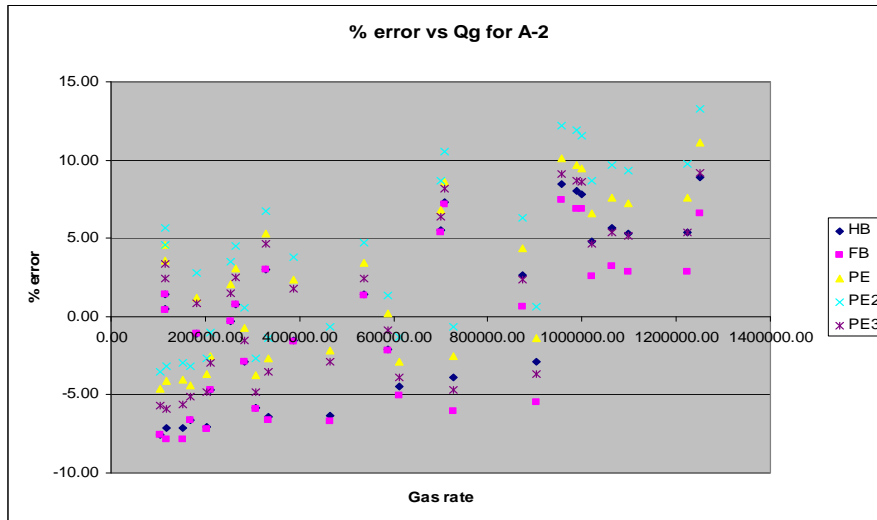


**Figure B.15:** Percentage error in predicted pressure drop versus gas rate for A-2

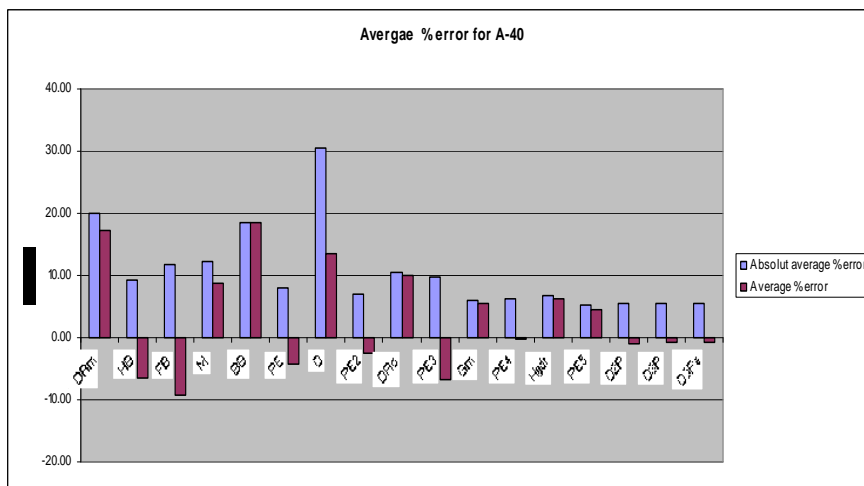


**Figure B.16:** Average percentage error in predicted pressure drop for A-40

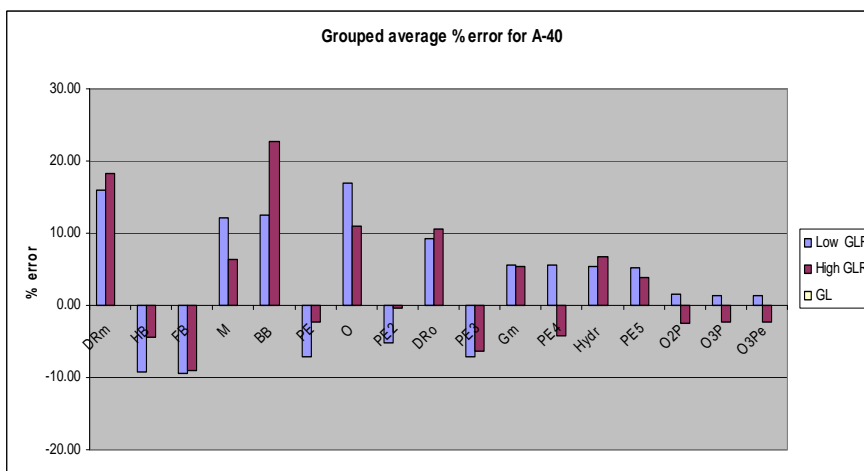


**Figure B.17:** Average percentage error for A-40, divided in groups of high and low GLR and tests including gas-lift

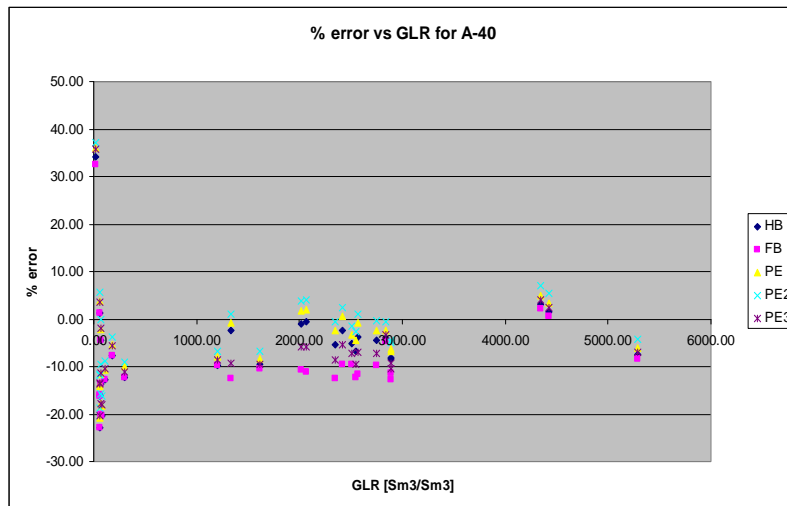


**Figure B.18:** Percentage error in predicted pressure drop versus GLR for A-40

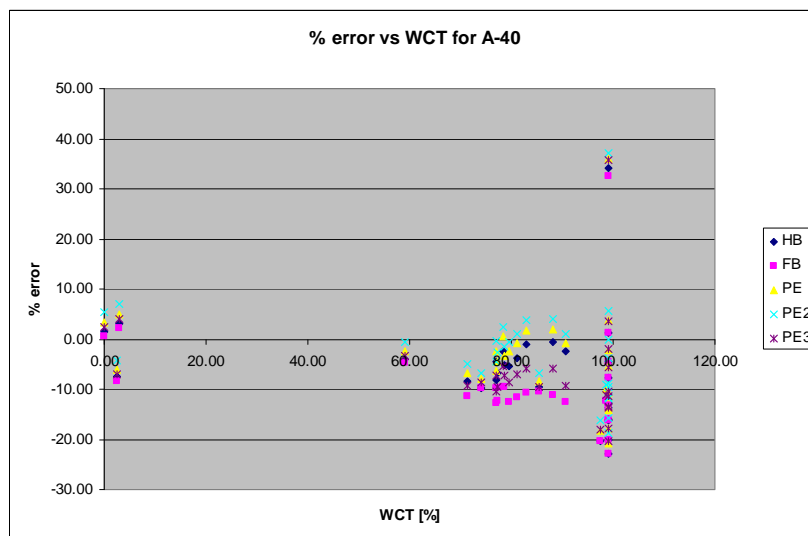


**Figure B.19:** Percentage error in predicted pressure drop versus WCT for A-40

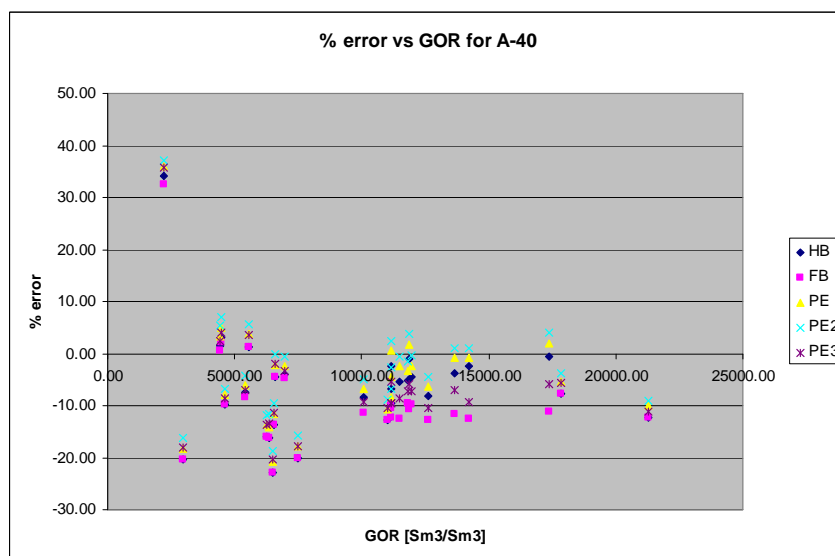


**Figure B.20:** Percentage error in predicted pressure drop versus GOR for A-40

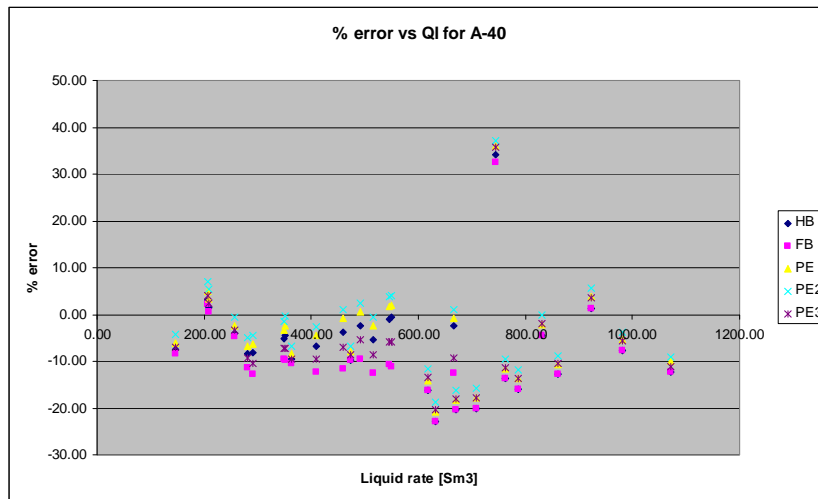


**Figure B.21:** Percentage error in predicted pressure drop versus liquid rate for A-40

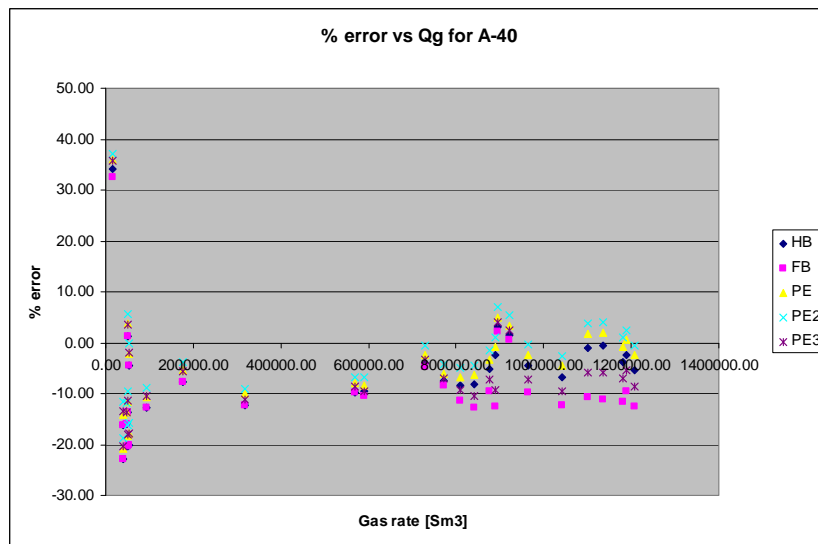


**Figure B.22:** Percentage error in predicted pressure drop versus gas rate for A-40

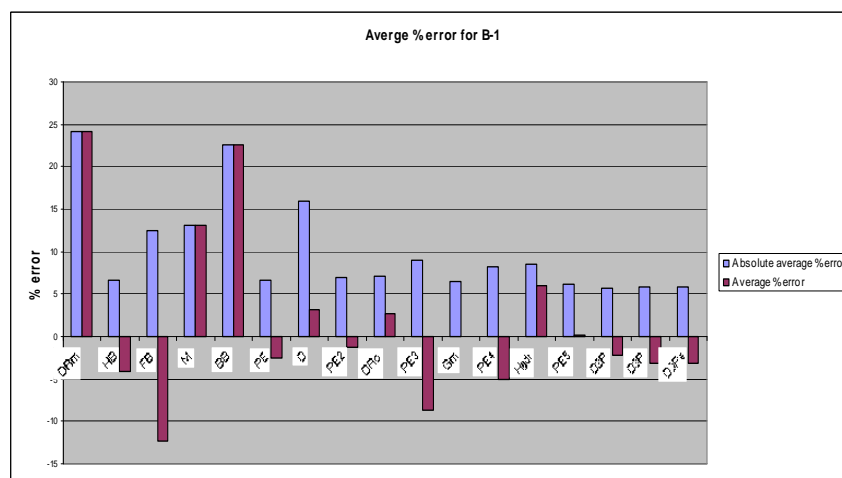


**Figure B.23:** Average percentage error in predicted pressure drop for B-1



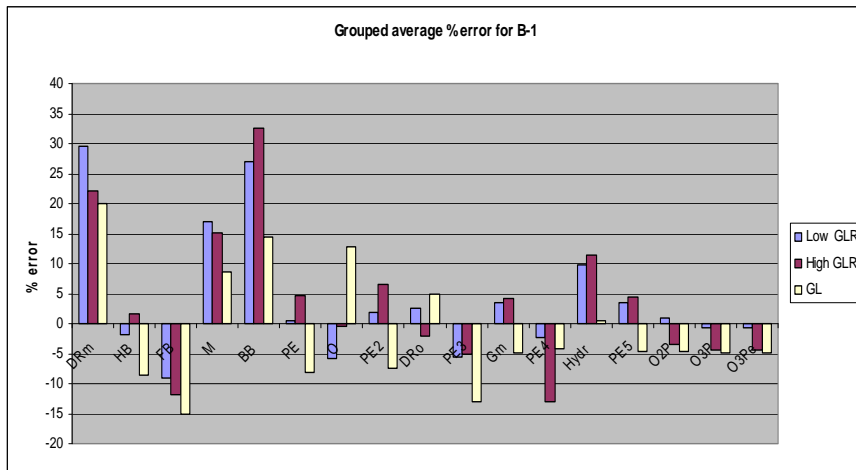


**Figure B.24:** Average percentage error for B-1, divided in groups of high and low GLR and tests including gas-lift

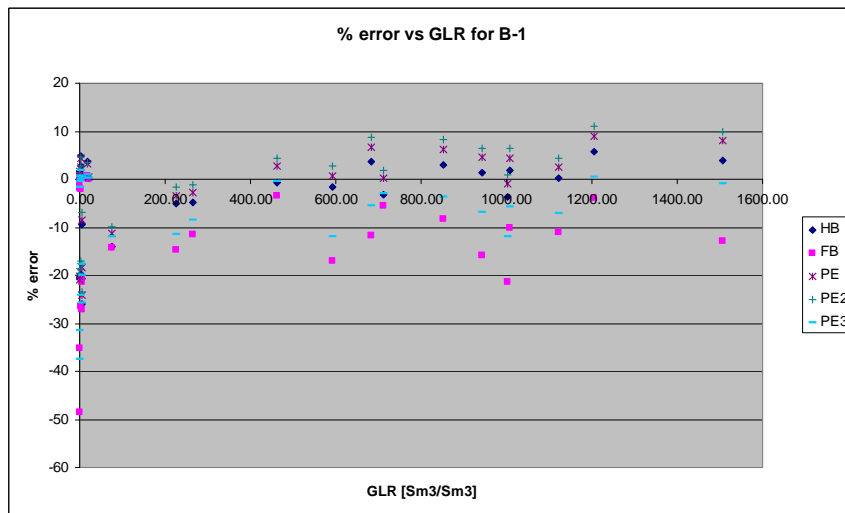


**Figure B.25:** Percentage error in predicted pressure drop versus GLR for B-1

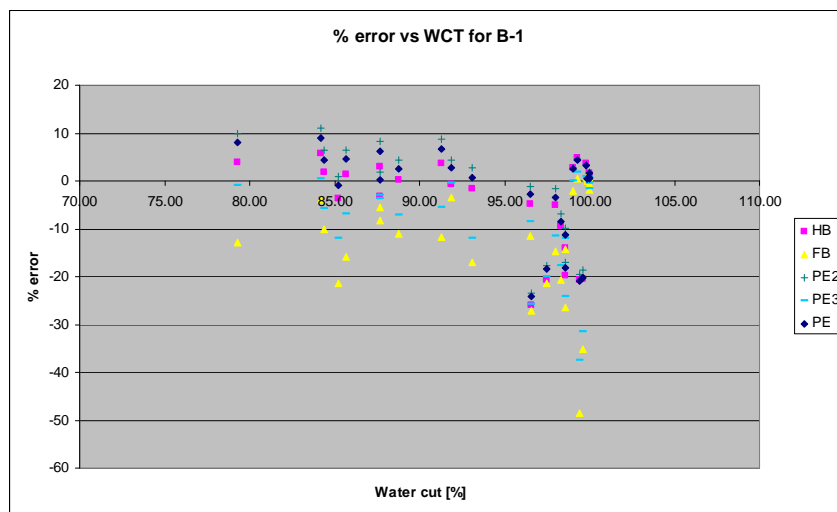


**Figure B.26:** Percentage error in predicted pressure drop versus WCT for B-1

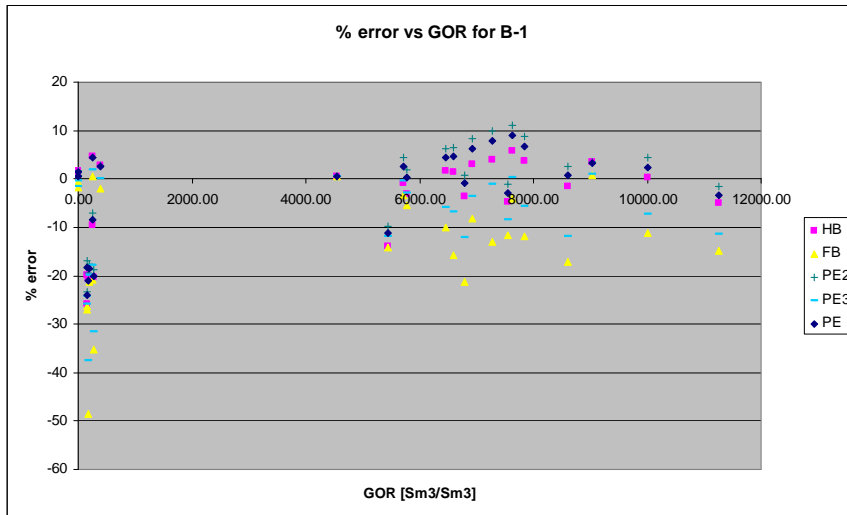


**Figure B.27:** Percentage error in predicted pressure drop versus GOR for B-1

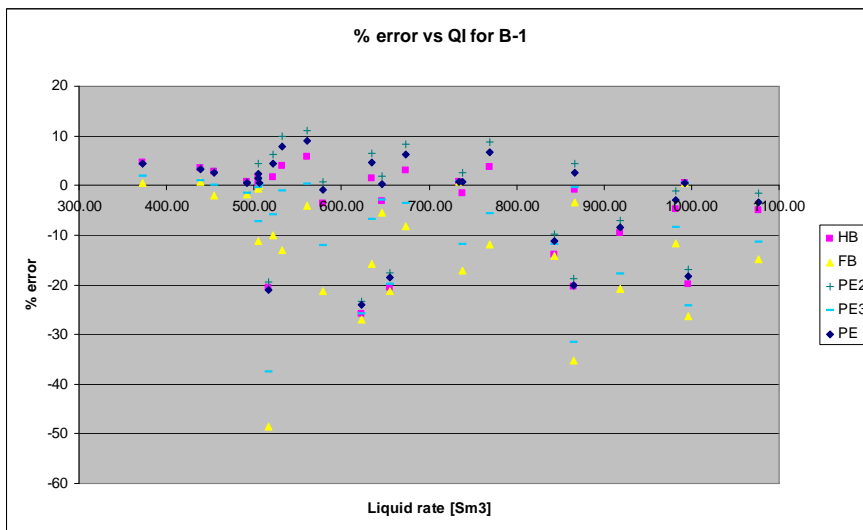


**Figure B.28:** Percentage error in predicted pressure drop versus liquid rate for B-1

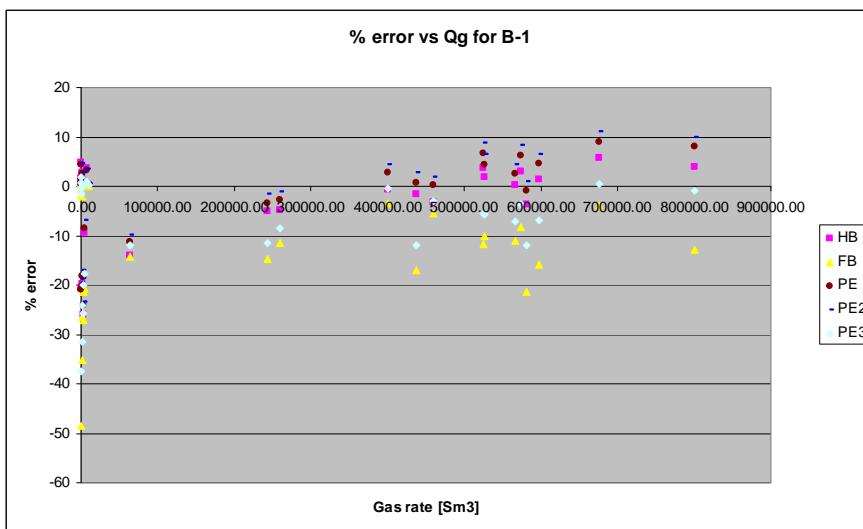


**Figure B.29:** Percentage error in predicted pressure drop versus gas rate for B-1

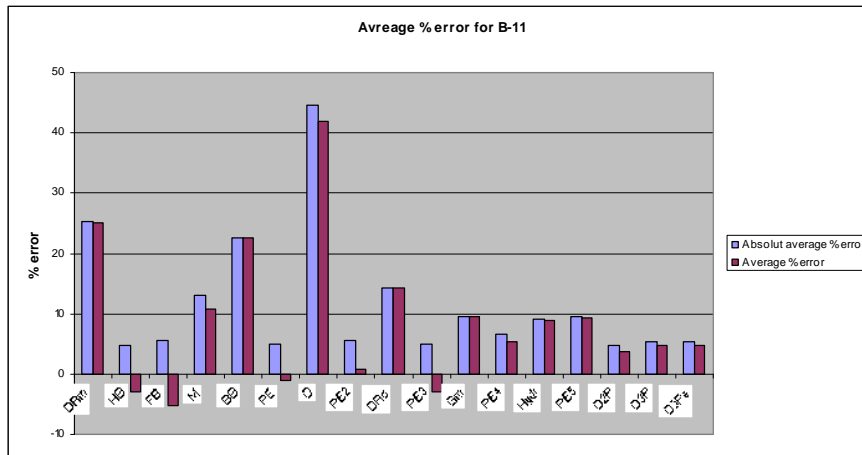


Figure B.30: Average percentage error in predicted pressure drop for B-11

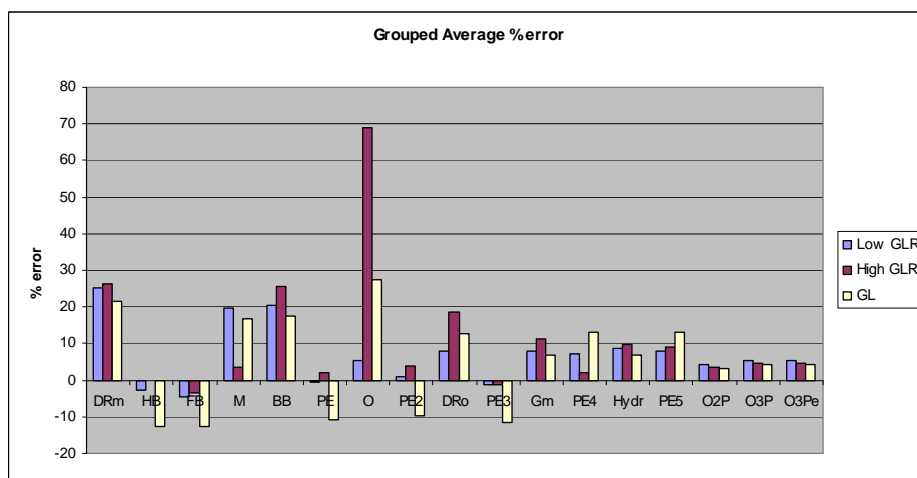


Figure B.31: Average percentage error for B-11, divided in groups of high and low GLR and tests including gas-lift

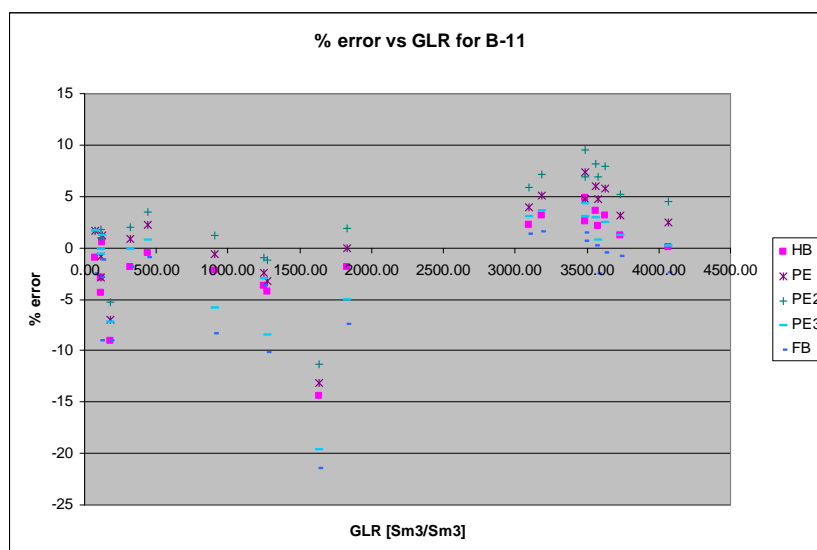
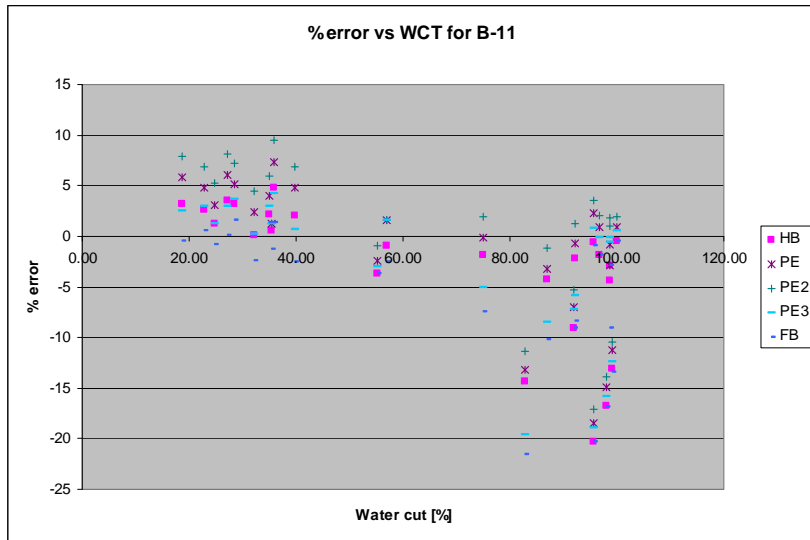
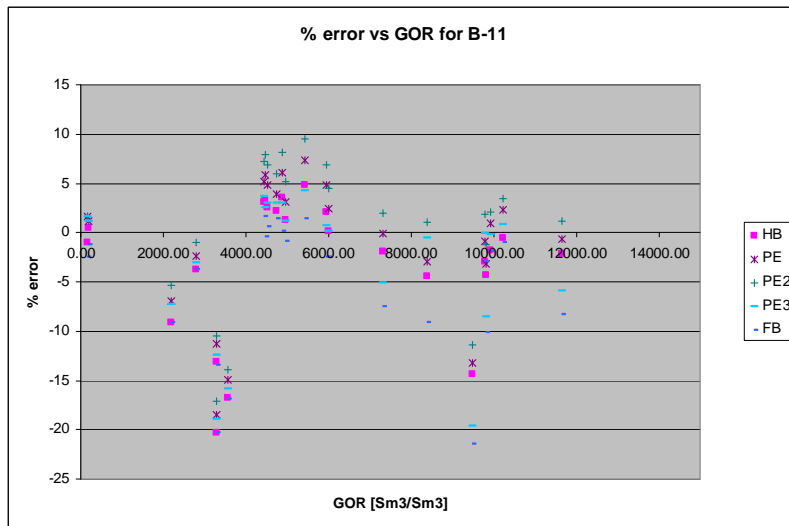


Figure B.32: Percentage error in predicted pressure drop versus GLR for B-11



**Figure B.33:** Percentage error in predicted pressure drop versus WCT for B-11



**Figure B.34:** Percentage error in predicted pressure drop versus GOR for B-11

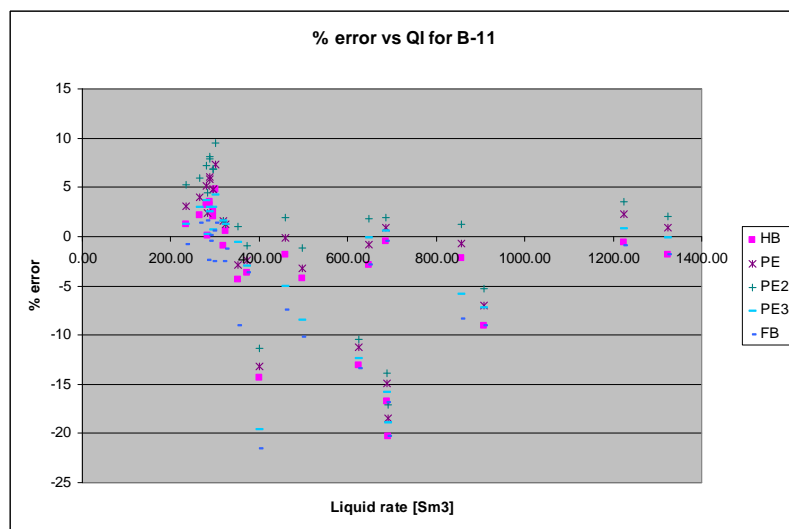


**Figure B.35:** Percentage error in predicted pressure drop versus liquid rate for B-11

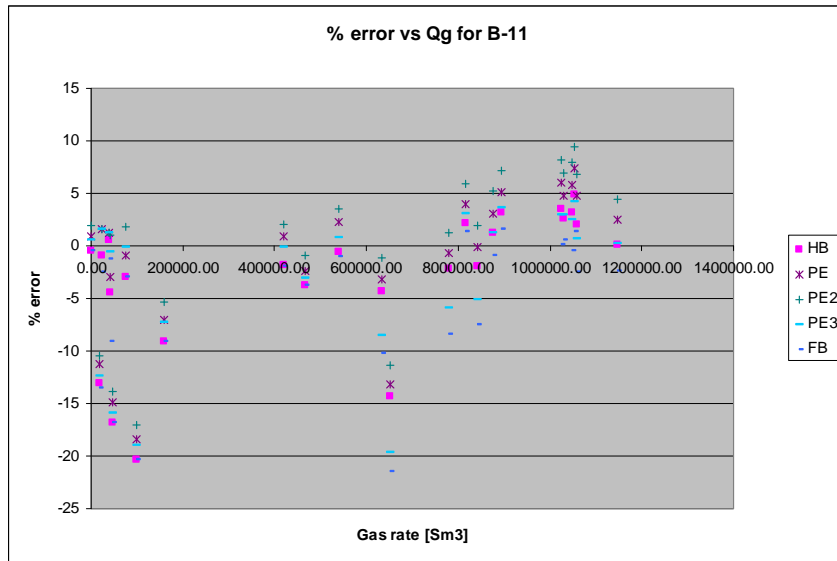


**Figure B.36:** Percentage error in predicted pressure drop versus gas rate for B-11

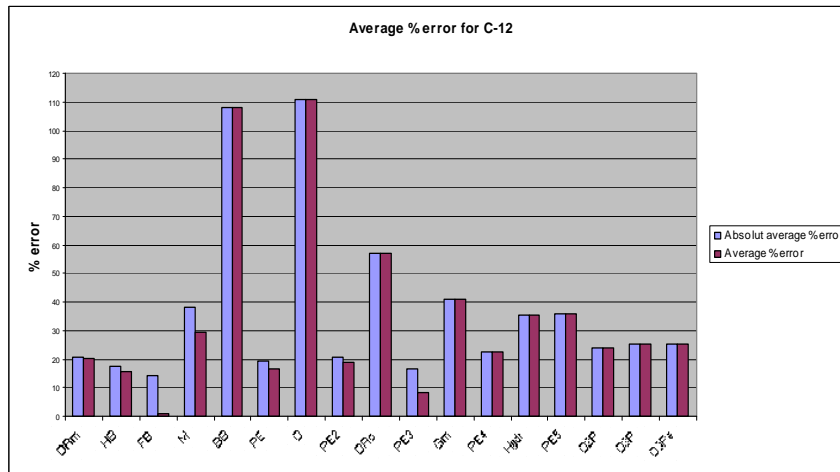


**Figure B.37:** Average percentage error in predicted pressure drop for C-12

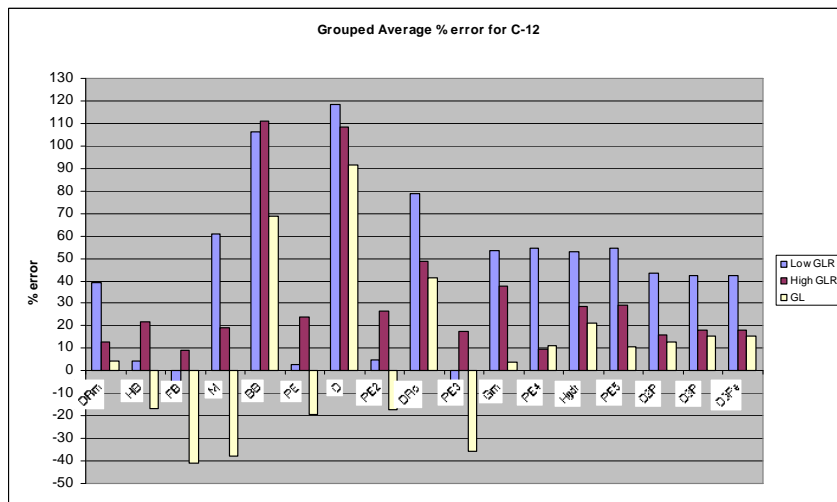


**Figure B.38:** Average percentage error for C-12, divided in groups of high and low GLR and tests including gas-lift

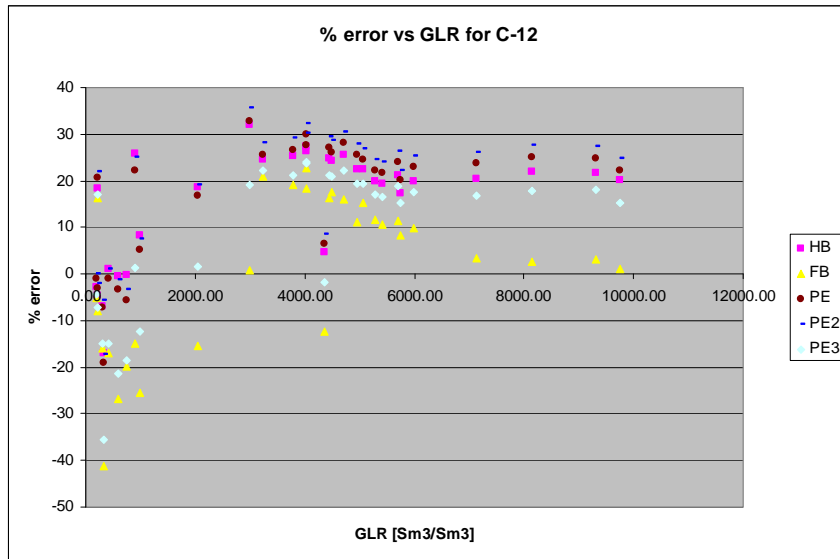


**Figure B.39:** Percentage error in predicted pressure drop versus GLR for C-12

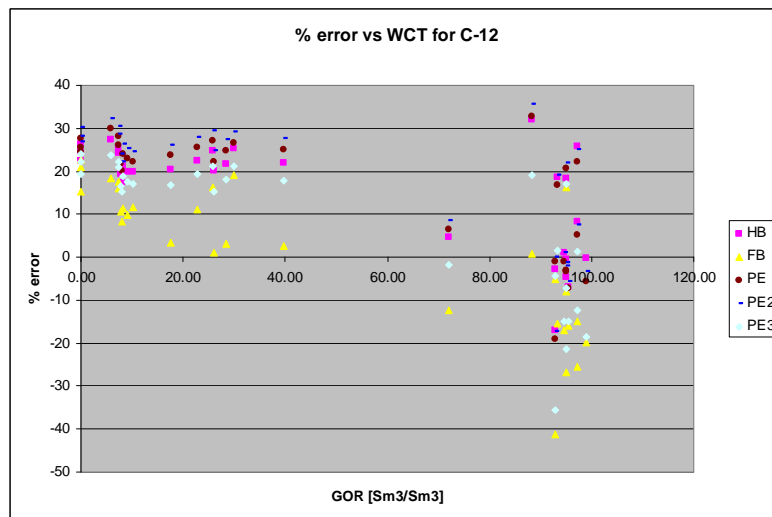


**Figure B.40:** Percentage error in predicted pressure drop versus WCT for C-12

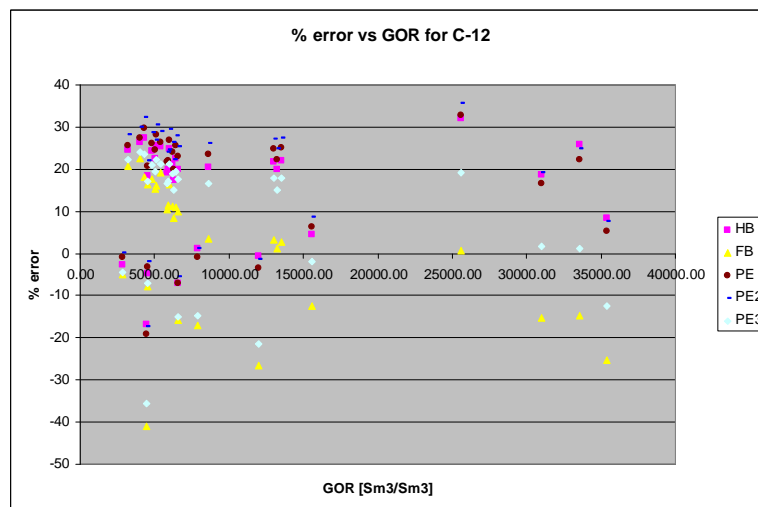


**Figure B.41:** Percentage error in predicted pressure drop versus GOR for C-12

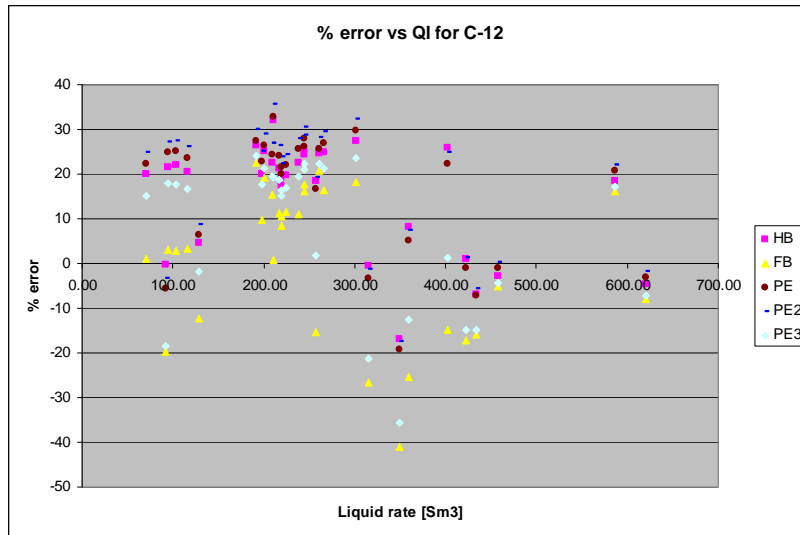


**Figure B.42:** Percentage error in predicted pressure drop versus liquid rate for C-12

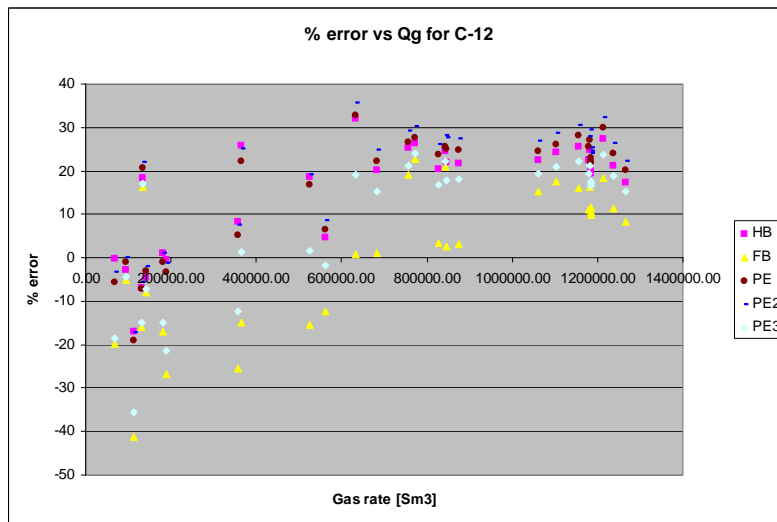


**Figure B.43:** Percentage error in predicted pressure drop versus gas rate for C-12

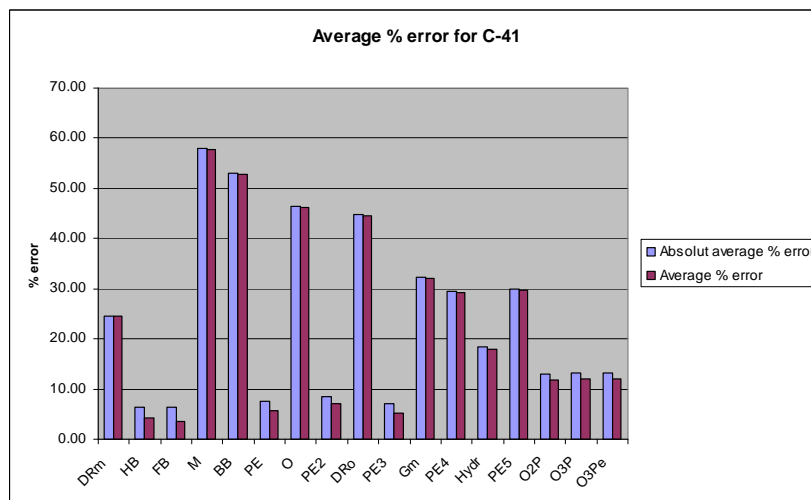


**Figure B.44:** Average percentage error in predicted pressure drop for C-41

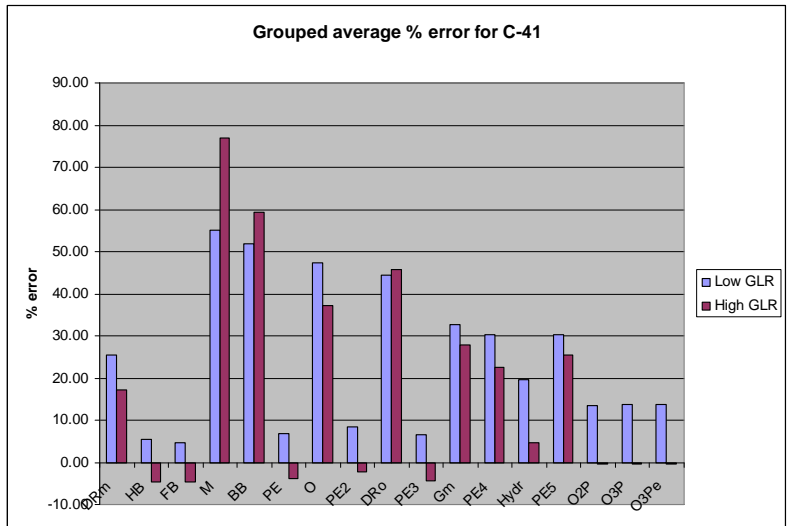


**Figure B.45:** Average percentage error for C-41, divided in groups of high and low GLR and tests including gas-lift

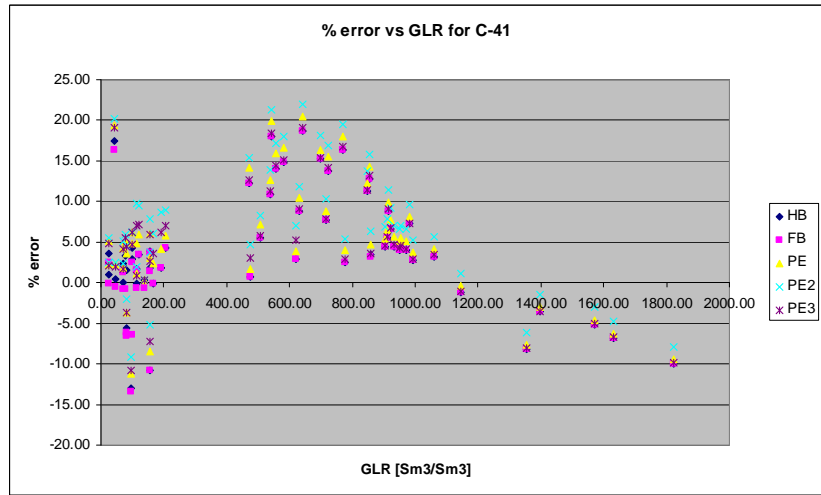


**Figure B.46:** Percentage error in predicted pressure drop versus GLR for C-41

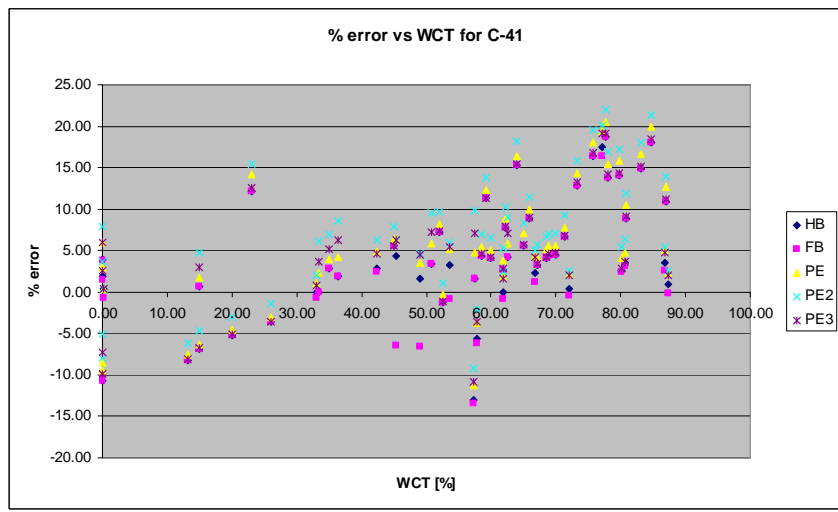


**Figure B.47:** Percentage error in predicted pressure drop versus WCT for C-41



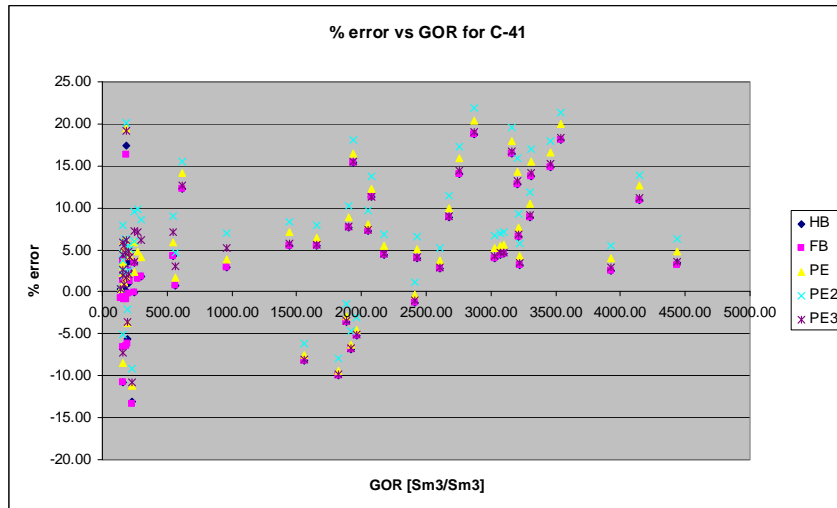


**Figure B.48:** Percentage error in predicted pressure drop versus GOR for C-41

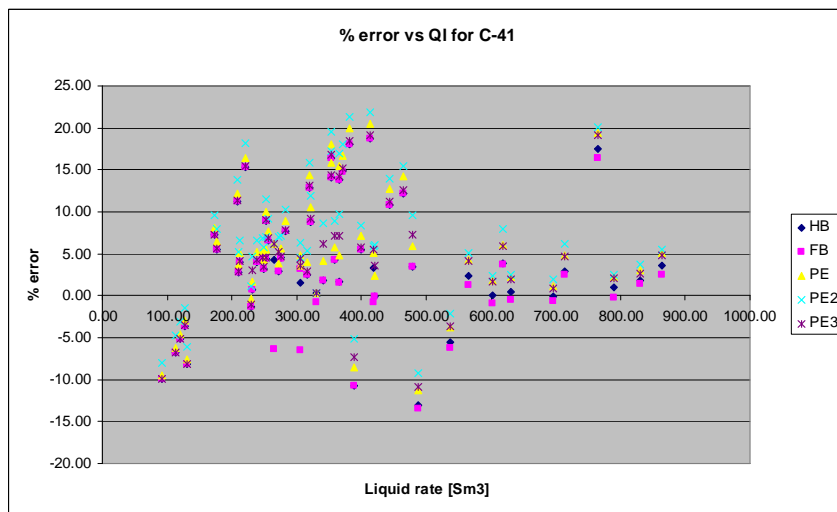


**Figure B.49:** Percentage error in predicted pressure drop versus liquid rate for C-41

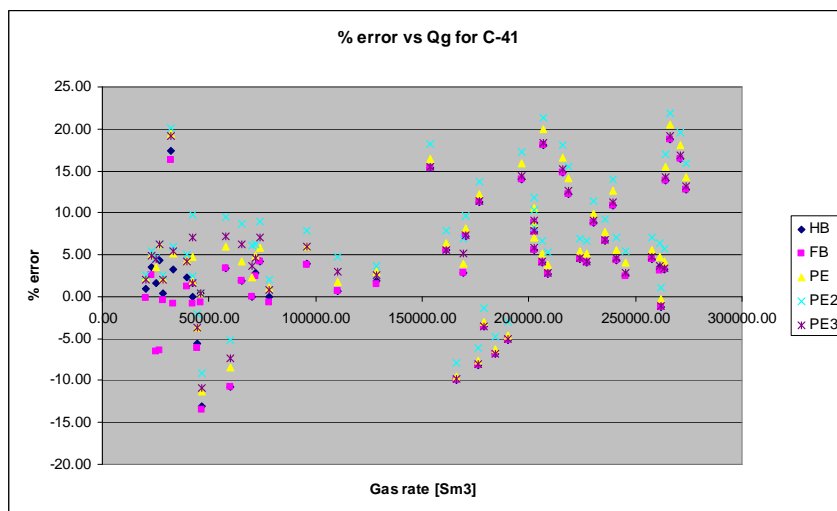


**Figure B.50:** Percentage error in predicted pressure drop versus gas rate for C-41

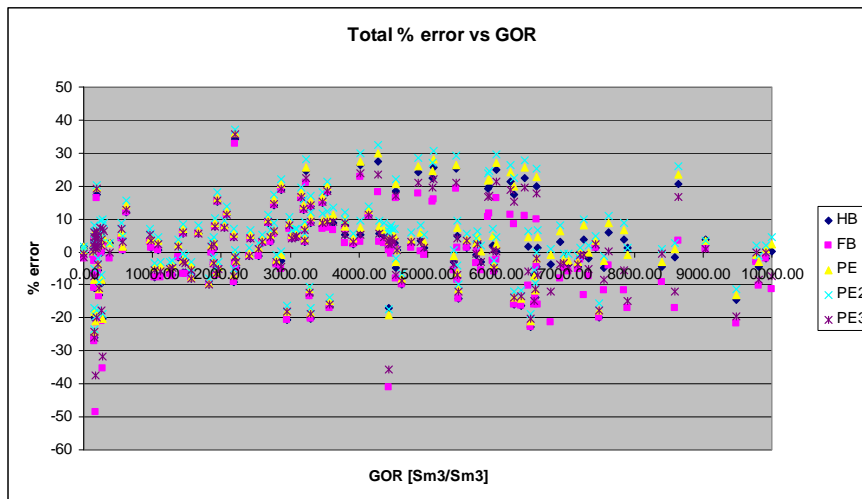


**Figure B.51:** Percentage error in predicted pressure drop versus GOR for all tests



**Figure B.52:** Percentage error in predicted pressure drop versus liquid rate for all tests

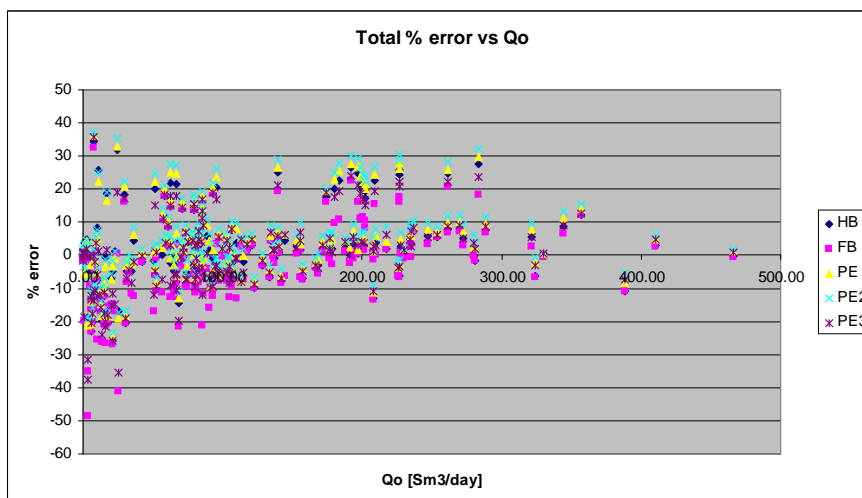


**Figure B.53:** Percentage error in predicted pressure drop versus oil rate for all tests

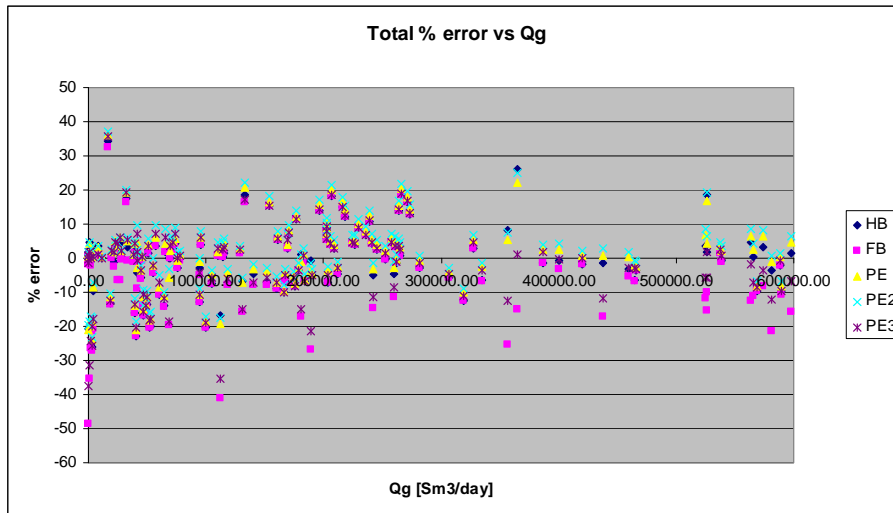


**Figure B.54:** Percentage error in predicted pressure drop versus gas rate for all tests

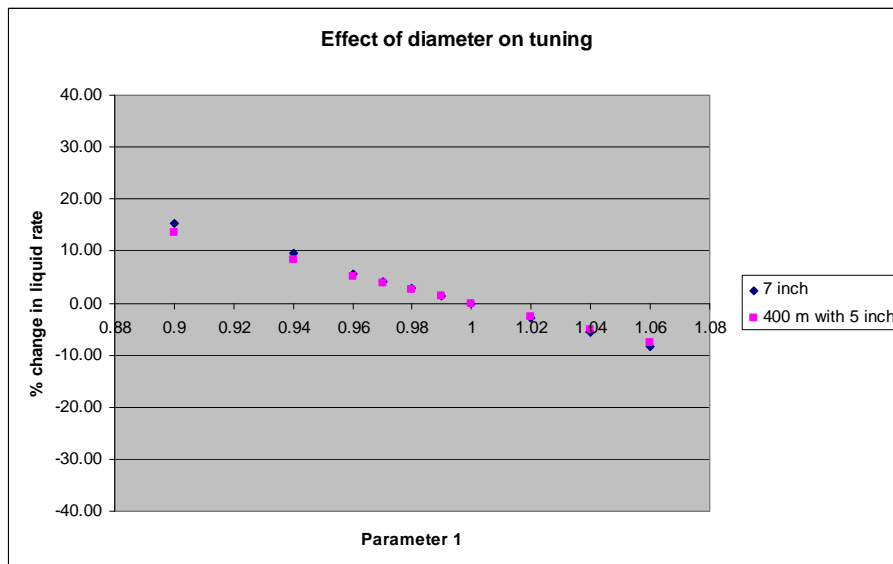


**Figure B.55:** Percentage change in liquid rate, effect of changing diameter on tuning